

Chapter 1

Notion and Structure of Sensor Data Fusion

Sensor data fusion is an omnipresent phenomenon that existed prior to its technological realization or the scientific reflection on it. In fact, all living creatures, including human beings, by nature or intuitively perform sensor data fusion. Each in their own way, they combine or “fuse” sensations provided by different and mutually complementary sense organs with knowledge learned from previous experiences and communications from other creatures. As a result, they produce a “mental picture” of their individual environment, the basis of behaving appropriately in their struggle to avoid harm or successfully reach a particular goal in a given situation.

1.1 Subject Matter

As a sophisticated technology with significant economic and defence implications as well as a branch of engineering science and applied informatics, modern sensor data fusion aims at automating this capability of combining complementary pieces of information. Sensor data fusion thus produces a “situation picture,” a reconstruction of an underlying “real situation,” which is made possible by efficiently implemented mathematical algorithms exploiting even imperfect data and enhanced by new information sources. Emphasis is not only placed on advanced sensor systems, technical equivalents of sense organs, but also on spatially distributed networks of homogeneous or heterogeneous sensors on stationary or moving platforms and on the integration of data bases storing large amounts of quantitative context knowledge. The suite of information sources to be fused is completed by the interaction with human beings, which makes their own observations and particular expertise accessible.

The information to be fused may comprise a large variety of attributes, characterized, for example, by sensor ranges from less than a meter to hundreds of kilometers, by time scales ranging from less than a second to a few days, by nearly stationary or rapidly changing scenarios, by actors behaving cooperatively, in-cooperatively, or even hostile, by high precision measurements or sensor data of poor quality.

Sensor data fusion systems emerging from this branch of technology have in effect the character of “cognitive tools”, which enhance the perceptive faculties of human beings in the same way conventional tools enhance their physical strength. In this type of interactive assistance system, the strengths of automated data processing (dealing with mass data, fast calculation, large memory, precision, reliability, robustness etc.) are put into service for the human beings involved. Automated sensor data fusion actually enables them to bring their characteristically “human” strengths into play, such as qualitatively correct over-all judgment, expert knowledge and experience, intuition and creativity, i.e. their “natural intelligence” that cannot be substituted by automated systems in the foreseeable future. The user requirements to be fulfilled in a particular application have a strong impact on the actual fusion system design.

1.1.1 Origins of Modern Development

Sensor data fusion systems have been developed primarily for applications, where a particular need for support systems of this type exists, for example in time-critical situations or in situations with a high decision risk, where human deficiencies must be complemented by automatically or interactively working data fusion techniques. Examples are fusion tools for compensating decreasing attention in routine and mass situations, for focusing attention on anomalous or rare events, or complementing limited memory, reaction, and combination capabilities of human beings. In addition to the advantages of reducing the human workload in routine or mass tasks by exploiting large data streams quickly, precisely, and comprehensively, fusion of mutually complementary information sources typically produces qualitatively new and important knowledge that otherwise would remain unrevealed.

The demands for developing such support systems are particularly pressing in defence and security applications, such as surveillance, reconnaissance, threat evaluation, and even weapon control. The earliest examples of large sensor data fusion projects were designed for air defence against missiles and low-flying bombers and influenced the development of civilian air traffic control systems. The development of modern sensor data fusion technology and the underlying branch of applied science was stimulated by the advent of sufficiently powerful and compact computers and high frequency devices, programmable digital signal processors, and last but not least by the “Strategic Defence Initiative (SDI)” announced by US President RONALD REAGAN on March 23, 1983.

After a certain level of maturity has been reached, the Joint Directors of Laboratories (JDL), an advisory board to the US Department of Defense, coined the technical term “Sensor Data and Information Fusion” in George Orwell’s very year 1984 and undertook the first attempt of a scientific systematization of the new technology and the research areas related to it [1, Chap. 2, p. 24]. To the present day, the scientific fusion community speaks of the “JDL Model of Information Fusion” and its subsequent generalizations and adaptations [1, Chap. 3], [2]. The JDL model provides a structured and integrated view on the complete functional chain from dis-

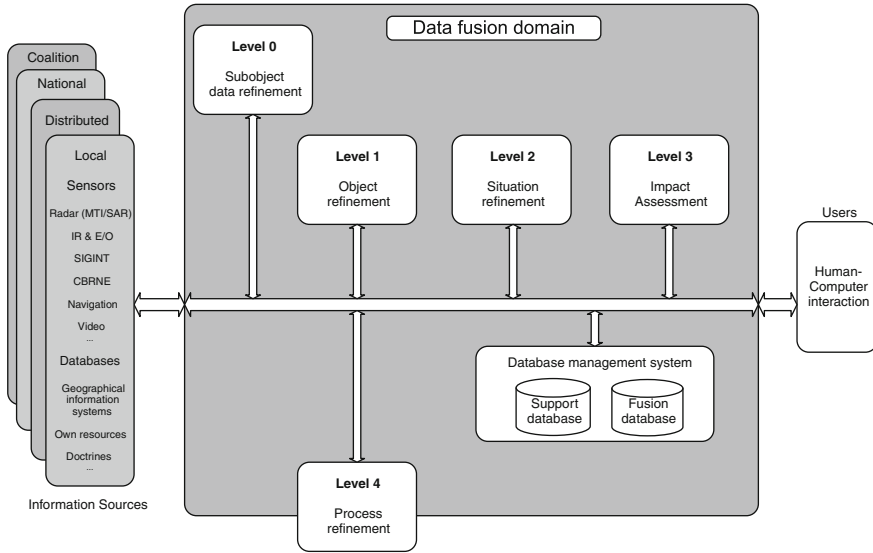


Fig. 1.1 Overview of the JDL-Model of Sensor Data and Information Fusion [1, Chap. 3], which provides a structured and integrated view on the complete functional chain from distributed sensors, data bases, and human reports to the users and their options to act including various feed-back loops at different levels

tributed sensors, data bases, and human reports to the users and their options to act including various feed-back loops at different levels (Fig. 1.1). It seems to be valid even in the upcoming large fields of civilian applications of sensor data fusion and cyber security [3]. Obviously, the fundamental concepts of sensor data fusion have been developed long before their full technical feasibility and robust realizability in practical applications.

1.1.2 General Technological Prerequisites

The modern development of sensor data fusion systems was made possible by substantial progress in the following areas over the recent decades:

1. Advanced and robust *sensor systems*, technical equivalents of sense organs with high sensitivity or coverage are made available that may open dimensions of perception usually inaccessible to most living creatures.
2. *Communication links* with sufficient bandwidths, small latencies, stable connectivity, and robustness against interference are the backbones of spatially distributed networks of homogeneous or heterogeneous sensors.

3. Mature *navigation systems* are prerequisites of (semi-)autonomously operating sensor platforms and common frames of reference for the sensor data based on precise space–time registration including mutual alignment.
4. *Information technology* provides not only sufficient processing power for dealing with large data streams, but also efficient data base technology and fast algorithmic realizations of data exploitation methods.
5. *Technical interoperability*, the ability of two or more sub-systems or components to interact and to exchange and to information mutually understood, is inevitable to build distributed “systems of systems” for sensor exploration and data exploitation [4].
6. Advanced and ergonomically efficient *Human–Machine Interaction (HMI)* tools are an integral part of man-machine-systems presenting the results of sensor data fusion systems to the users in an appropriate way [5].

The technological potential enabled by all these capabilities is much enhanced by integrating them in an overall sensor data fusion system.

1.1.3 Relation to Information Systems

According to this technological infrastructure, human decision makers on all levels of hierarchy, as well as automated decision making systems, have access to vast amounts of data. In order to optimize use of this high degree of data availability in various decision tasks, however, the data continuously streaming in must not overwhelm the human beings, decision making machines, or actuators involved. On the contrary, the data must be fused in such a way that at the right instant of time the right piece of high-quality information relevant to a given situation is transmitted to the right user or component and appropriately presented. Only if this is the case, the data streams can support goal-oriented decisions and coordinated action planing in practical situations and on all levels of decision hierarchy.

In civilian applications, management information or data warehouse systems are designed in order to handle large information streams. Their equivalents in the defence and security domain are called C⁴ISTAR Systems [4]. This acronym denotes computer-assisted functions for C⁴ (Command, Control, Communications, Computers), I (Intelligence), and STAR (Surveillance, Target Acquisition and Reconnaissance) in order to enable the coordination of defence-related operations. While management information or data warehouse systems are primarily used to obtain competitive advantages in economic environments, C⁴ISTAR systems aim at information dominance over potential military opponents. The observation that more or less the same terminology is used in both areas for characterizing the struggle to avoid harm or successfully reach goals, is an indication of far-reaching fundamental commonalities of decision processes in defence command & control as well as in product development and planing, in spite of different accentuations in particular aspects.

A basic component of C⁴ISTAR information systems, modular and flexibly designed as “systems of systems,” is the combination of sensor systems and data bases with appropriate sensor data and information fusion sub-systems. The objective at this level is the production of timely, consistent and, above all, sufficiently complete and detailed “situation pictures,” which electronically represent a complex and dynamically evolving overall scenario in the air, on the ground, at sea, or in an urban environment. The concrete operational requirements and restrictions in a given application define the particular information sources to be considered and data fusion techniques to be used.

A Characteristic Example

A particularly mature example of an information system, where advanced sensor data fusion technology is among its central pillars, is given by a distributed, coalition-wide C⁴ISTAR system of systems for wide-area ground surveillance. It mirrors many of the aspects previously addressed and has been carried out within the framework of a multinational technology program called MAJIC (Multi-Sensor Aerospace-Ground Joint ISR Interoperability Coalition) [4, Chap. 20]. By collaboratively using interoperable sensor and data exploitation systems in coalition operations, MAJIC has been designed to improve situational awareness of military commanders over the various levels of the decision making hierarchy.

Based on appropriate concepts of deployment and the corresponding tactical procedures, technological tools for Collection, Coordination and Intelligence Requirements Management (CCIRM) are initiated by individual sensor service requests of deployed action forces. The CCIRM tools produce mission plans according to superordinate priorities, task sensor systems with appropriate data acquisition missions, initiate data exploitation and fusion of the produced sensor data streams in order to obtain high-quality reconnaissance information, and, last but not least, guarantee the feedback of the right information to the requesting forces at the right instant of time.

Under the constraint of leaving existing C⁴ISTAR system components of the nations participating in MAJIC unchanged as far as possible, the following aspects are addressed with particular emphasis:

1. The integration of advanced sensor technology for airborne and ground-based wide-area surveillance is mainly based on Ground Moving Target Indicator Radar (GMTI), Synthetic Aperture Radar (SAR), electro-optical and infrared sensors (E/O, IR) producing freeze and motion imagery, Electronic Support Measures (ESM), and artillery localization sensors (radar- or acoustics-based).
2. Another basic issue is the identification and implementation of common standards for distributing sensor data from heterogeneous sources including appropriate data and meta-data formats, agreements on system architectures as well as the design and implementation of advanced information security concepts.
3. In addition to sensor data fusion technology itself, tools and procedures have been developed and are continuously enhanced for co-registration of hetero-

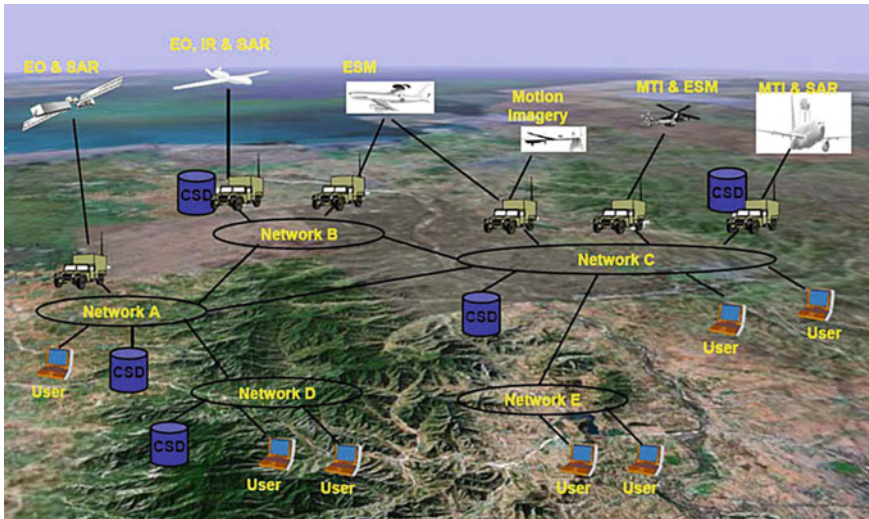


Fig. 1.2 MAJIIC system architecture emphasizing the deployed sensors, databases, and distributed sensor data fusion systems (Interoperable ISR Exploitation Stations)

geneous sensors, cross-cueing between the individual sensors of a surveillance system, the sensors of different systems, and between sensors and actuators, as well as for exploitation product management, representation of the “Coalition Ground Picture,” for coordinated mission planning, tasking, management, and monitoring of the MAJIIC sub-systems.

4. MAJIIC-specific communications have been designed to be independent of network-types and communication bandwidths, making it adaptable to varying requirements. Commercially available and standardized internet- and crypto-technology has been used in both the network design and the implementation of interfaces and operational features. Important functionalities are provided by collaboration tools enabling ad-hoc communication between operators and exchange of structured information.
5. The central information distribution nodes of the MAJIIC C⁴ISTAR system of systems are so-called Coalition Shared Data servers (CSD) making use of modern database technology. Advanced Data Mining and Data Retrieval tools are part of all MAJIIC data exploitation and fusion systems.
6. From an operational point of view, a continuous interaction between Concept Development and Experimentation (CD&E process, [6]) by planning, running, and analyzing simulated and live C⁴ISTAR experiments is an essential part of the MAJIIC program, fostering the transfer of MAJIIC capabilities into national and coalition systems.

Figure 1.2 provides an overview of the MAJIIC system architecture and the deployed sensor systems.

1.2 Characterization as a Branch of Applied Science

The object of knowledge in sensor data fusion as a branch of applied science is sensor data fusion technology discussed previously. In other words, it aims at the acquisition of knowledge required to build automated sensor data fusion systems, often being part of larger information systems, by using appropriately developed scientific methodologies. This includes the elicitation, collection, analysis, modeling, and validation of this knowledge.

In order to reach this goal, scientific research in sensor data fusion is performed in an interdisciplinary way by applying fundamental results gathered from other sciences, such as natural sciences dealing with physical object properties perceptible by sensors and the underlying sensing principles, engineering sciences, mainly sensor engineering, metrology, automation, communications, and control theory, but also applied mathematics and statistics, and, last but not least, applied informatics. Two characteristic features of sensor data fusion can be identified.

1. The available sensor data and context knowledge to be fused typically provide incomplete and imperfect pieces of information. These deficiencies have manifold reasons and are unavoidable in real-world applications. For dealing with imperfect sensor and context data, sophisticated mathematical methodologies and reasoning formalisms are applied. Certain aspects of them are developed by extending the underlying methodology, thus providing contributions to fundamental research. Reasoning with uncertain information by using probabilistic or other formalisms is therefore a major scientific feature characterizing sensor data fusion.
2. As a branch of applied science, sensor data fusion is closely related to the practical design of surveillance and reconnaissance components for information systems. In implementing fundamental theoretical concepts, a systematic way of finding reasonable compromises between mathematical exactness and pragmatic realization issues as well as suitable approximation methodologies are therefore inevitable. System aspects such as robustness and reliability even in case of unforeseeable nuisance phenomena, priority management, and graceful degradation are of particular importance in view of practicability. This is equally true for comprehensive evaluation and prediction of fusion system performance and identification of relevant factors for system control and operation, based, for example, on extensive Monte-Carlo-simulations and the analysis of theoretical bounds [7].

1.2.1 Pioneers of Sensor Data Fusion

Since sensor data fusion can be considered as a branch of automation with respect to imperfect sensor data and non-sensor information, a historical reflection on its roots could identify numerous predecessors in automation engineering, cybernetics,

and Bayesian statistics, who developed fundamental notions and concepts relevant to sensor data fusion. Among many other pioneers, CARL FRIEDRICH GAUSS, THOMAS BAYES and the Bayesian statisticians, as well as RUDOLF E. KALMAN have created the methodological and mathematical prerequisites of sensor data fusion that made the modern development possible.

Carl Friedrich Gauß

Many achievements in science and technology that have altered today's world can be traced back to the great mathematician, astronomer, geodesist, and physicist CARL FRIEDRICH GAUSS (1777–1855). This general tendency seems also to be true in the case of sensor data fusion. After finishing his opus magnum on number theory, GAUSS re-oriented his scientific interests to astronomy. His motive was the discovery of the planetoid Ceres by the Theatine monk GIUSEPPE PIAZZI (1746–1826) on Jan 1, 1801, whose position was lost shortly after the first astronomical orbit measurements. GAUSS succeeded in estimating the orbit parameters of Ceres from a few noisy measurements by using a recursively defined least-squares error compensation algorithm [8], a methodology, which can be interpreted as a limiting case of Kalman filtering, one of the most important backbone algorithms of modern target tracking and sensor data fusion. Based on his results, HEINRICH OLBERS (1758–1840) was able to rediscover Ceres on Jan 1, 1802. The discovery of three other planetoids followed (Pallas 1802, Juno 1804, Vesta 1807). Although until then, GAUSS was well-known to mathematical experts only, this success made his name popular, leading to his appointment at Göttingen University in 1807 as a Professor of Astronomy and Director of the Observatory. GAUSS' personal involvement in this new scientific branch of reasoning with imprecise observation data is indicated by the fact that he called his first borne child Joseph, after Father GUISEPPE PIAZZI [9, p. 15]. Three others of his children were named after the discoverers of Pallas, Juno, and Vesta.

Bayesian Statisticians

In sensor data fusion, the notion of “Bayesian probability” is of fundamental importance. It interprets the concept of probability as “a measure of a state of knowledge” (see [10], e.g.) and not as a relative frequency as in classical statistics. According to this interpretation, the probability of a hypothesis given the sensor data is proportional to the product of the likelihood function multiplied by the prior probability. The likelihood function represents the incomplete and imperfect information provided by the sensor data themselves as well as context information on the sensor performance and the sensing environment, while the prior probability the belief in the hypothesis before the sensor data were available (see Chap. 3 *Bayesian Knowledge Propagation* of this book).

The term ‘Bayesian’ refers to THOMAS BAYES (1702–1761), a British mathematician and Presbyterian minister, who proved a special case of this proposition,

which is now called Bayes' theorem (published posthumously by his friend RICHARD PRICE (1723–1791) in 1763, [11]). The roots of 'subjective probability' can even be traced back to the great Jewish philosopher MOSES MAIMONIDES (1135/38–1204) and the medieval rabbinic literature [12, Chap. 10]. It was PIERRE-SIMON LAPLACE (1749–1827), however, who introduced a more general version of Bayes' theorem, apparently unaware of Bayes' work, and used it to approach problems in celestial mechanics, medical statistics, reliability, and jurisprudence [13, Chap. 3]. In the sequel, the foundations of Bayesian statistics were laid by many eminent statisticians.

Of particular importance is ABRAHAM WALD (1902–1950, [14]), an Austro-Hungarian mathematician, who immigrated to the USA in 1938, where he created *Sequential Analysis*, a branch of applied statistical decision making, which is of enormous importance for sensor data fusion, especially in track management and consistency testing (see Chap. 4 *Sequential Track Extraction* of this book). In his influential work on *Statistical Decision Functions* [15], he recognized the fundamental role of Bayesian methods and called his optimal decision methods 'Bayes strategies'.

Rudolf E. Kalman and his Predecessors

The beginning of modern sensor data fusion is inextricably bound up with the name of RUDOLF E. KALMAN (*1930), a Hungarian-American system theorist, though he had many predecessors. The Kalman filter is a particularly influential example of a processing algorithm for inferring a time variable object state from uncertain data assuming an uncertain object evolution, which can elegantly be derived from Bayesian statistics. Among Kalman's predecessors, THORVALD NICOLAI THIELE (1838–1910), a Danish astronomer, actuary and mathematician, derived a geometric construction of a fully developed Kalman filter in 1889 [16, Chap. 4]. Also RUSLAN L. STRATONOVICH (1930–1997), a Russian physicist, engineer, probabilist, and PETER SWERLING (1929–2000), one of the most influential RADAR theoreticians in the second half of the twentieth century [17, Appendix], developed Kalman-type filtering algorithms earlier using different approaches.

STANLEY F. SCHMIDT (*1926) is generally credited with developing the first application of a Kalman filter to the problem of trajectory estimation for the NASA Apollo Spaceflight Program in 1960, leading to its incorporation in the Apollo navigation computer. The state-of-the-art until 1974 is summarized in the influential book *Applied Optimal Estimation*, edited by ARTHUR GELB [18].

Contemporary Researchers

Independently of each other, GÜNTHER VAN KEUK (1940–2003) and SINGER first applied Kalman filtering techniques to single air target tracking problems in multiple radar data processing [19, 20]. The foundations of multiple hypothesis tracking methods for dealing with data of uncertain origin related to multiple objects were

laid by ROBERT W. SITTLER, who first posed the problem [21], while DONALD B. REID published a method for solving it [22]. VAN KEUK, SAM S. BLACKMAN, and YAAKOV BAR-SHALOM were among the first, who transformed Reid's method into practical algorithms (see [23, 24] for an overview of the development until 2004).

In the vast research literature published since then, however, it is impossible to identify all important scientists and engineers. The following discussion of significant contributions is therefore by no means complete, reflects the author's personal point of view, and is related to methodological framework presented in Part 1 of this book.

In particular due to their monographs on target tracking and sensor data fusion issues, YAAKOV BAR-SHALOM [25], SAM S. BLACKMAN [26], and ALFONSO FARINA [27] are highly influential researchers and have inspired many developments. HENK A. P. BLOM introduced stochastic hybrid processes into data fusion [28], which under the name of "Interacting Multiple Models" still define the state-of-the-art in target dynamics modeling. He in particular applied Bayesian data fusion to large air traffic control systems under severe reliability constraints. Countless realization aspects in fusion systems design are covered by OLIVER DRUMMOND's contributions. Already in his PhD thesis [29], where he has addressed many important issues in multiple object tracking at a very early time. LARRY STONE is a pioneer in Bayesian sonar tracking and data fusion in complex propagation environments [30]. NEIL GORDON was among the first, who applied sequential random Monte-Carlo-techniques to non-linear tracking problems, known under the name of "Particle Filtering", and inspired a rapid development in this area [31]. Numerous contributions to problems at the borderline between advanced signal processing, distributed detection theory, and target tracking were made by PETER K. WILLETT. XIAO-RONG LI provided important solutions to radar data fusion. The integration of modern mathematical non-linear filtering to practical radar implementation is among the merits of FRED DAUM. Numerous achievements in non-linear filtering, distributed sensing, and resources management were provided by UWE D. HANEBECK. HUGH FRANCIS DURRANT-WHYTE is generally credited with creating decentralized data fusion algorithms as well as with simultaneous localization and navigation. The stormy development of efficient multitarget tracking based on random set theory with Probabilistic Hypothesis Density Filtering (PHD) as an efficient realization has been developed by RONALD MAHLER [32]. Finally, ROY STREIT first introduced Expectation Maximization techniques to solve efficiently the various data association problems in target tracking and sensor data fusion and exploited the use of Poisson-point processes in this area [33].

A well readable introduction to sensor data fusion was published by H. B. MITCHELL [34]. The handbook "Advanced Signal Processing: Theory and Implementation for Sonar, Radar, and Non-Invasive Medical Diagnostic Systems" [35] deals with many advanced sensor data fusion applications. MARTIN E. LIGGINS, JAMES LLINAS, AND DAVID L. HALL edited the compendium "Handbook of Multisensor Data Fusion: Theory and Practice" [1]. An excellent introduction to more advanced techniques with emphasis on particle filtering is provided by FREDRIK GUSTAFSSON [36].

1.2.2 Organization of the Research Community

The interdisciplinary significance of sensor data fusion is illustrated by the fact that numerous institutions with different profiles are working world-wide on particular aspects of it. For this reason, the “International Society of Information Fusion (ISIF)” was founded in 1998 as a scientific framework organization. According to its constitution, it is “an independent, non-profit organization dedicated to advancing the knowledge, theory and applications of information fusion” [37]. Since that year, ISIF has been organizing the annual *International Conferences on Information Fusion*, the main scientific conference of the international scientific information fusion community.

1.2.3 Important Publication Platforms

To publish high-quality scientific papers on sensor data and information fusion, several well-established scientific journals are available, such as the *IEEE Transactions on Aerospace and Electronic Systems* and *on Signal Processing*, the most visible publication platforms, the *ISAF Journal of Advances in Information Fusion*, or the *Elsevier Journal on Information Fusion*. Besides the proceedings of the FUSION conferences, the annual SPIE Conference Series *Signal and Data Fusion of Small Targets (SPIE SMT)* organized by OLIVER E. DRUMMOND since 1989 in the USA, numerous special sessions at radar and automated control conferences as well as several national fusion workshops, such as the German IEEE ISIF Workshop Series *Sensor Data Fusion: Trends, Solutions, Applications (SDF)* [41], provide forums, where the latest advances and research results are presented and discussed among researchers and application engineers.

1.3 From Imperfect Data to Situation Pictures

Sensor data fusion typically provides answers to questions related to objects of interest such as: Do objects exist at all and how many of them are moving in the sensors’ fields of view? Where are they located at what time? Where will they be in the future with what probability? How can their overall behavior be characterized? Are anomalies or hints to their possible intentions recognizable? What can be inferred about the classes the objects belong to or even their identities? Are there clues for characteristic interrelations between individual objects? In which regions do they have their origin? What can be said about their possible destinations? Are there observable over-all object flows? Where are sources or sinks of traffic? and many other questions.

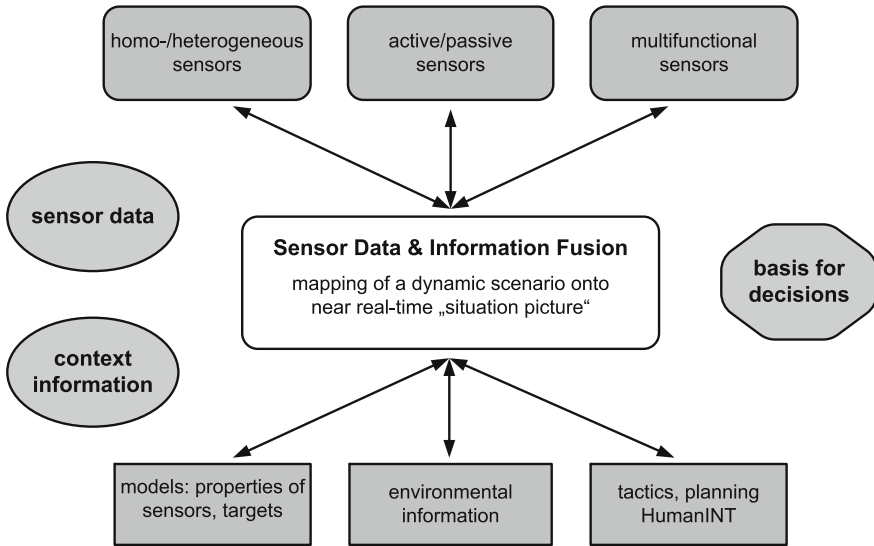


Fig. 1.3 Sensor data and information fusion for situation pictures: overview of characteristic aspects and their mutual interrelation

The answers to those questions are the constitutive elements, from which near real-time situation pictures can be produced that electronically represent a complex and dynamically evolving overall scenario in the air, on the ground, at sea, under water, as well as in out- or in-door urban environments, and even more abstract spaces. According to the previous discussion, these “situation elements” must be gained from the currently received sensor data streams while taking into account all the available context knowledge and pre-history. Since situation pictures are fundamental to any type of computer-aided decision support, the requirements of a given application define which particular information sources are to be fused.

The sensor data to be fused are usually inaccurate, incomplete, or ambiguous. Closely spaced moving objects are often totally or partially irresolvable. The measured object parameters may be false or corrupted by hostile measures. The context information is in many cases hard to formalize and even contradictory in certain aspects. These deficiencies of the information to be fused are unavoidable in any real-world application. Therefore, the extraction of ‘information elements’ for situation pictures is by no means trivial and requires a sophisticated mathematical methodology for dealing with imperfect information. Besides a precise requirement analysis, this is one of the major scientific features that characterizes and shapes sensor data fusion as branch of applied science.

1.3.1 Discussion of Characteristic Aspects

Figure 1.3 provides an overview of different aspects within this context and their mutual interrelation, which should be emphasized:

1. The underlying sensor systems can be located in different ways (collocated, distributed, mobile) producing measurements of the same or of different type. A multisensor system potentially increases the coverage or data rate of the total system and may help to resolve ambiguities.
2. Even by fusing homogeneous sensors, information can be obtained that is unaccessible to each sensor individually, such as in stereoscopic vision, where range information is provided by fusing two camera images taken from different viewpoints.
3. Fusion of heterogeneous sensor data is of particular importance, such as the combination of kinematic measurements with measured attributes providing information on the classes to which objects belongs to. Examples for measured attributes are Signal Intelligence (SIGINT), Jet Engine Modulation (JEM), radial or lateral object extension, chemical signatures, etc.
4. Especially for defense and security applications, the distinction between active and passive sensing is important as passive sensors enable covert surveillance, which does not reveal itself by actively emitting radiation.
5. Multi-functional sensor systems, such as phased-array radar, offer additional operational modes, thus requiring more intelligent strategies of sensor management that provide feedback to the process of information acquisition via appropriate control or correction commands. By this, the surveillance objectives can often be reached much more efficiently.
6. Context information is given, for example, by available knowledge on sensor and object properties, which is often quantitatively described by statistical models. Context knowledge is also given by environmental information on roads or topographical occlusions and provided by Geographical Information Systems (GIS). Seen from a different perspective, context information, such as road-maps, can also be extracted from real-time sensor data directly.
7. Relevant context knowledge (e.g. doctrines, planning data, tactics) and human observer reports (HUMINT: Human Intelligence) is also important information in the fusion process. The exploitation of context information of this kind can significantly improve the fusion system performance.

1.3.2 Remarks on the Methods Used

Situation elements for producing timely situation pictures are provided by integratively and spatio-temporally processing various pieces of information that in themselves often may have only limited value for understanding the situation. Essentially, logical cross-references, inherent complementarity, and redundancy are exploited.

More concretely speaking, the methods used are characterized by a stochastic approach (estimating relevant state quantities) and a more heuristically defined knowledge-based approach (modeling actual human behavior when exploiting information).

Among the data exploitation products of data fusion systems, object ‘tracks’ are of particular importance. Tracking faces an omnipresent aspect in every real-world application insofar as it is dealing with fusion of data produced at *different instants of time*; i.e. tracking is important in all applications where particular emphasis is placed on the fact that the sensor data to be exploited have the character of a time series.

Tracks thus represent currently available knowledge on relevant, time-varying quantities characterizing the instantaneous “state” of individual targets or target groups of interest, such as aircraft, ships, submarines, vehicles, or moving persons. Quantitative measures that reliably describe the quality of this knowledge are an integral part of a track. The information obtained by ‘tracking’ algorithms [25, 26, 42] also includes the history of the targets. If possible, a one-to-one association between the target trajectories in the sensors’ field of view and the produced tracks is to be established and has to be preserved as long as possible (track continuity). The achievable track quality does not only depend on the performance of the sensors used, but also on target properties and the operational conditions within the scenario to be observed. If tracks ‘match’ with the underlying real situation within the bounds defined by inherent quality measures being part of them, we speak of ‘track consistency.’”

Tracking algorithms, including Bayesian multiple hypothesis trackers as particularly well-understood examples, are iterative updating schemes for conditional probability density functions representing all available knowledge on the kinematic state of the objects to be tracked at discrete instants of time t_l . The probability densities are conditioned on both, the sensor data accumulated up to some time t_k , typically the current data acquisition time, as well as on available context information, such as on sensor characteristics, the object dynamics, the environment, topographical maps, or on certain rules governing the object behavior. Depending on the time instant t_l at which estimates for the state \mathbf{x}_l are required, the related estimation process is referred to as prediction ($t_l > t_k$), filtering ($t_l = t_k$), or retrodiction ($t_l < t_k$) [43, 44].

1.3.3 A Generic Sensor Data Fusion System

Figure 1.4 shows a generic scheme of functional building blocks within a multiple sensor tracking and data fusion system along with its relation to the underlying sensors. In the case of multi-functional sensors, there is feedback from the tracking system to the process of sensor data acquisition (sensor management). The following aspects should be emphasized:

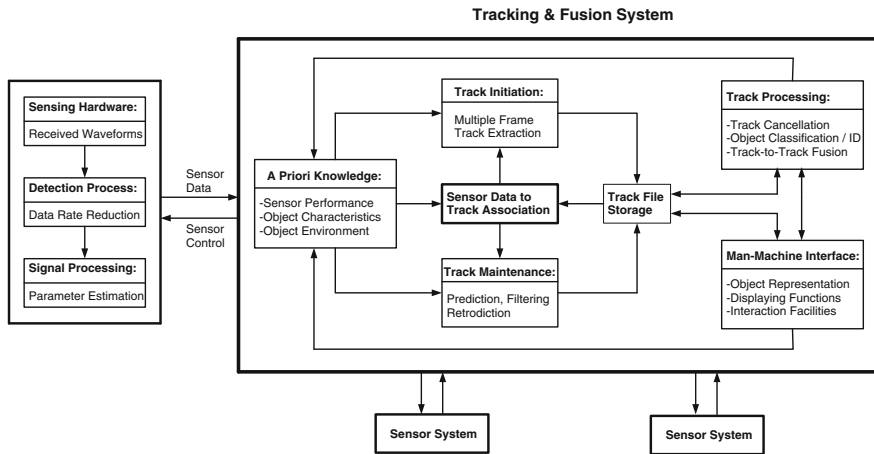


Fig. 1.4 Generic scheme of functional building blocks within a tracking/fusion system along with its relation to the sensors (centralized configuration, type IV according to O. Drummond)

Sensor Systems

After passing a detection process, essentially working as a means of data rate reduction, the signal processing provides estimates of parameters characterizing the waveforms received at the sensors’ front ends (e.g. radar antennas). From these estimates sensor reports are created, i.e. measured quantities possibly related to objects of interest, which are the input for the tracking and sensor data fusion system. By using multiple sensors instead of one single sensor, among other benefits, the reliability and robustness of the entire system is usually increased, since malfunctions are recognized easier and earlier and often can be compensated without risking a total system breakdown.

Interoperability

A prerequisite of all further processing steps, which at first sight seems to be trivial, is technical interoperability. It guarantees that all relevant sensor data are transmitted properly, in a timely way, and completely including all necessary meta-data describing the sensor performance, the platform parameters, and environmental characteristics. This type of meta-data is necessary to transform the sensor data into common frames of reference, to identify identical pieces of data, and to merge similar pieces of data into one single augmented piece of information. The process of combining data from different sources and providing the user with a unified view of these data is sometimes also referred to as data integration. Often interoperability acts as a bottleneck in designing real-world data fusion systems of systems [4, Chap. 20].

Fusion Process

All sensor data that can be associated to existing tracks are used for track maintenance (using, e.g., prediction, filtering, and retrodiction). The remaining data are processed for initiating new tentative tracks (multiple frame track extraction). Association techniques thus play a key role in tracking/fusion applications. Context information in terms of statistical models (sensor performance, object characteristics, object environment) is a prerequisite for track maintenance and initiation. Track confirmation/termination, classification/identification, and fusion of tracks related to the same objects or object groups are part of the track management functionalities.

Human–Machine Interface

The scheme is completed by a human–machine interface with display and interaction functions. Context information can be updated or modified by direct human interaction or by the track processor itself, for example as a consequence of object classification or road-map extraction. For an introduction to the vast literature on the related problems in human factors engineering and on practical systems solutions see Ref. [5].

1.3.4 On Measuring Fusion Performance

In sensor data fusion, the underlying ‘real’ situation is typically unknown. Only in expensive and time-consuming experiments certain aspects of a dynamically evolving situation are monitored, sometimes even with questionable accuracy. For this reason, experiments are valuable for demonstrating the “proof of concept” as well as to understand the underlying physical phenomena and operational problems, for example. They are of limited use, however, in performance evaluation and prediction. This underlines the role of comprehensive Monte-Carlo-simulations in fusion system performance evaluation.

According to the previous discussion, sensor data fusion systems try to establish one-to-one relations between objects in the sensors’ fields of view and identified object tracks in the situation picture. Strictly speaking, this is only possible under ideal conditions regarding the sensor performance and the underlying target scenario. It seems thus reasonable to measure the performance of a given tracking/fusion system by its characteristic deficiencies when compared to this ideal goal. In general, two categories of deficiencies can be distinguished that are either caused by mismatch regarding the input data or by non-optimal processing and unfavorable application constraints.

Selected Performance Measures

Selected performance measures or ‘measures of deficiency’ in the sense of the previous discussion, which have practical relevance in fusion systems design should be emphasized in the following.

1. Usually a time delay is involved until a track has been extracted from the sensor data. A corresponding performance measure is thus given by the ‘extraction delay’ between the first detection of a target by a sensor and a confirmed track.
2. False tracks, i.e. tracks related to unreal or unwanted targets, are unavoidable in the case of a high density of false or unwanted data (e.g. by clutter, jamming/deception). Corresponding ‘deficiencies’ are: mean number of falsely extracted targets per time and mean life time of a false track before its deletion.
3. Targets should be represented by one and the same track until leaving the field of view. Related performance measures are: mean life time of true target tracks, probability of an ‘identity switch’, and probability of a target not being represented by a track.
4. The track inaccuracy (given by the error covariance matrix of a state estimate, e.g.) should be as small as possible. Furthermore, the deviations between the estimated and actual target characteristics should correspond with the error covariance matrices produced (consistency). If this is not the case, ‘track loss’ usually occurs.

In a given application it is by no means simple to achieve a reasonable compromise between the various, competing performance measures and the user requirements. Optimization with respect to one measure may easily degrade other performance measures, finally deteriorating the entire system performance. This is especially true under more challenging conditions.

1.3.5 Tracking-Derived Situation Elements

The primary objective of multiple sensor target tracking is to explore the underlying target kinematics such as position, velocity, or acceleration. In other words, standard target tracking applications gain information related to ‘Level 1 Fusion’ according to the well-established terminology of the JDL model of information fusion (see e.g. [1, Chap. 2] and the literature cited therein). Kinematic data of this type, however, are by no means the only information to be derived from target tracks. In many cases, reliable and quantitative higher level information according to the JDL terminology can be obtained. To be more concrete, wide-area air and ground surveillance is considered here as an important real-world example serving as a paradigm for other challenging tracking and fusion applications.

Inferences based on Retrodicted Tracks

The first type of higher JDL level information to be inferred from tracking data is based on a closer analysis of the histories of the kinematic object states provided by retrodiction techniques. The statements derived typically refer to object characteristics that are either time invariant or change with time on a much larger scale than kinematics quantities usually tend to do. This is the main reason why the gain in accuracy achievable by retrodiction techniques can be exploited.

- *Velocity History.* The analysis of precisely retrodicted velocity histories enables the distinction of objects belonging to different classes such as moving persons, boats, vehicles, vessels, helicopters, or jet aircraft. If the object speed estimated with sufficiently high accuracy has exceeded a certain threshold, certain object classes can be reliably be excluded. As an example, uncertainty whether an object is a helicopter or a wing aircraft can be resolved if in the track history a velocity vector 'Zero' exists. Depending on the context of the underlying application, classifications of this type can be essential to generate an alert report.
- *Acceleration History.* Similar considerations are valid if acceleration histories are taken into account. High normal accelerations, e.g., are a clear indication of a fighter aircraft. Moreover, one can safely conclude that a fighter aircraft observed with a normal acceleration > 6 g, for example, is not carrying a certain type of weaponry (any more). In other words, conclusions on the threat level connected with the objects observed can be drawn by analyzing kinematic tracks.
- *Heading, Aspect Angle.* Precise reconstructions of the targets' heading vectors are not only important input information for threat evaluation and weapon assignment in themselves, but also enable estimates of the aspect angle of an object at a given instant of time with respect to other sensors, such as those producing high range or Doppler resolution spectra. Track-derived information of this type is basic for fusing spectra distributed in time and can greatly improve object classification thus providing higher-JDL-level information.
- *Rare Event Detection.* Analysis of JDL-level-1 tracks can be the key to detecting rare or anomalous events by fusing kinematic tracks with other context information such as annotated digital road-maps and general rules of behavior. A simple example in the area of continuous-time, wide-area ground surveillance can be the production of an alert message if a large freight vehicle is observed at an unusual time on a dirt road in a forest region. There are analogous examples in the maritime or air domain.

Inferences based on Multiple Target Tracking

A second type of higher JDL level information related to mutual object interrelations can be inferred from JDL level 1 tracking data if emphasis is placed on the results of *multiple target tracking*.

- *Common History*. Multiple target tracking methods can identify whether a set of targets belongs to the same collectively moving group, such as an aircraft formation or a vehicle convoy, whose spatial extension may be estimated and tracked. If an aircraft formation has split off after a phase of penetration, e.g., the interrelation between the individual objects is to be preserved and provides valuable higher-JDL-level information that is important, e.g., when a former group target is classified as ‘hostile’ since this implies that all other targets originally belonging to the same group are likely to be hostile as well.
- *Object Sources and Sinks*. The analysis of large amounts of target tracks furthermore enables the recognition of sources and sinks of moving targets. By this type of reasoning, certain areas can be identified as air fields, for example, or an area of concentration of military forces. In combination with available context information, the analysis of multiple object tracks can also be used for target classification by origin or destination. A classification as hostile or suspect directly leads to an alert report.
- *Split-off Events*. By exploiting multiple target tracking techniques, certain split-off events can be identified as launches of air-to-air or air-to-surface missiles. The recognition of such an event from JDL-level-1 tracking information not only has implications on classifying the original target as a fighter aircraft, but can also establish a certain type of ‘book-keeping’, such as counting the number of missile launches. This enables estimates of the residual combat strength of the object, which has direct implications on countermeasures, e.g.
- *Stopping Events*. In the case of MTI radar (Moving Target Indicator), Doppler blindness can be used to detect the event ‘A target under track has stopped’, provided this phenomenon is described by appropriate sensor models. If there is previous evidence for a missile launcher, e.g., missing data due to Doppler blindness may indicate preparation for launch with implications on potential countermeasures. In combination with other tracks, a stopping event may also establish new object interrelations, for example, when a target is waiting for another and then moving with it.

1.3.6 Selected Issues in Anomaly Detection

Anomaly detection can be regarded as a process of information fusion that combines incomplete and imperfect pieces of mutually complementary sensor data and context information in such a way that the attention of human decision makers or decision making systems is focused on particular events that are “irregular” or may cause harm and thus require special actions, such as exploiting more specialized sensors or initiating appropriate activities by military or security personnel [45]. Fusion-based anomaly detection thus improves situational awareness. What is actually meant by “regular” or “irregular” events is higher-level information itself that depends on the context of the underlying application. Here, it is either assumed to be a priori known or to be learned from statistical long-time analysis of typical situations.

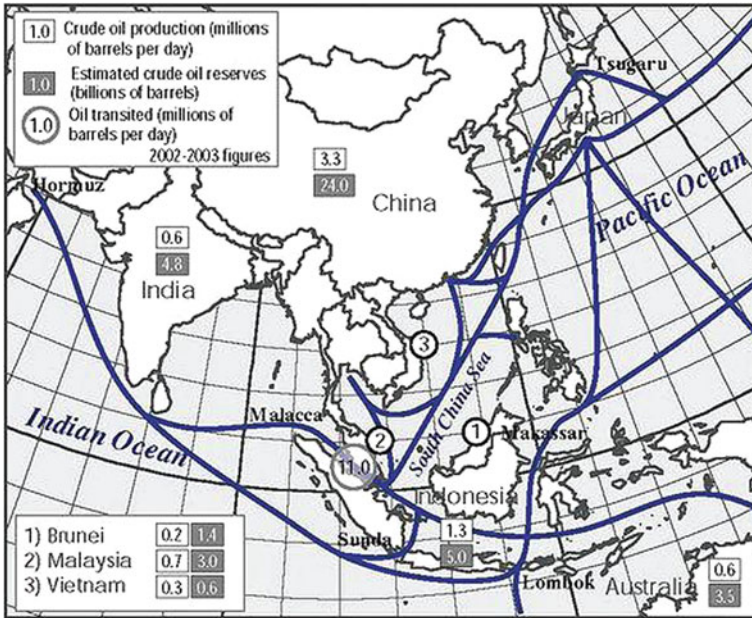


Fig. 1.5 Illustration of sea lanes and strategic passages in Pacific Asia

In complex surveillance applications, we can often take advantage of context information on the sensing environment insofar as it is the stationary or slowly changing “stage” where a dynamic scenario evolves. Typical examples of such environmental information are digital road or sea-/air-lane maps and related information, which can essentially be regarded as spatial motion constraints (see Fig. 1.5 as an illustration). In principle, this information is available by Geographical Information Systems (GIS). Another category of context information is provided by visibility models and littoral or weather maps indicating regions, where a high clutter background is to be taken into account, for example. Moreover, rather detailed planning information is often available. This category of information is not only important in mission planning or in the deployment and management of sensor systems, but can be used to decide whether an object is moving on a lane or leaving it, for example. In addition, ground-, sea- or air-lane information can be used to improve the track accuracy of lane-moving vehicles and enhance track continuity. See Sect. 9.1 for a more detailed discussion.

Integration of Planning Information

In certain applications, rather detailed planning information is available, which provides valuable context knowledge on the temporal evolution of the objects involved

and can in principle be incorporated into the tracking formalism. Planning information is often approximately described by space–time waypoints that have to be passed by the individual objects during a preplanned operation, i.e. by a set of position vectors to be reached at given instants of time and possibly via particular routes (roads, lanes) between the waypoints. In addition, we assume that the acceptable tolerances related to the arrival of the objects at the waypoints are characterized by known error covariance matrices, possibly individually chosen for each waypoint and object, and that the association between the waypoints and the objects is predefined.

The impact of waypoints on the trajectory to be estimated from future sensor data (under the assumption that the plan is actually kept) can simply be obtained by processing the waypoints as additional artificial ‘measurements’ via the standard Bayesian tracking paradigm, where the tolerance covariance matrices are taken into account as the corresponding ‘measurement error covariances’. If this is done, the processing of sensor measurements with a younger time stamp are to be treated as “out-of sequence” measurements with respect to the artificial waypoint measurements processed earlier. For dealing with out-of-sequence measurements see Sect. 5.1. According to these considerations, planning information can well improve both track accuracy and continuity as well as facilitate the sensor-data-to-track association problems involved, provided the plan is actually kept.

Detecting Regularity Pattern Violation

A practically important class of anomalies results from a violation of regularity patterns such as those previously discussed (motion on ground-, sea-, or air-lanes or following preplanned waypoints and routes). An anomaly detector thus has to decide between two alternatives:

- The observed objects obey an underlying pattern.
- The pattern is not obeyed (e.g. off-lane, unplanned).

Decisions of this type are characterized by decision errors of first and second kind. In most cases, it is desirable to make the decisions between both alternatives for given decision errors to be accepted. A “sequential likelihood ratio” test fulfills this requirement and has enormous practical importance. For a more detailed discussion see Chap. 9.2. As soon as the test decided that the pattern is obeyed, the calculation of the likelihood ratio can be restarted since it is more or less a by-product of track maintenance. The output of subsequent sequential ratio tests can serve to re-confirm “normality” or to detect a violation of the pattern at last. The most important theoretical result on sequential likelihood ratio tests is the fact that the test has a *minimum decision length on average* given predefined statistical decision errors of first and second kind.

Tracking-derived Regularity Patterns

We have discussed moving targets that obey certain space–time constraints that are a priori known (roads/lanes, planned waypoints). A violation of these constraints was quite naturally interpreted as an anomaly. Seen from a different perspective, however, moving targets that are assumed to obey a priori *unknown* space–time constraints and to be observed by wide-area sensors, such as vehicles on an unknown road network, produce large data streams that can also be used for extracting the underlying space–time constraint, e.g. a road-map. After a suitable post-processing, the produced tracks of motion-constrained targets simply define the corresponding constraints and can thus be extracted from tracking-based results. See Sect. 9.2 for a more detailed discussion. Extracted road-maps can be highly up-to-date and precise. A discussion where such ideas are used in wide-area maritime surveillance using AIS data can be found in [46] (AIS: Automatic Identification System).

1.4 Future Perspectives of Sensor Data Fusion

Due to the increasing availability of inexpensive, but powerful sensor, communication, and information technology, its technical prerequisites, sensor data fusion, or more general, information fusion, increasingly emancipates from its roots in defense related applications. A commonplace example of this trend is the advent of navigation systems, which have developed a mass market by fusing military global navigation satellite system data with digital road-maps in combination with an appealing graphical interface. We can therefore expect that information fusion will become a key technology driver for developing numerous innovative products penetrating everyone’s daily life and changing it profoundly. In this context, many new research questions are expected to emerge that will foster the further evolution of information fusion as an also economically eminent branch of applied informatics.

1.4.1 New Everyday Life Applications

Even now, intelligent filtering, analysis, evaluation, and graphical presentation of multiple sensor information enable numerous products that make everyday life safer or more secure. For example, in intelligent car-driver assistance systems, image and video data from cameras and miniaturized automotive radar sensors are automatically fused in order to perceive road obstacles and pedestrians or to exclude “ghost objects.” At airport security checks, assistance systems can be used, which directly take advantage of military surveillance technology. By fusing signatures of stand-off chemical sensors and miniaturized gamma-spectrometers, for example, with person trajectories, carry-on items contaminated with hazardous materials or explosives can be detected. This may be a contribution to avert threats or avoid terrorist attacks.

Other areas where information fusion based assistance systems will increasingly be important are medical and health care, process control, logistics, industrial production, precision agriculture, and traffic monitoring. A particularly stormy evolution can currently be observed for assistance systems, where physical activities and the health status of elderly or handicapped human beings can be monitored, allowing them to live in their usual everyday environment much longer than now. In the vast fields of fire, disaster, and pollution control, quick exploitation and fusion of complex data streams can be essential for safety analysis and designing corresponding concepts as well as for developing sophisticated emergency information and management systems.

Since sensor data fusion has actually evolved into a mature technology in major fields and provides a coherent and powerful inventory of methodologies and algorithms already proven in ambitious applications, the further realization of its inherent application potential is much alleviated by the very fact that research and development for new products can be done on a sound technology base that does not need to be created in a time-consuming and expensive way. For this reason, the expected development cycles for innovative products are short, while the development risks involved are calculable. Due to its traditional strengths in high-tech industries, such as system technology or software engineering, sensor or RFID technology, highly industrialized and research-intensive countries like Germany can use their potential especially in those branches where they are traditionally well-positioned—for example in automotive technology, automation and aerospace industries, in security, safety and medical technology, and last but not least, in information system technology in general.

1.4.2 Discussion of Large-Scale Trends

More generally speaking, information fusion technology already provides mature results with profitable market opportunities, especially in those areas where physical or technical sensor data are to be fused with quantitative context information on the basis of well-understood mathematical algorithms, often making use of Bayesian reasoning.

Human Assistance Systems

Typically “human” fusion processes, however, characterized by associative reasoning, negotiating of reasonable compromises, or extrapolating incomplete information creatively and in an intuitive way, seem to be still unfit for automation, perhaps fundamentally unfit. Nevertheless, technical data fusion systems can offer assistance functionalities also here, by which specifically human competencies of judgment are freed from routine or mass tasks, quite in the sense of a “cognitive tool” as discussed earlier. Moreover, highly promising research areas are and will increasingly be those

that aim at modeling and formalizing this specific human expert knowledge and expertise of situation assessment and incorporate it into the process of automated multiple sensor data.

Context Data Integration

Furthermore, a large-scale technology tend to be highlighted is given by the large potential of quantitative non-sensor information available in comprehensive databases, such as Geographical Information Systems (GIS), which is still waiting to be integrated into multiple sensor data fusion systems. This is especially true in the vast area of ground, air, sea, and underwater robotics, but has also strong implications in guaranteeing high levels of air transportation security, even in the case of high traffic densities, and in advanced logistics support systems, such as container monitoring and tracking, topics with direct implications for global economy.

Network-centric Operations

A predominant trend in defence applications is given by the demand of supporting “Network-centric Operations”, which will still be in effect for the next decade. Sensor data and information fusion technology is one of the major forces shaping this process of transformation from more standard operational doctrines. Especially for out-of-area operations and operations in an urban terrain, as well as for dealing with “asymmetric” opponents, distributed high-performance reconnaissance is inevitable. In particular, wide-area ground, sea, and underwater surveillance, belong to this field, specially by making use of unmanned reconnaissance robots (unmanned ground, aerial, or underwater vehicles). Moreover, intelligent security systems for harbors, critical infrastructure, or camp protection are likely to raise many research intensive data fusion problem.

Pervasive Passive Surveillance

A particularly exciting topic of recent research is advanced distributed signal and data fusion for passive radar systems, where radio, TV, or mobile phone base stations are used as sources for illuminating targets of interest. Even in remote regions of the world, each transmitter of electromagnetic radiation becomes a potential radar transmitter station, which enables air surveillance by passively receiving reflections of non-cooperatively emitted signals of opportunity. In this way, the reconnaissance process remains covert and is not revealed by actively transmitting radiation. Analogous considerations are valid for sub-sea surveillance.

Fusion-driven Communications

The communications sub-systems within a large sensor network are typically characterized by many internal degrees of freedom, which can be controlled and adapted. This opens the vast area of fusion-driven communications, where communications and the distributed data fusion system architectures are closely tied and optimized with respect to the particular surveillance goals to be reached [48]. In the focus are multi-component system consisting of sensors, data bases, and communication infrastructures that collectively behave as a single dynamically adaptive system. Important aspects are network scalability given a limited communication bandwidth, adaptive and optimal spectrum sharing protocols, sensor data against network objectives, and in-network information. In addition, the growing use and ubiquitous nature of sensor networks pose issues when networks deployed for multiple applications need to be combined or need to exchange information at the network level.

'Add-on' Research Efforts

Since a stormy evolution of civilian information fusion applications is to be expected in the near future, defence-related research and development on information fusion technology will increasingly show the character of “add-on” research, which adapts existing civilian problem solutions to specifically military requirements. This trend is analogous to the evolution in advanced communication systems, a technology that also had its roots in the military domain, before the civilian market opportunities became the predominant force driving its technological and scientific progress.

References

1. M.E. Liggins, D.L. Hall, J. Llinas (eds.), *Handbook of Multisensor Data Fusion—Theory and Practice*, 2nd edn. (CRC Press, Boca Raton, 2008)
2. E. Bosse, J. Roy, S. Wark, *Concepts, Models, and Tool for Information Fusion* (Artech House, Norwood, 2007)
3. B.V. Dasarathy (ed.), A special Issue on information fusion in computer security, in *Information Fusion*, vol 10, No. 4 (Elsevier, New York, 2009)
4. M. Wunder, J. Grosche (eds.), *Verteilte Führungsinformationssysteme* (Springer, New York, 2009)
5. L. Schmidt, C.M. Schlick, J. Grosche (eds.), *Ergonomie und Mensch-Maschine-Systeme* (Springer, Berlin, 2008)
6. D.S. Alberts, R.E. Hayes, *Code of Best Practice for Experimentation* (CCRP Publication series, Washington, DC, 2002)
7. H.L.V. Trees, K.L. Bell (eds.), *Bayesian Bounds for Parameter Estimation and Nonlinear Filtering/Tracking* (Wiley-IEEE Press, New York, 2007)
8. H.W. Sorenson, Least-squares estimation: from Gauss to Kalman. *IEEE Spectr.* **7**, 63–68 (1970)
9. K.-R. Biermann (ed.), *Carl Friedrich Gauß in Briefen und Gesprächen* (C. H. Beck, München, 1990)

10. E.T. Jaynes, *Probability Theory: The Logic of Science* (Cambridge University Press, Cambridge, 2003)
11. T. Bayes, An essay towards solving a problem in the doctrine of chances. *Philos. Trans. Roy. Soc. London* **53**, 370418 (1763) (Reprinted in *Biometrika*, **45**, 1958. <http://www.stat.ucla.edu/history/essay.pdf>)
12. N.L. Rabinovitch, *Probability and Statistical Inference in Ancient and Medieval Jewish Literature* (University of Toronto Press, Toronto, 1973)
13. S.M. Stigler, *The History of Statistics* (Harvard University press, Cambridge, 1986)
14. J. Wolfowitz, Abraham Wald, 1902–1950. *Ann. Math. Stat.* **23**(1), 1–13 (1952)
15. A. Wald, *Statistical Decision Functions* (Wiley, New York, 1950)
16. S.L. Lauritzen, *Thiele—Pioneer in Statistics* (Oxford University Press, Oxford, 2002)
17. E. Brookner, *Tracking and Kalman Filtering Made Easy* (Wiley, Sudbury, 1998)
18. A. Gelb (ed.), *Applied Optimal Estimation* (M.I.T Press, Cambridge, 1974)
19. G. van Keuk, Description of a tracking strategy for phased array radar, in *Proceedings of Advanced Radar Systems, NATO AGARD Advisory Group for Aerospace Research and Development Conference*, No. 66, p. 36-1–36-10, Istanbul, Turkey, May 1970
20. R.A. Singer, Estimating optimal tracking filter performance for manned maneuvering targets. *IEEE Trans. Aerosp. Electron. Syst.* **TAES 5**, 473–483 (1970)
21. R.W. Sittler, An optimal data association problem in surveillance theory. *IEEE Trans. Mil. Electron.* **MIL-8**, 2 (1964)
22. D.B. Reid, An algorithm for tracking multiple targets. *IEEE Trans. Autom. Control* **AC-24**, 6 (1979)
23. G. van Keuk, PDAB—Ein Verfahren zur Einzelzielverfolgung in stark gestörter Umgebung. FFF Research Report 363, Wachtberg (1987)
24. S.S. Blackman, Multiple hypothesis methods. *IEEE AES Mag.* **19**(1), 41–52 (2004)
25. Y. Bar-Shalom, P.K. Willett, X. Tian, *Tracking and Data Fusion. A Handbook of Algorithms* (YBS Publishing, Storrs, 2011)
26. S.S. Blackman, R. Popoli, *Design and Analysis of Modern Tracking Systems* (Artech House, Norwood, 1999)
27. A. Farina, & F.A. Studer, *Radar Data Processing*, Vol. 1 Introduction and Tracking (Wiley, New York, 1985) (Vol. 2 Advanced Topics and Applications, 1986)
28. H.A.P. Blom, J. Jygeros (eds.), *Stochastic Hybrid Systems: Theory and Safety Critical Applications* (Springer, Berlin, 2006)
29. O.E. Drummond, Multiple-Object Tracking, PhD Thesis, University of California (1975)
30. L.D. Stone, T.L. Corwin, C.A. Barlow, *Bayesian Multiple Target Tracking* (Artech House, Norwood, 1999)
31. B. Ristic, S. Arulampalam, N. Gordon, *Beyond the Kalman Filter: Particle Filters for Tracking Applications* (Artech House Radar Library, Norwood, 2004)
32. R.P.S. Mahler, *Statistical Multisource-Multitarget Information Fusion* (Artech House, Norwood, 2007)
33. R.L. Streit, *Poisson Point Processes. Imaging, Tracking, and Sensing* (Springer, New York, 2010)
34. H.B. Mitchell, *Multi-Sensor Data Fusion* (Springer, Berlin, 2007)
35. S. Stergiopoulos (ed.), *Advanced Signal Processing: Theory and Implementation for Sonar, Radar, and Non-Invasive Medical Diagnostic Systems* (CRC Press, Boca Raton, 2001)
36. F. Gustafsson, *Statistical Sensor Fusion* (Gazelle, Lancaster, 2010)
37. <http://www.isif.org>
38. W.-D. Wirth, *Radar Techniques Using Array Antennas* (IEE Press, London, 2001)
39. G. van Keuk, S. Blackman, On phased-array tracking and parameter control. *IEEE Trans. Aerosp. Electron. Syst.* **AES-29**(1), 186 (1993)
40. R. Baltes, G. van Keuk, Tracking multiple maneuvering targets in a network of passive radars, in *Proceedings of the IEEE International Radar Conference, RADAR'95*, Washington DC (1995)

41. W. Koch (ed.), IEEE ISIF Sensor Data Fusion: Trends, Solutions, Applications. Annual Workshop published in IEEE Xplore. 2005: Bonn, 2006: Dresden, 2007: Bremen, 2009: Lübeck, 2010: Leipzig, 2011: Leipzig, since 2012: Bonn
42. W. Koch, Target tracking, Chap. 8, in *Advanced Signal Processing: Theory and Implementation for Sonar, Radar, and Non-Invasive Medical Diagnostic Systems*, ed. by S. Stergiopoulos (CRC Press, Boca Raton, 2001)
43. O.E. Drummond, Target tracking with retrodicted discrete probabilities. Proc. of SPIE Sig. Data Process Small Targets **3163**, 249 (1997)
44. W. Koch, Fixed-interval retrodiction approach to Bayesian IMM-MHT for maneuvering multiple targets. IEEE Trans. Aerosp. Electron. Syst. **AES-36**(1), 2–14 (2000)
45. W. Koch, J. Biermann, Anomaly detection from tracking-derived situation elements, in *Proceedings of the NATO Workshop on Data Fusion and Anomaly Detection for Maritime Situational Awareness—MSA 2009*, La Spezia, Italy, September 2009
46. B. Ristic, B. La Scala, M. Morelande, & N. Gordon, Statistical analysis of motion patterns in AIS data: Anomaly detection and motion prediction, in Proceedings of the 11th International Conference on Information Fusion, FUSION 2008, Cologne, July 2008
47. D. Fox, Activity recognition from wearable sensors. Keynote Lecture at 11th International Conference on Information Fusion, Cologne (2008)
48. S.C. Mukhopadhyay, H. Leung, P.K. Varshney, & R. Schober (eds.), Guest editorial special issue. IEEE Sens. J. Spec. Issue Cogn. Sens. Netw. **11**(3), 519–521 (2010)

Part I
Sensor Data Fusion: Methodological
Framework

Chapter 2

Characterizing Objects and Sensors

In most cases, not all properties characterizing observed objects in a certain application have the same importance for producing a situation picture or can be inferred by the sensor systems involved. At the very beginning, we have to identify suitable object properties relevant to the underlying requirements, which are called *state quantities*. In the context discussed here, state quantities are completely described by numbers or appropriate collections of numbers and may be time-dependent. All relevant properties characterizing an object of interest at a certain instant of time t_k , $k \in \mathbb{N}$, are gathered in a collection X_k of state quantities, which is called *object state* at time t_k . Object states can also be composed of the individual object states of an object group.

2.1 Examples of State Quantities

1. As a first example, consider a vehicle moving on a road approximately modeled by a curve. If the vehicle's position or speed on the road at a time t_k only has interest, the corresponding object state is composed by two real numbers: the arc-length x_k of a point on the curve, representing its position, and its temporal derivative \dot{x}_k , representing its speed. The corresponding object state is thus given by a two-dimensional vector: $X_k = \mathbf{x}_k$ with $\mathbf{x}_k = (x_k, \dot{x}_k)^\top \in \mathbb{R}^2$.
2. Another practically important example is the kinematic state X_k of an object moving in the three-dimensional space at a given instant of time t_k , which is typically given by its position \mathbf{r}_k , velocity $\dot{\mathbf{r}}_k$, and acceleration $\ddot{\mathbf{r}}_k$ at this time. X_k is thus represented by a 9-dimensional vector $X_k = \mathbf{x}_k$ with $\mathbf{x}_k = (\mathbf{r}_k^\top, \dot{\mathbf{r}}_k^\top, \ddot{\mathbf{r}}_k^\top)^\top \in \mathbb{R}^9$.
3. A natural generalization of this concept is the notion of the joint state of two or more objects of interest that form an object group. If kinematic object characteristics are of interest, the corresponding object state X_k is given by a possibly high-dimensional vector $X_k = \mathbf{x}_k$ with $\mathbf{x}_k = (\mathbf{x}_k^{1\top}, \mathbf{x}_k^{2\top}, \dots)^\top$.

4. The notion of object states, however, is broader and includes other characteristic state quantities. In certain applications, object attributes can be described by positive real numbers $x_k \in \mathbb{R}^+$, related to the object's backscattering properties, for example, such as its characteristic mean radar cross section. In this case, a relevant object state may be given by $X_k = (\mathbf{x}_k, x_k)$, where the individual state quantities \mathbf{x}_k (e.g. kinematics) and x_k (e.g. cross section) are taken from different sets of numbers.
5. Stationary or moving objects may belong to distinct classes. Let the object property "object belongs at time t_k to class i_k " be denoted by $i_k \in \mathbb{N}$. Moving objects, for example, can be classified according to the dynamics mode currently in effect, or according to certain characteristic features indicating, e.g., their chemical signatures. Examples of object classes relevant to air surveillance are: *bird, glider, helicopter, sporting airplane, passenger jet, fighter aircraft, missile*. In this case, a characteristic object state is given by $X_k = (\mathbf{x}_k, i_k)$.
6. For describing spatially extended objects or collectively moving object clusters, the kinematic state vector \mathbf{x}_k must be complemented by an additional state quantity characterizing their spatial extension. For the sake of simplicity and to deal with the extended object or cluster tracking problem as rigorously as possible, we confine the discussion to the practically important case of *ellipsoidal* object or cluster extensions. In this case, the current extension at time t_k can be described mathematically by a symmetric and positively definite matrix \mathbf{X}_k . According to this approach, the following object properties are covered:
 - *Size*: volume of the extension ellipsoid
 - *Shape*: ratio of the corresponding semi-axes
 - *Orientation*: direction of the semi-axes.

The corresponding object state is thus given by $X_k = (\mathbf{x}_k, \mathbf{X}_k)$.

Since object states must be inferred from incomplete and imperfect information sources, the collection of state quantities such as

$$X_k = (\mathbf{x}_k, x_k, \mathbf{X}_k, i_k) \quad (2.1)$$

or some of them are interpreted as *random variables*. The application of other, more general notions of uncertainty is possible (see [1], e.g.), but excluded here. According to the Bayesian interpretation of probability theory, all available knowledge on the objects of interest at time t_k is mathematically precisely represented by probability densities of their corresponding states $p(X_k)$. If only one state quantity is of interest, for example in \mathbf{x}_k , $p(\mathbf{x}_k)$ is given by a marginal density:

$$p(\mathbf{x}_k) = \sum_{i_k} \int dx_k d\mathbf{X}_k p(\mathbf{x}_k, x_k, \mathbf{X}_k, i_k). \quad (2.2)$$

Methods to calculate the probability density functions related to object states with at least approximate accuracy is the main goal in Bayesian sensor data fusion.

2.2 Object Evolution Models

Object states usually change in time. Their temporal evolution, however, is imperfectly known in most cases. This fundamental ignorance can often be described by a probability density function of the object state at time t_k , which is conditioned on the previous state X_{k-1} , called transition density $p(X_k|X_{k-1})$, i.e. . With an underlying Markov assumption, knowledge about future object states can be predicted from prior knowledge via the Chapman-Kolmogorov equation:

$$p(X_k) = \int dX_{k-1} p(X_k|X_{k-1}) p(X_{k-1}). \quad (2.3)$$

The temporal evolution described by $p(X_k|X_{k-1})$ mirrors the real object evolution insofar as it allows a Monte-Carlo-simulation of a subsequent state X_k by generating random realizations of it according to the density $p(X_k|X_{k-1})$. It is thus reasonable to call the conditional probability density $p(X_k|X_{k-1})$ the *evolution model* of an object. In the sequel, the notion of an evolution model is illustrated by examples. A wide variety of object evolution models for kinematic object states has been described in the handbook [2, Chap. 1.5] and a series of survey papers [3–7], which are adapted to the particular requirements of the underlying application.

2.2.1 Van-Keuk's Evolution Model

An early and particularly intuitive example of state evolution models in the context of tracking and sensor data fusion was proposed by Günther van Keuk in 1971 [8]. According to van Keuk, the motion of an object is described by a linear equation with additive white Gaussian noise:

$$\mathbf{x}_k = \mathbf{F}_{k|k-1}\mathbf{x}_{k-1} + \mathbf{G}_{k|k-1}\mathbf{v}_k, \quad (2.4)$$

referring to kinematic object states given by $\mathbf{x}_k = (\mathbf{r}_k^\top, \dot{\mathbf{r}}_k^\top, \ddot{\mathbf{r}}_k^\top)^\top$. The Gaussian random vector \mathbf{v}_k is described by a zero-mean, unit-covariance Gaussian probability density $p(\mathbf{u}_k) = \mathcal{N}(\mathbf{u}_k; \mathbf{0}, \mathbf{1})$. More generally, let a Gaussian be denoted by $\mathcal{N}(\mathbf{x}; \mathbb{E}[\mathbf{x}], \mathbb{C}[\mathbf{x}]) = |\mathbb{C}[\mathbf{x}]|^{-\frac{1}{2}} \exp\{-\frac{1}{2}(\mathbf{x} - \mathbb{E}[\mathbf{x}])^\top \mathbb{C}[\mathbf{x}]^{-1}(\mathbf{x} - \mathbb{E}[\mathbf{x}])\}$ with an expectation vector $\mathbb{E}[\mathbf{x}]$ and a symmetric, positively definite covariance matrix $\mathbb{C}[\mathbf{x}]$. The matrix $\mathbf{F}_{k|k-1}$ is called *evolution matrix*,

$$\mathbf{F}_{k|k-1} = \begin{pmatrix} \mathbf{1} & (t_k - t_{k-1}) \mathbf{1} & \frac{1}{2}(t_k - t_{k-1})^2 \mathbf{1} \\ \mathbf{0} & \mathbf{1} & (t_k - t_{k-1}) \mathbf{1} \\ \mathbf{0} & \mathbf{0} & e^{-(t_k - t_{k-1})/\theta_t} \mathbf{1} \end{pmatrix} \quad (2.5)$$

with a modeling parameter θ_t , while the matrix $\mathbf{G}_{k|k-1}$ is given by:

$$\mathbf{G}_{k|k-1} = q_t \sqrt{1 - e^{-2(t_k - t_{k-1})/\theta_t}} (\mathbf{O}, \mathbf{O}, \mathbf{1})^\top, \quad (2.6)$$

implying a second modeling parameter q_t . According to this evolution model, straightforward calculations show that the acceleration $\ddot{\mathbf{r}}_k$ is described by an ergodic, zero-mean Gauß-Markov process with an autocorrelation function given by:

$$\mathbb{E}[\ddot{\mathbf{r}}_k \ddot{\mathbf{r}}_l^\top] = q_t^2 \exp[-(t_k - t_l)/\theta_t] \mathbf{1}, \quad l \leq k. \quad (2.7)$$

This expression clearly defines the modeling parameters q_t (*acceleration bandwidth*) and θ_t (*maneuver correlation time*), which have characteristic values for different classes of maneuvering objects. The corresponding Gauß-Markov transition density is given by:

$$p(\mathbf{x}_k | \mathbf{x}_{k-1}) = \mathcal{N}(\mathbf{x}_k; \mathbf{F}_{k|k-1} \mathbf{x}_{k-1}, \mathbf{D}_{k|k-1}) \quad (2.8)$$

where $\mathbf{D}_{k|k-1} = \mathbf{G}_{k|k-1} \mathbf{G}_{k|k-1}^\top$ is called *evolution covariance matrix*.

2.2.2 Interacting Multiple Models

In practical applications, it might be uncertain which evolution model out of a set of r possible alternatives is currently in effect. In the case of air targets, for example, we can distinguish between different flight phases (no turn, slight maneuver, high-g, turn etc.). According to the previous discussion, the maneuvering class $1 \leq i_k \leq r$, to which an object belongs at time t_k , can be considered as a part of its state. In general, Markovian evolution models for object states $X_k = (\mathbf{x}_k, i_k)$ are expressed by:

$$p(x_k, i_k | x_{k-1}, i_{k-1}) = p(x_k | i_k, x_{k-1}, i_{k-1}) p(i_k | x_{k-1}, i_{k-1}). \quad (2.9)$$

A special case that implies additional assumptions is defined by:

$$p(x_k, i_k | x_{k-1}, i_{k-1}) = p(x_k | i_k, x_{k-1}) p(i_k | i_{k-1}) \quad (2.10)$$

$$= p_{i_k i_{k-1}} \mathcal{N}(\mathbf{x}_k; \mathbf{F}_{k|k-1}^{i_k} \mathbf{x}_{k-1}, \mathbf{D}_{k|k-1}^{i_k}) \quad (2.11)$$

and is called *IMM evolution model* (IMM: Interaction Multiple Models, see [7] and the literature cited therein) and has been introduced by HENK BLOM [9]. IMM models are characterized by r purely kinematic transition densities $p(\mathbf{x}_k | \mathbf{x}_{k-1}, i_k)$, for instance of the van Keuk type, and class transition probabilities $p_{i_k i_{k-1}} = p(i_k | i_{k-1})$ that must be specified and are part of the modeling assumptions. The transition probabilities $p_{i_k i_{k-1}}$ define a stochastic matrix. According to $\sum_{i_k=1}^r p(i_k | i_{k-1}) = 1$ the columns of such matrices must add up to one.

Note that Eq. 2.11 assumes that $p(x_k | x_{k-1}, i_k, i_{k-1})$ is independent of the past maneuvering class i_{k-1} and $p(i_k | \mathbf{x}_{k-1}, i_{k-1})$ does not depend on the object's kinematic state \mathbf{x}_{k-1} . While the first assumption seems to be quite natural, the second

may be an oversimplification in certain cases. As an example, let us consider two evolution models describing low and strong maneuvers, respectively. The probability $p(i_k = 1|i_k = 1, \mathbf{x}_{k-1})$ that an object stays in the low maneuver model increases as the object acceleration diminishes, while $p(i_k = 2|i_k = 2, \mathbf{x}_{k-1})$ increases as the acceleration increases. If q is a measure of the maximum acceleration, state-dependent transition matrices of the form

$$\begin{pmatrix} p_{11}e^{-\frac{1}{2}\frac{|\ddot{\mathbf{x}}_k|^2}{q^2}} & 1 - p_{22}(1 - e^{-\frac{1}{2}\frac{|\ddot{\mathbf{x}}_k|^2}{q^2}}) \\ 1 - p_{11}e^{-\frac{1}{2}\frac{|\ddot{\mathbf{x}}_k|^2}{q^2}} & p_{22}(1 - e^{-\frac{1}{2}\frac{|\ddot{\mathbf{x}}_k|^2}{q^2}}) \end{pmatrix} \quad (2.12)$$

can model this type of object behavior [10]. For $r = 1$, the linear-Gauß-Markov models result as a limiting case.

2.3 Sensor Likelihood Functions

Over time, one or several sensors produce sets of measurement data Z_k that potentially carry information on object states X_k characterizing one or more objects of interest at time t_k . This information is typically imprecise and corrupted by unavoidable measurement errors, e.g. In several applications, a sensor output Z_k can refer to individual properties of several neighboring objects of interest, but it is usually unknown to which particular object. In addition, some or all sensor data can be false, i.e. be originated by unwanted objects or unrelated to really existing objects. It is furthermore not necessarily true that sensors always produce measurements of objects of interest when an attempt is made. Moreover, several closely-spaced objects may produce irresolved measurements originated by two or more objects.

At discrete instants of time t_k , we consider the set $Z_k = \{Z_k^j\}_{j=1}^{m_k}$ of m_k sensor data. The accumulation of the sensor data Z_l , $1 \leq l \leq k$, up to and including the time t_k , typically the present, is an example of a time series recursively defined by $Z^k = \{Z_k, m_k, Z^{k-1}\}$. The time series produced by the measurements of individual sensors s involved are denoted by $Z_s^k = \{Z_l^s, m_l^s\}_{l=1}^k$, $1 \leq s \leq S$.

Within the framework of Bayesian reasoning, imperfect knowledge about what measured sensor data Z_k can actually say about the states of the objects involved is modeled by interpreting Z_k as a set of random variables. The statistical properties of Z_k are characterized by a probability density function $p(Z_k|X_k)$, which is conditioned on the corresponding object state X_k referring to the same time t_k . The probability densities $p(Z_k|X_k)$ are also called *likelihood functions* when considered as functions of the random variable X_k for a given sensor output Z_k . Typically, likelihood functions need to be known only up to a factor independent of X_k ,

$$\ell(X_k; Z_k) \propto p(Z_k|X_k), \quad (2.13)$$

as will become clear below. The sensor data Z_k explicitly enter into the likelihood function, while all sensor properties describing the sensors' physical and technical characteristics and their measurement performance are implicitly part of it and shape its concrete functional form. In particular, all relevant sensor parameters, such as measurement accuracy, detection probability, false alarm density, sensor resolution, minimum detectable velocity, radar beam width, pulse repetition frequency etc., must be present in the likelihood function. A likelihood function thus describes what information on an object state X_k is provided by the sensor data Z_k at a given instant of time t_k . For physical reasons, often $p(Z_k|X_I, Y) = p(Z_k|X_k)$ holds for any other random variable Y that is not part of the object state.

Likelihood functions $p(Z_k|X_k)$ model the real sensor output (and thus the physics of the underlying measurement process and its interaction with the object environment). For this reason, they provide the basis for Monte-Carlo-simulations of the sensor measurements by generating random realizations of Z_k according to $p(Z_k|X_k)$. For this reason, likelihood functions are simply called "sensor models" in direct analogy to "evolution models" given by $p(X_k|X_{k-1})$. Obviously, a sensor model is more correct, the more it provides simulated measurements that correspond on average to the real sensor output.

In the sequel, the notion of a likelihood function is illustrated by selected examples.

2.3.1 Gaussian Likelihood Functions

For well-separated objects, perfect detection, and in absence of false sensor data, let us consider measurements \mathbf{z}_k related to the kinematic state vector $\mathbf{x}_k = (\mathbf{r}_k^\top, \dot{\mathbf{r}}_k^\top, \ddot{\mathbf{r}}_k^\top)^\top$ of an object at time t_k . In constructing a sensor model $p(\mathbf{z}_k|\mathbf{x}_k)$, two questions must be answered:

1. The first question aims at what aspect of the state vector is currently in the focus of the sensor, i.e. at the identification of a *measurement function*,

$$\mathbf{h}_k : \mathbf{x}_k \mapsto \mathbf{h}_k(\mathbf{x}_k), \quad (2.14)$$

describing what is actually measured. Sensors characterized by the same measurement function \mathbf{h}_k are called *homogeneous sensors*, in contrast to *heterogeneous sensors*, where this is not the case.

2. The second question asks for the quality of such a measurement. In many applications, additive measurement errors \mathbf{u}_k can be considered, given by bias-free and Gaussian distributed random variables characterized by a *measurement error covariance matrix* \mathbf{R}_k . The measurement errors produced at different times or by different sensors can usually be considered as independent of each other.

In this case, the measurement process can be described by a *measurement equation* $\mathbf{z}_k = \mathbf{h}_k(\mathbf{x}_k) + \mathbf{v}_k$, which is equivalent to a Gaussian likelihood function:

$$\ell(\mathbf{x}_k; \mathbf{z}_k) = \mathcal{N}(\mathbf{z}_k; \mathbf{h}_k(\mathbf{x}_k), \mathbf{R}_k). \quad (2.15)$$

Range-Azimuth Measurements

In a two-dimensional plane, we may, for example, consider measurements of an object's range r_k and azimuth angle φ_k with respect to the sensor position in a given Cartesian coordinate system. Let the range and azimuth measurements be independent of each other with Gaussian measurement errors described by the standard deviations σ_r, σ_φ . Hence, in polar coordinates, the measurement error covariance matrix is diagonal: $\text{diag}[\sigma_r^2, \sigma_\varphi^2]$. A transformation of the original measurements into the Cartesian coordinate system, where the state vectors \mathbf{x}_k are formulated, is provided by the transform $\mathbf{t}(r_k, \varphi_k) = r_k(\cos \varphi_k, \sin \varphi_k)^\top$. A well-known result on affine transforms of Gaussian random variables (see Appendix A.3) is applicable, if the non-linear function $\mathbf{t}(r_k, \varphi_k)$ is expanded in a Taylor series up to the first order. The corresponding Jacobian can be written as the product of a rotation matrix \mathbf{D}_{φ_k} by φ_k and a dilation matrix \mathbf{S}_{r_k} defined by r_k :

$$\mathbf{T}_k = \frac{\partial \mathbf{t}(r_k, \varphi_k)}{\partial (r_k, \varphi_k)} \quad (2.16)$$

$$= \underbrace{\begin{pmatrix} \cos \varphi_k & -\sin \varphi_k \\ \sin \varphi_k & \cos \varphi_k \end{pmatrix}}_{\text{rotation } \mathbf{D}_{\varphi_k}} \underbrace{\begin{pmatrix} 1 & 0 \\ 0 & r_k \end{pmatrix}}_{\text{dilation } \mathbf{S}_{r_k}}. \quad (2.17)$$

The transformed measurements $\mathbf{z}_k = \mathbf{t}(r_k, \varphi_k)$ can thus be approximately characterized as Gaussian random variables with measurement error covariance matrices \mathbf{R}_k given by:

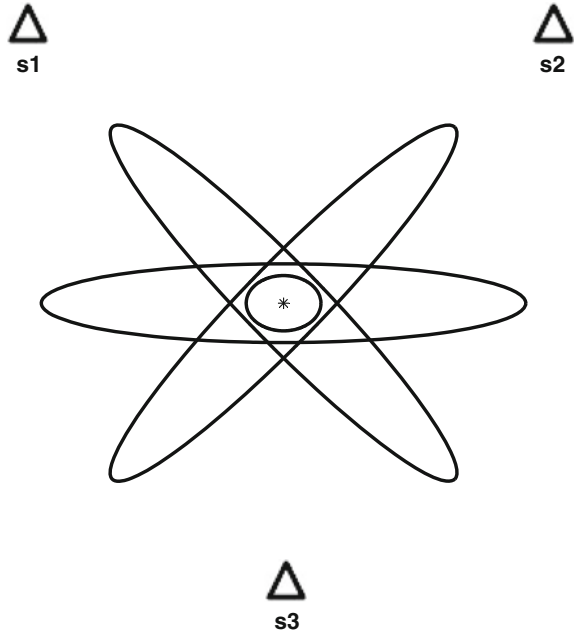
$$\mathbf{R}_k = \mathbf{D}_{\varphi_k} \begin{pmatrix} \sigma_r^2 & 0 \\ 0 & r_k^2 \sigma_\varphi^2 \end{pmatrix} \mathbf{D}_{\varphi_k}^\top. \quad (2.18)$$

according to Eq. A.20. Obviously, the measurement error covariance matrix \mathbf{R}_k depends on the underlying sensor-to-object geometry, i.e. differently located sensors with the same parameters σ_r, σ_φ produce measurements of the same object that are characterized by differently oriented measurement error ellipses as illustrated in Fig. 2.1. The cross-range semi-axis of the measurement error ellipses increases with increasing range, while the other semi-axis remains constant. The orientation of the measurement ellipse depends on the object's azimuth angle φ_k . With a matrix $\mathbf{H}_k = (\mathbf{1}, \mathbf{0}, \mathbf{0})$ that projects the position vector from the object state vector, $\mathbf{H}_k \mathbf{x}_k = \mathbf{r}_k$, the resulting likelihood function is thus given by:

$$\ell(\mathbf{x}_k; \mathbf{z}_k) \propto \mathcal{N}(\mathbf{z}_k; \mathbf{H}_k \mathbf{x}_k, \mathbf{R}_k). \quad (2.19)$$

For a discussion of problems and improvements, e.g. ‘‘Unbiased Converted Measurements’’, see [2, Chap. 1.7]. In many other applications, we are analogously looking for

Fig. 2.1 Schematic representation of the approximate measurement error ellipses of three sensors located at s_1, s_2, s_3 measuring range and azimuth of an object at $*$ and the impact of the sensor-to-object geometry on their mutual orientation, basic for the geometric fusion gain



formulations where a non-linear measurement function \mathbf{h}_k is linearly approximated by a *measurement matrix* \mathbf{H}_k , possibly depending on time.

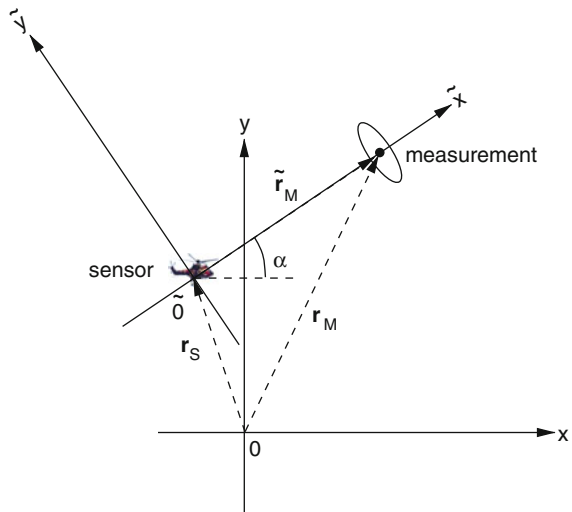
Doppler Measurements

By exploiting the Doppler effect, sensors that receive electromagnetic or acoustic wave forms reflected or emitted by objects of interest, such as radar, sonar, or ultrasonic devices, can measure the radial component \dot{r}_k of an object's relative velocity $\dot{\mathbf{r}}_k - \dot{\mathbf{p}}_k$ with respect to the sensor, where $\dot{\mathbf{p}}_k$ denotes the velocity vector of the sensor platform (see Fig. 2.2). Such frequency-based measurements are often highly precise and important in certain applications such as threat evaluation. The measurement triple $(r_k, \varphi_k, \dot{r}_k)$, however, cannot be transformed into Cartesian coordinates in analogy to the previous considerations. With $(\mathbf{r}_k - \mathbf{p}_k)/|\mathbf{r}_k - \mathbf{p}_k|$, the unit vector pointing from the sensor platform at the position \mathbf{p}_k to the object located at \mathbf{r}_k , the measurement function for range-rate measurements r_k is non-linear and given by:

$$h : \mathbf{x}_k \mapsto h(\mathbf{x}_k; \mathbf{p}_k, \dot{\mathbf{p}}_k) = \frac{(\dot{\mathbf{r}}_k - \dot{\mathbf{p}}_k)^\top (\mathbf{r}_k - \mathbf{p}_k)}{|(\dot{\mathbf{r}}_k - \dot{\mathbf{p}}_k)^\top (\mathbf{r}_k - \mathbf{p}_k)|}. \quad (2.20)$$

Note that in a practical realization sufficiently accurate navigation systems are required to estimate the platform state vector. As mentioned before, an expression following Eq. 2.19 can be obtained by a first-order Taylor expansion of the measurement function.

Fig. 2.2 Transformation of underlying Cartesian coordinates into a measurement-adapted system by a translation and rotation defined by the object's azimuth. Note that the \tilde{x} -axis points towards the object: r_k is thus a measurement of \tilde{x}



This type of non-linear measurement functions, however, can be handled alternatively. Consider a transformation of the underlying coordinates into a Cartesian system, where the origin is at the sensor location, while one of the axes points in a direction defined by the angular measurements (Fig. 2.2). Obviously, this transformation is simply a translation followed by a rotation. In the new coordinate system, the range-rate measurement can be interpreted as a measurement of one of the Cartesian components of the relative velocity vector of the object [11]. This means that the likelihood has a form as in Eq. 2.19 with a linear measurement equation. If a processing scheme is to be applied that requires likelihood functions of this form, a coordinate transform is therefore necessary at each processing step. In this context, Eq. A.20 is relevant, stating that a Gaußian density remains a Gaußian after this transformation. Similar considerations apply if measurements of the radial or lateral object extension is considered [12].

Evaluations with real data show that this type of dealing with range-rate measurements is significantly more robust than approaches based on Taylor expansions. The example leads to the more general observation that the appropriate formulation of sensor models requires a careful study of the individual physical quantity to be measured, quantitative performance evaluations, and comparisons with alternatives in order to achieve efficient and robust sensor models, the basic elements of sensor data fusion systems.

TDoA and FDoA Measurements

In a plane, let the kinematic state of an object emitting electromagnetic signals at time t_k be given by $\mathbf{x}_k = (\mathbf{r}_k^T, \dot{\mathbf{r}}_k^T)^T$. The emitter is observed by $S = 2$ sensors on possibly moving platforms with known state vectors $(\mathbf{p}_k^{sT}, \dot{\mathbf{p}}_k^{sT})^T$, $s = 1, 2$ that passively receive the emitted radiation. The *Time of Arrival (ToA)*, the time interval

from transmitting a signal at the emitter position \mathbf{r}_k and receiving it at a sensor position \mathbf{p}_k^s , is equal to the time the signal needs to travel from the emitter to the sensor. Since we know the propagation speed of the signal (speed of light c), ToA is given by $|\mathbf{r}_k - \mathbf{p}_k^s|/c$. A sensor model for *Time Difference of Arrival (TDoA)* measurements z_k^t directly follows:

$$\ell_t(\mathbf{x}_k; z_k^t) = \mathcal{N}(z_k^t c; h_t(\mathbf{x}_k), \sigma_t/c) \quad (2.21)$$

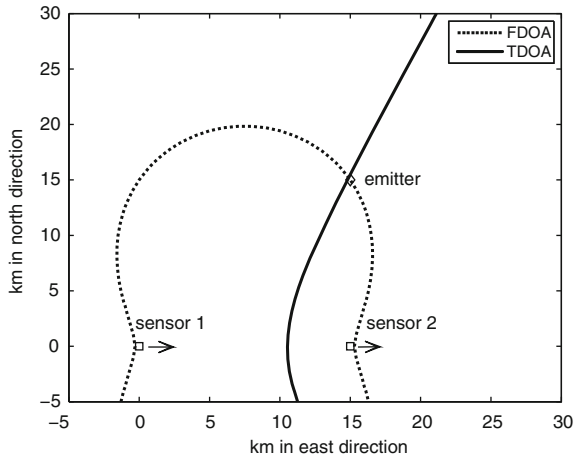
with a measurement function h_t given by:

$$h_t(\mathbf{x}_k; \mathbf{p}_k^1, \mathbf{p}_k^2) = |\mathbf{r}_k - \mathbf{p}_k^1| - |\mathbf{r}_k - \mathbf{p}_k^2|, \quad (2.22)$$

where σ_t denotes the standard deviation of the corresponding TDoA measurement errors. The locations of the sensor platforms enter as parameters. The sign of an individual measurement indicates which of the sensors is closer to the emitter. Without loss of generality, we can thus limit the discussion to one of these cases. The solid line in Fig. 2.3, a hyperbola, shows all potential emitter positions producing the same TDoA measurements, i.e. having the same distance difference from the sensors.

The Doppler shift in frequency is proportional to the radial velocity component of an emitter moving with respect to a Cartesian sensor coordinate system. The inverse wave length λ of the emitted radiation is the proportionality constant. Let $(\mathbf{r}_k - \mathbf{p}_k^s)/|\mathbf{r}_k - \mathbf{p}_k^s|$ denote the unit vector pointing from the sensor position \mathbf{p}_k^s at time t_k to the emitter located at \mathbf{r}_k , moving with the velocity $\dot{\mathbf{r}}_k$. As before, the radial component of the relative velocity of the emitter with respect to the sensor s is given by $(\dot{\mathbf{r}}_k - \dot{\mathbf{p}}_k^s)^\top (\mathbf{r}_k - \mathbf{p}_k^s)/|\mathbf{r}_k - \mathbf{p}_k^s|$. The measurement function for *Frequency Difference of Arrival (FDoA)* measurements is thus given by:

Fig. 2.3 Localization of an emitter using TDoA and FDoA measurements by two moving sensors: constant TDoA/FDoA emitter location curve



$$h_f(\mathbf{x}_k) = \frac{(\dot{\mathbf{r}}_k - \dot{\mathbf{p}}_k^1)^\top (\mathbf{r}_k - \mathbf{p}_k^1)}{|\mathbf{r}_k - \mathbf{p}_k^1|} - \frac{(\dot{\mathbf{r}}_k - \dot{\mathbf{p}}_k^2)^\top (\mathbf{r}_k - \mathbf{p}_k^2)}{|\mathbf{r}_k - \mathbf{p}_k^2|}. \quad (2.23)$$

A constant FDoA curve for a non-moving emitter is shown by the dashed curve in Fig. 2.3, where the arrows indicate the direction of the platform velocities. In this example, TDoA and FDoA are complementary in that TDoA takes the (approximate) role of bearings measurement, and FDoA, the (approximate) role of distance measurement. TDoA and FDoA measurements may be obtained simultaneously by calculating the Complex Ambiguity Function (CAF, [13]), which cross-correlates the signals received by the sensors. The likelihood functions that result from the measurement functions h_t and h_f are shown in Fig. 2.4. Techniques discussed in [14] and applied to emitter localization and tracking, make it possible to approximate the likelihood functions by sums of appropriately chosen individual Gaussians with a linear approximation of the measurement function according to Eq. 2.19.

2.3.2 Multiple Sensor Likelihood

Assume S homogeneous sensors are located at different positions that measure, at the same instant of time t_k , the same linear function $\mathbf{H}_k \mathbf{x}_k$ of an individual kinematic object state \mathbf{x}_k . Under conditions as considered before, let the individual likelihood functions of the sensors be given by:

$$\ell_s(\mathbf{x}_k; \mathbf{z}_k^s) \propto \mathcal{N}(\mathbf{z}_k^s; \mathbf{H}_k \mathbf{x}_k, \mathbf{R}_k^s), \quad s = 1, \dots, S. \quad (2.24)$$

Since independently working sensors were assumed, the over-all likelihood function describing the information on an object state, which is provided by all sensors at time t_k , can be written as a product of the individual likelihood functions:

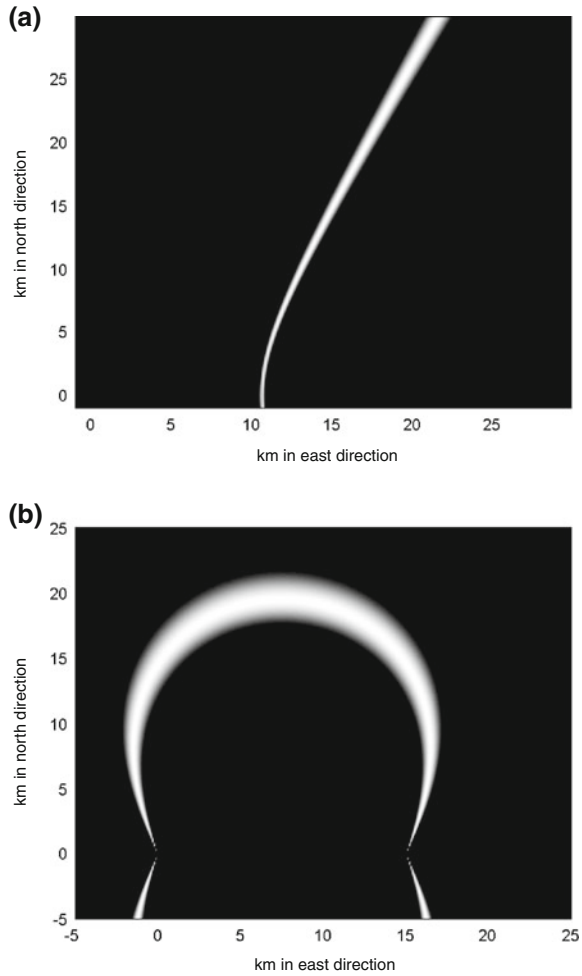
$$\ell(\mathbf{x}_k; \mathbf{z}_k^1, \dots, \mathbf{z}_k^S) \propto \prod_{s=1}^S \mathcal{N}(\mathbf{z}_k^s; \mathbf{H}_k \mathbf{x}_k, \mathbf{R}_k^s). \quad (2.25)$$

In Appendix A.5, a product formula for Gaussians is proven, which is well-suited for simplification of the product representation of the over-all likelihood function. An induction argument directly yields that $\ell(\mathbf{x}_k; \mathbf{z}_k^1, \dots, \mathbf{z}_k^S)$ can be represented by a single Gaussian,

$$\ell(\mathbf{x}_k; \mathbf{z}_k^1, \dots, \mathbf{z}_k^S) \propto \mathcal{N}(\mathbf{z}_k; \mathbf{H}_k \mathbf{x}_k, \mathbf{R}_k) \quad (2.26)$$

with an *effective measurement* \mathbf{z}_k and a corresponding *effective measurement error covariance* \mathbf{R}_k defined by:

Fig. 2.4 Likelihood functions for TDoA and FDoA measurements. Idea: approximate the likelihood functions by a sum of appropriately chosen Gaussians with a linear approximation of the measurement function. **a** Likelihood of TDoA and FDoA measurements. **b** Likelihood of FDoA measurements.



$$\mathbf{R}_k = \left(\sum_{s=1}^S \mathbf{R}_k^s \right)^{-1} \quad (2.27)$$

$$\mathbf{z}_k = \mathbf{R}_k \sum_{s=1}^S \mathbf{R}_k^s \mathbf{z}_k^s. \quad (2.28)$$

The effective measurement is thus represented by a *weighted arithmetic mean* of the measurements \mathbf{z}_k^s provided by the individual sensors involved, where the corresponding matrix-valued weighting factors are given by the inverses of the corresponding measurement error covariance matrices \mathbf{R}_k^s . Obviously, “poor” measurements, characterized by large measurement errors, provide smaller contributions to the effec-

tive measurement \mathbf{z}_k than “good” ones. Dealing with data from multiple sensors in this way is an example of centralized or distributed *measurement fusion* as opposed to *track-to-track fusion* (see the discussion in Sect. 3.1.1). Figure 2.1 illustrates the *geometric fusion gain* \mathbf{R}_k according to Eq. 2.27.

Geometric Fusion Gain

From these considerations several conclusions can be drawn:

1. If all individual measurement covariance matrices are identical, $\mathbf{R}_k^s = \mathbf{R}'_k$, $s = 1, \dots, S$, the effective measurement is the simple arithmetic mean of the individual measurements: $\mathbf{z}_k = \frac{1}{S} \sum_s \mathbf{z}_k^s$. For the effective measurement error covariance, we obtain the ‘square-root’ law: $\mathbf{R}_k = \frac{1}{S} \mathbf{R}'_k$.
2. If all measurement error ellipses involved differ significantly in their geometrical orientation relative to each other, a much greater effect can be observed (geometrical fusion gain).
3. The ‘intersection’ of error ellipses is obtained by calculating the *harmonic mean* of the related error covariance matrices. The harmonic mean of error covariances quantitatively describes the gain by fusing sensor data from several sources and has been referred to as the *Fusion Equation*.
4. In the limiting case of very narrow measurement error ellipses, such as those characterized by $\sigma_r \gg r_k \sigma_\varphi$, the triangulation of an object’s position from bearings only is obtained. Analogously, range-only measurements can be used (trilateration).

These considerations are also valid in three spatial dimensions as well as in more sophisticated sensor data, such as bistatic range or range-rate measurements (see for example [15, 16]).

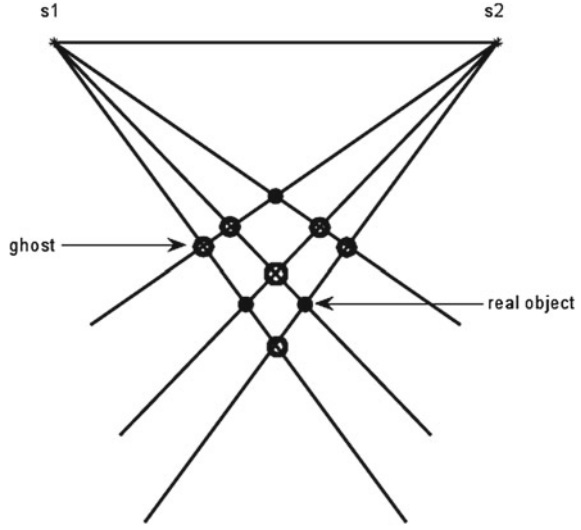
If there is more than one object in the common field of view of bearing-only sensors, not every intersection of two bearings actually corresponds to a real object position. Figure 2.5 illustrates this situation as well as the appearance of *ghosts* that do not correspond to real objects. Of course, in the case of inaccurate, false, missing, or even irresolved bearings, the *de-ghosting* is by no means trivial. For more details and possible solutions of de-ghosting problems in certain applications, see for example [17] (bearing-only tracking) or [18] (passive radar).

Cumulative Detection

In applications with relatively large data innovation intervals between successive data collections, such as in air-to-ground wide-area surveillance, sensor data fusion is particularly important for enhancing the data rate. Assuming measurement fusion as before, we consider the *mean cumulative data innovation intervals* ΔT_c [19] resulting from the individual innovation intervals ΔT_s , $s = 1, \dots, S$ of S sensors, which is defined by:

$$\frac{1}{\Delta T_c} = \sum_{s=1}^S \frac{1}{\Delta T_s}. \quad (2.29)$$

Fig. 2.5 Two objects observed by two bearings-only sensors s_1, s_2 . Not all intersections of bearing correspond to real objects. Typically, the number of “ghosts” is much higher than the number of objects involved



The *cumulative detection probability* is given by $P_D^S = 1 - \prod_{s=1}^S (1 - P_D^s)$, where P_D^s denotes the individual detection probability of sensor s , possibly depending on the corresponding sensor-to-object geometry (see the discussion in Sect. 3.1.2). It is appropriate to introduce the notion of the *mean cumulative detection probability* P_D^C , referring to ΔT_c and defined by:

$$P_D^C = 1 - \prod_{s=1}^S (1 - P_D^s)^{\frac{\Delta T_c}{\Delta T_s}}. \quad (2.30)$$

The data innovation intervals ΔT_s also enter into this formula, which describes the mean improvement of the overall detection performance to be expected by sensor data fusion. The larger ΔT_s , the smaller is the effect of sensor s on the overall performance, even if the corresponding individual detection probability P_D^s is large.

2.3.3 Likelihood for Ambiguous Data

A sensor output at time t_k , consisting of m_k measurements collected in the set Z_k , can be ambiguous, i.e. the origin of the sensor data has to be explained by a set of data interpretations, which are assumed to be exhaustive and mutually exclusive. As an example, let us consider measurements $Z_k = \{\mathbf{z}_k^j\}_{j=1}^{m_k}$ possibly related to the kinematic state \mathbf{x}_k of well-separated objects. ‘Well-separated’ here means that measurements potentially originated by one object could not have been originated by another. Even in this simplified situation, ambiguity can arise from imperfect

detection, false measurements, often referred to as *clutter*, or measurements from unwanted objects.

Illustration

As a schematic illustration of a more general case, let us consider six measurements produced by two closely-spaced objects (see Fig. 2.6). Among other data interpretations, the black dots indicate two measurements assumed as real, while all other data are assumed to be false (Fig. 2.6a). The asterisks denote predicted measurements provided by the tracking system. Under assumptions discussed in (Sect. 3.2.2), object measurements are Gaussian distributed about the predicted measurements with a covariance matrix $\mathbf{S}_{k|k-1}$ determined by the ignorance on the object state as well as by the sensor and the evolution model. The difference vector $\mathbf{v}_{k|k-1}$ between an actual and a predicted measurement is called *innovation*. As will become clear below, the statistical properties of the innovation related to a particular interpretation hypothesis are essential to evaluating its statistical weight. *Gating* means that only those sensor data are considered whose innovations are smaller than a certain predefined threshold in the sense of a Mahalanobis norm: $\mathbf{v}_{k|k-1}^\top \mathbf{S}_{k|k-1}^{-1} \mathbf{v}_{k|k-1} < \chi^2(P_c)$. Expectation gates thus contain the measurements with a given (high) *correlation probability* P_c . Obviously, the ambiguities involved with the situation in Fig. 2.6 are not completely resolved by gating.

More feasible hypotheses, however, compete with the data interpretation previously discussed. For instance, the targets could have produced a single unresolved measurement as indicated in Fig. 2.6b, all other data being false. Alternatively, one of the objects may not have been detected or no detection may have occurred at all. The expectation gates and therefore the ambiguity of the received sensor data grow larger according to an increasing number of false measurements and missed detections as well as to large measurement errors, data innovation intervals, or expected object maneuvers.

Well-separated Objects

Let $j_k = 0$ denote the data interpretation hypothesis that the object has not been detected at all by the sensor at time t_k , i.e. all sensor data have to be considered as false measurements, while $1 \leq j_k \leq m_k$ represents the hypothesis that the object has been detected, $\mathbf{z}_k^{j_k} \in Z_k$ being the corresponding measurement of the object properties, the remaining sensor data being false. Obviously, $\{0, \dots, m_k\}$ denotes a set of mutually exclusive and exhaustive data interpretations.

Due to the total probability theorem and with D or \neg D denoting that the object has or has not been detected, the conditional probability density $p(Z_k, m_k | \mathbf{x}_k)$ can be written as a weighted sum of conditional likelihood functions:

$$p(Z_k, m_k | \mathbf{x}_k) = p(Z_k, m_k, \neg D | \mathbf{x}_k) + p(Z_k, m_k, D | \mathbf{x}_k) \quad (2.31)$$

$$= p(Z_k, m_k | \neg D, \mathbf{x}_k) p(\neg D | \mathbf{x}_k) + p(Z_k, m_k | D, \mathbf{x}_k) p(D | \mathbf{x}_k). \quad (2.32)$$

The sensor model $p(Z_k, m_k | \mathbf{x}_k)$ can be traced back to intuitively understandable physical/technical phenomena and related sensor parameters. As a first consequence,

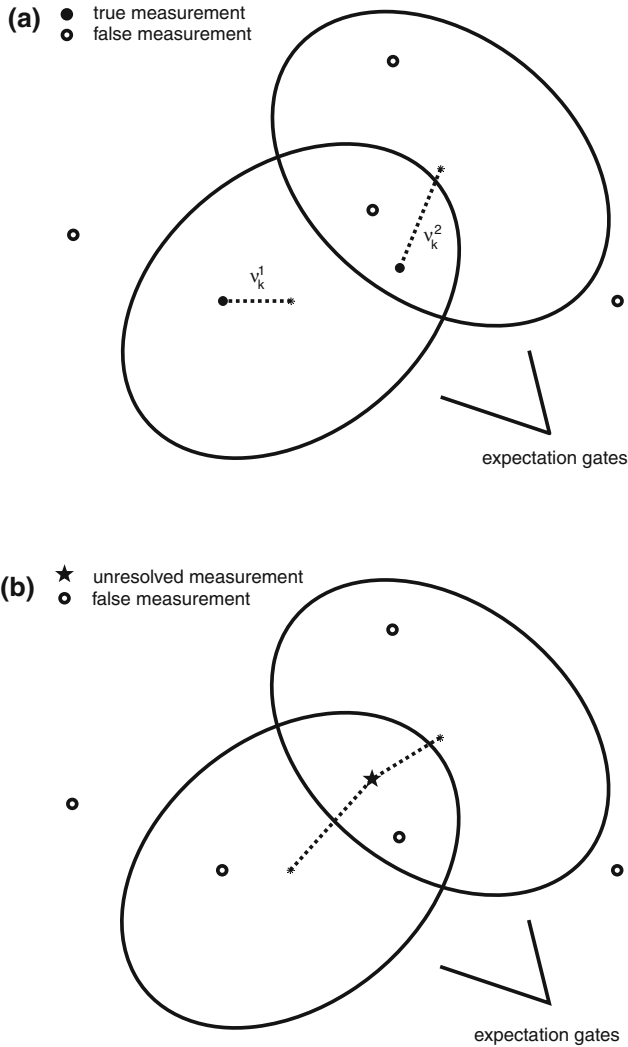


Fig. 2.6 Sensor measurements produced by two closely-spaced objects: competing data interpretations due to uncertain origin of the the sensor data including hypotheses assuming possibly unresolved measurements. **a** Two resolved targets. **b** Two unresolved targets

the *probability of detection*, $p(D|\mathbf{x}_k) =: P_D$, and non-detection, $p(-D|\mathbf{x}_k) = 1 - P_D$ enter into the likelihood as a characteristic parameter related to the detection process performed within a sensor system. For the sake of simplicity, we do not express by our notation here that detection probabilities may depend on the object state vectors \mathbf{x}_k . State-dependent detection probabilities, however, become relevant in several real-world applications (see the discussion in Sect. 3.1.2).

1. The conditional likelihood $p(Z_k, m_k | \neg D, \mathbf{x}_k)$ in Eq. 2.32 can be rewritten as:

$$p(Z_k, m_k | \neg D, \mathbf{x}_k) = p(Z_k | m_k, \neg D, \mathbf{x}_k) p(m_k | \neg D_k, \mathbf{x}_k) \quad (2.33)$$

$$= p_F(m_k) |\text{FoV}|^{-m_k}. \quad (2.34)$$

Here, the probability of having received m_k false measurements given the object was not detected, $p(m_k | \neg D_k, \mathbf{x}_k)$, is provided by a further modeling assumption, which relates the fluctuating number of false measurements to a mean *spatial clutter density* ρ_F characteristic of the sensor's detection process and the sensing environment. According to modeling assumptions, which are well-proven in many practical applications, let the probability of the number of false data involved $p(m_k | \neg D_k, \mathbf{x}_k)$ be given by a Poisson distribution

$$p_F(m_k) = (\bar{m}_F^{m_k} / m_k!) e^{-\bar{m}_F} \quad (2.35)$$

with a mean number of false measurements \bar{m}_F , which is related to the volume of the sensor's field of view $|\text{FoV}|$ and ρ_F via $\bar{m}_F = \rho_F |\text{FoV}|$. ρ_F may vary on a larger scale than the direct object neighborhood. Values for ρ_F can either be taken from so-called 'clutter maps', i.e. from related context information, or adaptively be estimated on-line [20–22]. Since false measurements are assumed to be independent from each other and equally distributed in the sensor's field of view (FoV), we have $p(Z_k | m_k, \neg D, \mathbf{x}_k) = \prod_{j=1}^{m_k} p(\mathbf{z}_k^j | \neg D, \mathbf{x}_k) = |\text{FoV}|^{-m_k}$.

2. For the conditional likelihood $p(Z_k, m_k | D, \mathbf{x}_k)$ in Eq. 2.32, we obtain analogously:

$$p(Z_k | m_k, D, \mathbf{x}_k) = \sum_{j_k=1}^{m_k} p(Z_k, m_k, j_k | D, \mathbf{x}_k) \quad (2.36)$$

$$= \sum_{j_k=1}^{m_k} p(Z_k | m_k, j_k, D, \mathbf{x}_k) p(m_k | j_k, D, \mathbf{x}_k) p(j_k | D, \mathbf{x}_k) \quad (2.37)$$

$$= \frac{p_F(m_k - 1)}{m_k |\text{FoV}|^{m_k - 1}} \sum_{j_k=1}^{m_k} \mathcal{N}(\mathbf{z}_k^{j_k}; \mathbf{H}_k \mathbf{x}_k, \mathbf{R}_k^{j_k}). \quad (2.38)$$

Under the assumption j_k , we assume a Gaussian likelihood function for describing $\mathbf{z}_k^{j_k}$ according to Eq. 2.19, the other $m_k - 1$ measurements being treated as equally distributed in the sensor field of view:

$$p(Z_k | m_k, j_k, D, \mathbf{x}_k) = |\text{FoV}|^{-(m_k - 1)} \mathcal{N}(\mathbf{z}_k^{j_k}; \mathbf{H}_k \mathbf{x}_k, \mathbf{R}_k^{j_k}). \quad (2.39)$$

$p(m_k | j_k, D, \mathbf{x}_k)$ is given by $p_F(m_k - 1)$, while a priori the m_k data association hypotheses j_k are assumed to equally distributed, $p(j_k | D, \mathbf{x}_k) = m_k^{-1}$.

By exploiting the definition of the Poisson distribution and re-arranging the terms, a likelihood function for ambiguous data is proportional to a weighted sum of Gaussians and a constant ($\rho_F > 0$):

$$\ell(\mathbf{x}_k; Z_k, m_k) \propto (1 - P_D)\rho_F + P_D \sum_{j_k=0}^{m_k} \mathcal{N}(\mathbf{z}_{j_k}; \mathbf{H}_k \mathbf{x}_k, \mathbf{R}_k). \quad (2.40)$$

In the special case of $\rho_F = 0$ (no false measurements to be expected), Kronecker symbols can be used to find an expression for the likelihood ($\delta_{ij} = 1$ for $i = j$, $\delta_{ij} = 0$ otherwise):

$$\ell(\mathbf{x}_k; Z_k, m_k) \propto (1 - P_D) \delta_{0m_k} + P_D \mathcal{N}(\mathbf{z}_k; \mathbf{H}_k \mathbf{x}_k, \mathbf{R}_k) \delta_{1m_k}. \quad (2.41)$$

Possibly Irresolved Measurements

Similar considerations can be applied to formulate appropriate likelihood functions in multiple object situations described by joint object states $\mathbf{x}_k = (\mathbf{x}_k^{1\top}, \mathbf{x}_k^{2\top}, \dots)^\top$, where possibly unresolved measurements are to be taken into account (see Fig. 2.6b).

Among other sensor properties, in such situations the limited capability of physical sensors to resolve closely-spaced objects must be part of the sensor model. The link from physical resolution phenomena to the likelihood functions is provided by considering the probability P_u of two objects being unresolved. P_u certainly depends on the relative distance vector \mathbf{d}_k in proper coordinates between the objects at a certain time t_k : $P_u = P_u(\mathbf{d}_k)$. We qualitatively expect that P_u will be close to One for small values of $|\mathbf{d}_k|$, while $P_u = 0$ for distances significantly larger than certain resolution parameters, such as the beam-width, band-width, or coherence length of a radar. We expect a narrow transient region. In a generic model of the sensor resolution, we may describe P_u by a Gaussian-type function of \mathbf{d}_k with a ‘covariance matrix’ serving as a quantitative measure of the sensor resolution capability, which in particular reflects the extension and spatial orientation of ellipsoidal resolution cells depending on the underlying sensor-to-object geometry.

According to these considerations, the notion of a *resolution probability* is crucial if suitable sensor models for object groups are to be designed. The underlying Gaussian structure significantly simplifies the mathematical reasoning involved and finally leads to a representation of the likelihood function by a weighted sum of Gaussians and a constant, i.e. we have to deal with the same mathematical structure as before in the case of well-separated objects. For details see the discussion in Sect. 3.1.1.

2.3.4 Incorporating Signal Strength

The strength z_k of an received object signal at time t_k carries information on the corresponding object strength x_k , which is in a radar application, for example, directly

related to the object's characteristic mean radar cross section via the radar equation [23]. An individual sensor measurement related to an object state $X_k = (\mathbf{x}_k, x_k)$ is thus given by $Z_k^j = (\mathbf{z}_k^j, z_k^j)$. With this notation, the previous discussion can directly be generalized:

$$p(Z_k, m_k | X_k) = p(Z_k, m_k | \neg D, X_k) p(\neg D | X_k) + \sum_{j_k=1}^{m_k} p(Z_k | m_k, j_k, D, X_k) p(m_k | j_k, D, X_k) p(j_k | D, X_k). \quad (2.42)$$

We only have to consider the following conditional likelihood functions:

$$p(Z_k, m_k | \neg D, X_k) = |\text{FoV}|^{-m_k} \prod_{j=1}^{m_k} p(z_k^j | \neg D, X_k) =: \Lambda \quad (2.43)$$

$$p(Z_k | m_k, j_k, D, X_k) = \mathcal{N}(\mathbf{z}_k^{j_k}; \mathbf{H}_k \mathbf{x}_k, \frac{1}{z_k} \mathbf{R}_k^{j_k}) \frac{\Lambda p(z_k^{j_k} | D, X_k)}{|\text{FoV}|^{-1} p(z_k^{j_k} | \neg D, X_k)}. \quad (2.44)$$

We here additionally assumed a measurement error covariance matrix $\frac{1}{z_k} \mathbf{R}_k$ depending on the received signal strength z_k . This can be justified by radar signal processing theory [23] and reflects the empirical phenomenon that the weaker the signals received are the less accurate the resulting measurements.

For the sake of simplicity, we furthermore assume that $p(z_k | \neg D, X_k)$ and $p(z_k | D, X_k)$ do not depend on the kinematic state vector, although the received signal strength may in principle depend on the sensor-to-object geometry. The often highly complex dependency on the aspect angle is instead described by so-called Swerling models of radar cross section fluctuations [24]. According to the practically important Swerling-I-model, the received signal strengths z_k are random variables, characterized by $p(z_k | x_k) = e^{-z_k/(1+x_k)}/(1+x_k)$, i.e. simple exponential densities. Let us furthermore assume that a detector decides on "detection", denoted by 'D', if z_k exceeds a certain threshold: $z_k > \lambda$. If there is actually an object present that has been detected, $P_D = p('D' | D)$ is thus given by:

$$P_D = \frac{1}{1+x_k} \int_{\lambda}^{\infty} dz_k e^{-z_k/(1+x_k)} = e^{-\lambda/(1+x_k)}. \quad (2.45)$$

The corresponding false alarm probability $P_F = p('D' | \neg D)$ is given by $P_F = \int_{\lambda}^{\infty} dz_k e^{-z_k} = e^{-\lambda}$. Here $x_k = 0$ is assumed for a noise-type target. This result directly leads to the famous *Swerling formula*, which relates the detection probability P_D to the object strength x_k and the false alarm probability P_F characterizing the detector:

$$P_D(x_k, P_F) = P_F^{\frac{1}{1+x_k}}. \quad (2.46)$$

A detected signal not belonging to a real object of interest is a clutter signal with a *clutter strength* c_k , a parameter characterizing context information on the sensing environment. After detection and according to Bayes Theorem, a received signal strength z_k is either distributed according to:

$$p(z_k | x_k, D) = \begin{cases} \frac{e^{(\lambda - z_k)/(1+x_k)}}{1+x_k} & \text{for } z_k > \lambda \\ 0 & \text{else} \end{cases} \quad (2.47)$$

or to:

$$p(z_k | x_k, -D) = \begin{cases} \frac{e^{(\lambda - z_k)/(1+c_k)}}{1+c_k} & \text{for } z_k > \lambda \\ 0 & \text{else.} \end{cases} \quad (2.48)$$

By inserting these densities in Eqs. 2.43 and 2.44, we directly obtain the modified likelihood function for ambiguous sensor data that include signal strength information:

$$\begin{aligned} \ell(\mathbf{x}_k, x_k; Z_k, m_k) &\propto (1 - e^{-\frac{\lambda}{1+x_k}}) \rho_F \\ &+ \sum_{j=1}^{m_k} \left(\frac{e^{(\lambda - z_k^j)/(1+c_k)}}{1+c_k} \right)^{-1} \frac{e^{-z_k^j/(1+x_k)}}{1+x_k} \mathcal{N}(\mathbf{z}_k^j; \mathbf{H}_k \mathbf{x}_k, \frac{1}{z_k^j} \mathbf{R}_k^j). \end{aligned} \quad (2.49)$$

Note that this likelihood function depends on the sensor parameters \mathbf{R}_k and λ , characterizing the measurement and the detection process, as well as the environmental parameters ρ_F and c_k . These parameters represent context information, which is a necessary input for the likelihood function besides the sensor data themselves.

2.3.5 Extended Object Likelihood

According to the discussion in Sect. 2.1, spatially extended objects or collectively moving object clusters, are characterized by an object state $X_k = (\mathbf{x}_k, \mathbf{X}_k)$, which consists of an kinematic state vector \mathbf{x}_k and a symmetric, positively definite matrix \mathbf{X}_k . For the sake of simplicity, let us exclude false or unwanted measurements at present. In a first approximation, the number m_k of measurements in Z_k is assumed to be independent of the object state X_k ,; i.e. $p(m_k | \mathbf{x}_k, \mathbf{X}_k)$ is assumed to be a constant.

In the case of extended or group targets, the significance of a single measurement is evidently dominated by the underlying object extension. The sensor-specific measurement error describing the precision by which a given scattering center is currently measured is the more unimportant, the larger the actual extension of the object is compared to the measurement error. The individual measurements must therefore rather be interpreted as measurements of the centroid of the extended or collective object, since it is unimportant, which of the varying scattering centers was actually responsible for the measurement.

We thus interpret each individual measurement produced by an extended object as a measurement of the object centroid with a corresponding ‘measurement error’ being proportional to the object extension \mathbf{X}_k to be estimated. By means of this ‘measurement error’, however, the object extension \mathbf{X}_k becomes explicitly part of the likelihood function $p(Z_k, m_k | \mathbf{x}_k, \mathbf{X}_k)$, which describes what the measured quantities Z_k, m_k can say about the state variables \mathbf{x}_k and \mathbf{X}_k . Elementary calculations, similar to those used in Sect. 2.3.2, yield the following factorization (see Appendix A.10 for details):

$$p(Z_k, m_k | \mathbf{x}_k, \mathbf{X}_k) \propto \prod_{j=1}^{m_k} \mathcal{N}(\mathbf{z}_k^j; \mathbf{H}_k \mathbf{x}_k, \mathbf{X}_k) \quad (2.50)$$

$$\propto \mathcal{N}(\mathbf{z}_k; \mathbf{H}_k \mathbf{x}_k, \frac{1}{m_k} \mathbf{X}_k) \mathcal{LW}(\mathbf{Z}_k; m_k - 1, \mathbf{X}_k) \quad (2.51)$$

up to a multiplicative constant independent of the state variables. In Eq. 2.51, the centroid measurement \mathbf{z}_k and the corresponding scattering matrix \mathbf{Z}_k are given by:

$$\mathbf{z}_k = \frac{1}{m_k} \sum_{j=1}^{m_k} \mathbf{z}_k^j \quad (2.52)$$

$$\mathbf{Z}_k = \sum_{j=1}^{m_k} (\mathbf{z}_k^j - \mathbf{z}_k)(\mathbf{z}_k^j - \mathbf{z}_k)^\top, \quad (2.53)$$

while $\mathcal{LW}(\mathbf{Z}_k; m_k - 1, \mathbf{X}_k)$ is proportional to a Wishart density with $m_k - 1$ degrees of freedom, a matrix-variate probability density function describing the properties of the random variable \mathbf{Z}_k (see Appendix A.11 for details):

$$\mathcal{LW}(\mathbf{Z}_k; m_k - 1, \mathbf{X}_k) = |\mathbf{X}_k|^{-\frac{m_k - 1}{2}} \text{etr}\left(-\frac{1}{2}(\mathbf{Z}_k \mathbf{X}_k^{-1})\right). \quad (2.54)$$

References

1. R.R. Yager, L. Liu (eds.). *Classic works of the Dempster-Shafer theory of belief functions* (Springer, Berlin, 2008)
2. Y. Bar-Shalom, P.K. Willett, X. Tian, Tracking and Data Fusion. in *A Handbook of Algorithms* (YBS Publishing, Storrs, 2011)
3. X. Rong, Survey of maneuvering target tracking. Part I. dynamic models. *IEEE Trans. Aerosp. Electron. Syst.* **39**(4), 1333–1364 (2003)
4. X.R. Li, V.P. Jilkov, A survey of maneuvering target tracking-part II: ballistic target models. in *Proceedings of the 2001 SPIE Conference on Signal and Data Processing of Small Targets*, vol. 4473, 559–581 (2001)
5. X.R. Li, V.P. Jilkov, A survey of maneuvering target tracking-part III: measurement models, in *Proceedings of the 2001 SPIE Conference on Signal and Data Processing of Small Targets*, vol. 4473, pp. 423–446, 2001

6. X.R. Li and V.P. Jilkov, A survey of maneuvering target tracking-Part IV: decision-based methods. in *Proceedings of the 2002 SPIE Conference on Signal and Data Processing of Small Targets*, vol. 4728, p. 60, 2002
7. X. Rong, Li, V.P. Jilkov, Survey of maneuvering target tracking. Part V. Multiple model methods". in *IEEE Transactions on Aerospace and Electronic Systems* vol. 41(4) (2005), pp.1255–1321
8. G.V. Keuk, Zielverfolgung nach Kalman-anwendung auf elektronisches radar. FFM-Bericht, 173 (1971)
9. H.A.P. Blom. An efficient filter for abruptly changing systems. In *Proceedings of the 23rd IEEE Conference on Decision and Control*, Las Vegas, 1984
10. M. Michaelis, F. Govaers, W. Koch, State dependent mode transition probabilities, in IEEE ISIF Workshop Sensor Data Fusion-Trends, Solutions, Applications, Bonn, Germany (IEEE Xplore), October 2013
11. D. Robinson, W. Seels, Kalman-Filter, European Patent No. EP0452797B1, April 1992
12. R. Klemm, M. Mertens, Tracking of convoys by airborne STAP radar. In IEEE international conference on information fusion, Cologne, 2008
13. D.J. Torrieri, Statistical theory of passive location systems. *IEEE Trans. Aerosp. Electron. Syst.* **AES-20**(2), 183–198 (1984)
14. D. Musicki, R. Kaune, W. Koch, Mobile Emitter Geolocation and Tracking Using TDOA and FDOA Measurements. In *IEEE Transactions on Signal Processing* vol. 58(3) pp.1863–1874 (2010)
15. K. Becker, Three-dimensional target motion analysis using angle and frequency measurements. *IEEE Trans. Aerosp. Electron. Syst.* **41**(1), 284–301 (2005)
16. C.R. Berger, M. Daun, W. Koch. Low complexity track initialization from a small set of non-invertible measurements. *EURASIP J. Adv. Sig. Process.* special issue on track-before-detect techniques, 15, (756414) **2008** doi:[10.1155/2008/756414](https://doi.org/10.1155/2008/756414)
17. R. Baltes, A triangulation system for tracking multiple targets with passive sensors. in *Proceedings of the DGON/ITG International Radar Symposium IRS'98*, Muenchen, 1998
18. M. Daun, U. Nickel, W. Koch, Tracking in multistatic passive radar systems using DAB/DVB-T illumination. In *Proceedings of Signal Processing* pp 1365–1386 (2012)
19. W. Koch, Ground target tracking with STAP radar: selected tracking aspects. Chapter 15 in: R. Klemm (ed.), *The Applications of Space-Time Adaptive Processing*, (IEE Publishers, London, 2004)
20. W. Koch, M. Blanchette, Tracking in densely cluttered environment—concepts and experimental results. In *Proceedings of ISATA Robotics, Motion, and Machine Vision*, p.215 ff, Aachen, 1994
21. W. Koch, Experimental results on Bayesian MHT for maneuvering closely-spaced objects in a densely cluttered environment. In *IEE International Radar Conference RADAR'97*, Edinburgh, 729 (1999)
22. W. Koch, Generalized smoothing for multiple model/multiple hypothesis filtering: experimental results, in *Proceedings of European Control Conference ECC'99*, Karlsruhe, CD ROM 1999
23. W.-D. Wirth, *Radar Techniques Using Array Antennas*. (IEE Press, London, 2001)
24. P.L. Bogler, *Radar Principles with Applications to Tracking Systems* (Wiley, New York, 1990)

Chapter 3

Bayesian Knowledge Propagation

Within the general framework of Bayesian reasoning and based on object evolution models and sensor likelihood functions, such as those previously discussed, we proceed along the following lines.

1. *Basis.* In the course of time, one or several sensors produce measurements of one or more objects of interest. The accumulated sensor data are an example of a time series. Each object is characterized by its current state.
2. *Objective.* Learn as much as possible about the object states X_l at each time of interest t_l by exploiting the sensor data collected in the times series Z^k , i.e. for past ($l < k$), present ($l = k$), or future ($l > k$) states.
3. *Problem.* The sensor information is usually imperfect, i.e. imprecise, of uncertain origin, false or corrupted, possibly unresolved, ambiguous etc. Moreover, the objects' temporal evolution is usually not well-known.
4. *Approach.* Interpret sensor measurements and object states as random variables and describe what is known about them by using conditional probability densities functions. In particular, information on an object state at time t_l obtained from the sensor data Z^k is represented by $p(X_l|Z^k)$.
5. *Solution.* Based on Bayes' Theorem, derive iteration formulae for calculating the probability density functions $p(X_l|Z^k)$ and develop a mechanism for initiating the iteration process. Derive state estimates from the probability densities along with appropriate quality measures for the estimates.

3.1 Bayesian Tracking Paradigm

A Bayesian tracking algorithm is an iterative updating scheme for calculating conditional probability density functions $p(X_l|Z^k)$ that represent all available knowledge on the object states X_l at discrete instants of time t_l . The densities are explicitly conditioned on the sensor data Z^k accumulated up to some time t_k , typically the present time. Implicitly, however, they are also determined by all available context

knowledge on the sensor characteristics, the dynamical object properties, the environment of the objects, topographical maps, or tactical rules governing the objects' overall behavior.

With respect to the instant of time t_l at which estimates of the object states X_l are required, the related density iteration process is referred to as *prediction* ($t_l > t_k$), *filtering* ($t_l = t_k$), or *retrodition* ($t_l < t_k$). The propagation of the probability densities involved is given by three basic update equations, which will be derived and discussed and illustrated by examples.

Prediction

The prediction density $p(X_k|Z^{k-1})$ is obtained by combining the evolution model $p(X_k|X_{k-1})$ with the previous filtering density $p(X_{k-1}|Z^{k-1})$:

$$p(X_{k-1}|Z^{k-1}) \xrightarrow[\text{constraints}]{\text{evolution model}} p(X_k|Z^{k-1}) \quad (3.1)$$

$$p(X_k|Z^{k-1}) = \int dX_{k-1} \underbrace{p(X_k|X_{k-1})}_{\text{evolution model}} \underbrace{p(X_{k-1}|Z^{k-1})}_{\text{previous filtering}}. \quad (3.2)$$

Filtering

The filtering density $p(X_k|Z^k)$ is obtained by combining the sensor model $p(Z_k, m_k|X_k)$ with the prediction density $p(X_k|Z^{k-1})$ according to:

$$p(X_k|Z^{k-1}) \xrightarrow[\text{sensor model}]{\text{current sensor data}} p(X_k|Z^k) \quad (3.3)$$

$$p(X_k|Z^k) = \frac{p(Z_k, m_k|X_k) p(X_k|Z^{k-1})}{\int dX_k \underbrace{p(Z_k, m_k|X_k)}_{\text{sensor model}} \underbrace{p(X_k|Z^{k-1})}_{\text{prediction}}}. \quad (3.4)$$

Retrodition

The retrodition density $p(X_l|Z^k)$ is obtained by combining the previous retrodition density $p(X_{l+1}|Z^k)$ with the object evolution model $p(X_{l+1}|X_l)$ and the previous prediction and filtering densities $p(X_{l+1}|Z^l)$, $p(X_l|Z^l)$ according to:

$$p(X_{l-1}|Z^k) \xleftarrow[\text{evolution model}]{\text{filtering, prediction}} p(X_l|Z^k) \quad (3.5)$$

$$p(X_l|Z^k) = \int dX_{l+1} \frac{\overbrace{p(X_{l+1}|X_l)}^{\text{evolution}} \overbrace{p(X_l|Z^l)}^{\text{prev. filtering}}}{\underbrace{p(X_{l+1}|Z^l)}_{\text{prev. prediction}}} \underbrace{p(X_{l+1}|Z^k)}_{\text{prev. retrodition}}. \quad (3.6)$$

The natural antonym of “prediction”, the technical term “retrodiction” was introduced by OLIVER DRUMMOND in a series of papers [1–3]. According to his definition, “The process of computing estimates of states, probability densities, or discrete probabilities for a prior time (or over a period of time) based on data up to and including some subsequent time, typically, the current time.” [1, p. 255], this term comprises not only standard smoothing, but also the concept of a retrodicted discrete probability that is analogous to a smoothed estimate in usual Kalman filtering. For this reason, the notion of “retrodiction” is general enough as well as adequate for the type of algorithms proposed above. Adopting the classical standard terminology [4], we could speak of *fixed-interval* retrodiction.

The Notion of a Track

According to this paradigm, an *object track* represents all relevant knowledge on a time-varying object state of interest, including its history and measures that describe the quality of this knowledge. As a technical term, ‘track’ is therefore either a synonym for the collection of densities $p(X_l|Z^k)$, $l = 1, \dots, k, \dots$, or of suitably chosen parameters characterizing them, such as estimates related to appropriate risk functions and the corresponding estimation error covariance matrices.

If possible, a one-to-one association between the objects in the sensors’ field of view and the produced tracks is to be established and has to be preserved as long as possible (*track continuity*). In many applications, track continuity is even more important than track accuracy. Obviously, the achievable track quality does not only depend on the performance of the underlying sensors, but also on the object properties and the operational conditions within the scenario to be observed.

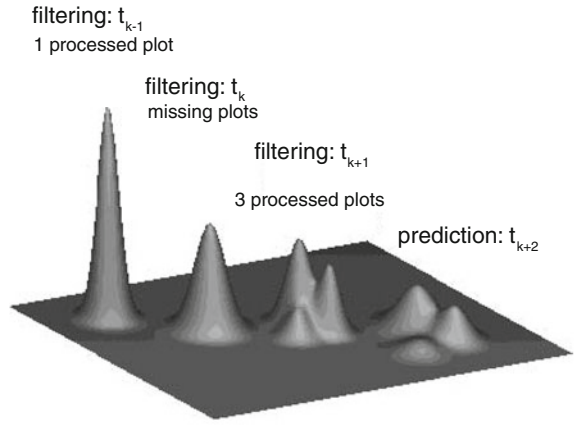
In this context, the notion of *track consistency* is important. It describes the degree of compliance between the inherent measures of track quality provided by the fusion process itself and the “real” tracking errors involved. Track consistency can be verified in experiments with an established ground truth or in Monte-Carlo-simulations (see the discussion on fusion performance measures in Sect. 1.3.3).

Graphical Illustration

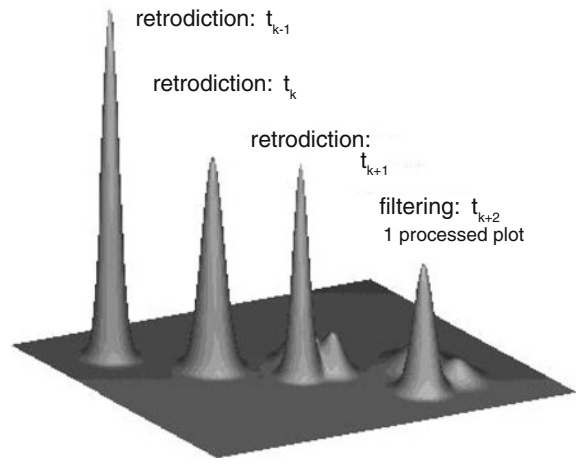
In Fig. 3.1a the conditional probability densities $p(\mathbf{x}_{k-1}|Z^{k-1})$, $p(\mathbf{x}_k|Z^k)$, and $p(\mathbf{x}_{k+1}|Z^{k+1})$ resulting from filtering at time instants t_{k-1} , t_k , and t_{k+1} are displayed along with the predicted density $p(\mathbf{x}_{k+2}|Z^{k+1})$. While at time t_{k-1} one sensor measurement has been processed, no measurement could be associated to it at time t_k . Hence, a missing detection is assumed. Due to the missing sensor information, the density $p(\mathbf{x}_k|Z^k)$ is broadened, since object maneuvers may have occurred. This in particular implies an increased region, where data at the subsequent time t_{k+1} are expected (gates). According to this effect, at time t_{k+1} three correlating sensor measurements are to be processed, leading to a multi-modal probability density function. The multiple modes reflect the ambiguity of the origin of the sensor data and also characterize the predicted density $p(\mathbf{x}_{k+2}|Z^{k+1})$. By this, the data-driven adaptivity of the Bayesian updating scheme is indicated.

In Fig. 3.1b, the density $p(\mathbf{x}_{k+2}|Z^{k+2})$, resulting from processing a single correlating sensor measurement at time t_{k+2} , along with the retrodicted densities

Fig. 3.1 Scheme of Bayesian density iteration: conditional probability density functions resulting from the *prediction*, *filtering*, and *retrodition* steps at different instants of times. **a** Forward iteration. **b** Backward iteration



(a) Forward Iteration.



(b) Backward Iteration.

$p(\mathbf{x}_{k+1}|Z^{k+2})$, $p(\mathbf{x}_k|Z^{k+2})$, and $p(\mathbf{x}_{k-1}|Z^{k+2})$ are shown. Obviously, available sensor data at the present time can significantly improve the estimates of the object states in the past.

3.1.1 Characteristic Aspects

The sensor data fusion process, i.e. the iterative calculation of conditional probability densities $p(X_l|Z^k)$ from multiple sensor data and context information on sensors,

objects, and the environment, can be characterized by several aspects. The emphasis, which is given to a particular aspect in a concrete application, has a strong impact on the design and architecture of a sensor data fusion system and on the requirements related to the underlying infrastructure, such as the bandwidth and reliability of communication links or navigation systems for sensor registration and alignment.

- In *optimal data fusion*, the conditional probability density functions involved are correctly calculated.
- In *centralized fusion*, only one fusion center exists, where the sensor data or object tracks are fused.
- In *distributed fusion*, the sensor data or object tracks are distributed and fused at several fusion centers.
- In *measurement fusion*, the sensor data and all relevant likelihood parameters are communicated to the fusion center(s).
- In *track-to-track fusion*, the local state estimates and covariances are communicated to the fusion center(s).
- In *full communication rate fusion*, all local sensor data or tracks are communicated to the fusion centers.
- In *reduced-rate communication fusion*, only selected sensor measurements or local tracks are communicated.

The likelihood function discussed in Sect. 2.3.2 is a typical example of centralized or distributed measurement fusion, while the fusion algorithms discussed in Sect. 6 can be characterized as distributed, full or reduced-rate track-to-track fusion. In general, measurement fusion architectures provide better approximations of optimal fusion. The choice of a fusion strategy depends on the particular requirements of a given application. See [5] for more a detailed discussion on benefits and problems of alternative fusion system architectures.

3.1.2 Remarks on Approximations

Under more realistic conditions, the probability densities involved typically have the structure of finite mixtures, i.e. they can be represented by weighted sums of individual probability densities that assume particular data interpretations or model hypotheses to be true. This general structure is a direct consequence of the uncertain origin of the sensor data and/or of the uncertainty related to the underlying object evolution. In concrete implementations, however, it is always necessary to apply certain approximations to handle such mixtures efficiently. Provided the densities $p(X_l|Z^k)$ are calculated at least approximately correctly, “good” estimators can be derived related to various risk functions adapted to the applications. What “good” means depends on the application considered and must often be verified by extensive Monte-Carlo-simulations and experiments.

Gaussian Mixtures

At least approximately correct closed-formula solutions for the Bayesian tracking paradigm can be derived if the prediction, filtering, and retrodiction densities as well as the sensor and evolution models belong to certain families of probability densities, so-called *mutually conjugate densities*. A wide and mathematically comfortable family of conjugate densities for random vectors \mathbf{x} is provided by *Gaussian mixtures* [6], i.e. by weighted sums of Gaussian probability densities, $p(\mathbf{x}) = \sum_i p_i \mathcal{N}(\mathbf{x}; \mathbf{x}_i, \mathbf{P}_i)$ with *mixture coefficients* $p_i \in \mathbb{R}$ that sum up to One, $\sum_i p_i = 1$, but need not necessarily be positive. A Gaussian mixture density is thus completely represented by a relatively small number of parameters $\{p_i, \mathbf{x}_i, \mathbf{P}_i\}_i$. As an early example see [7]. Other examples of families, which lead to at least approximately correct update formulae and are relevant to the work considered here, are Wishart and inverted Wishart mixtures or Gamma and inverted Gamma mixtures (see Appendix A.11).

For many real-world applications, it has been shown that even more sophisticated functional relationships describing the physics of the measurement process within a sensor system can be modeled by likelihood functions of the Gaussian mixture type. Of course, the accuracy of the sensor model, i.e. the number of mixture components that are actually to be taken into account to approximately describe the underlying phenomena, depends on the requirements of the underlying application. The same arguments are valid if the incorporation of context information, such as road-maps, is to be considered. They are also valid in the case of more complex dynamics models, such as those with a state dependent model transition matrix given by Eq. 2.12. Many examples of this type are discussed in Chap. 3.

It is the author's conviction that a large variety of relevant problems still exists in real-world applications of sensor data fusion and sensor management, which can efficiently be solved by using appropriately defined Gaussian mixtures. A particularly interesting indication of this general tendency seems to be the very fact that even in recent approaches, such as in Probability Hypothesis Density filtering (PHD, [8]), Gaussian mixture realizations provide the state-of-the-art solutions (GM-CPHD: Gaussian Mixture Cardinalized PHD). In view of practicality, these realizations are preferable compared to alternative approximation schemes, such as particle filtering. Moreover, explicit calculations in exploiting realistic sensor and evolution models are possible when using Gaussian mixture techniques, which provide a better understanding of the underlying physical and technical phenomena.

Particle Filtering

For implementing the Bayesian tracking paradigm, alternative approximation schemes are applicable that deal with the probability densities involved numerically. The most prominent method among these, *particle filtering*, was first introduced for tracking applications by Neil Gordon [9], who initiated and inspired a stormy development in this field (see [10] and the literature cited therein). Another early example of using particle filtering in a position estimation application for mobile robots is the work of D. Fox, W. Burgard, F. Dellaert, and S. Thrun [11].

Particle filtering techniques numerically represent probability density functions by random samples (called "particles") drawn from them by using random number

generators. The method is thus closely related to the random Monte-Carlo techniques, developed for problems in quantum field theory, for instance (see the discussion in [12]). For this reason, particle filtering techniques are computationally intensive. Their main advantage is the fact that they, in principle, provide “numerically exact” solutions at the cost of long computation times. These solutions can serve as benchmarks to test alternatives, such as Gaussian mixture realizations, which are often much less computation time consuming. In the context of the work presented here, performance comparisons using particle filters were done for “road-map assisted tracking” [13].

Particle filtering is a valuable approximation scheme for probability densities especially in applications, where the likelihood function $\ell(X_k; Z_k)$ can only be calculated pointwisely by an algorithm and no functional closed-formula expression is available. In the context of the work presented here, emitter localization and tracking in an urban environment is discussed (see [14] and the discussion in Sect. 3.2.3). Since this scenario is dominated by propagation phenomena, the key to the solution of this tracking problem lies in dealing with multipath phenomena appropriately. This can be done by using ray tracing algorithms for evaluating the most likely propagation channels for randomly chosen candidate emitter positions. Similar examples can be found wherever sophisticated propagation models can be exploited for localization and tracking (ionospheric propagation such as in communications or over-the-horizon radar, shallow-water sonar, indoor navigation) [15].

For advanced approximation techniques beyond classical particle filtering, which combines elements of Gaussian mixture reasoning with intelligent non-random sampling techniques, see the work of Uwe Hanebeck and his group (see [16], for example, and the literature cited herein).

3.1.3 On Track-to-Track Fusion

In certain applications, track-to-track fusion (see e.g. [17–20]) has considerable advantages:

- The communication channels are less overloaded with false tracks, provided these can be suppressed by local data processing.
- We may profit from reduced sensibility to sensor registration errors as local tracking is inherently robust regarding these effects. In this case, the problem is transferred to track-to-track fusion, but on this level its solution profits from efficient track-to-track correlation algorithms in situations that are not too dense.
- Disturbances of individual sensor sites and their corresponding local processors do not lead to the loss of the total system function.

Disadvantages result from suboptimal performance with respect to reaction time, track quality, lacking profit from redundancy, and the lower data rate for sensor individual tracking, which particularly affects track initiation, e.g. Moreover, track-to-track fusion is problematic if data collected by active and passive sensors have

to be fused (e.g. position data and bearings), since the production of local, sensor individual tracks may be difficult in non-trivial situations.

We speak of *optimal* track-to-track fusion in a Bayesian sense if the conditional probability density functions $p(X_k|Z^k) = p(X_k|\{Z_s^k\}_{s=1}^S)$, conditioned on all measurements of all sensors, can be correctly reconstructed from the locally produced tracks $p(X_k|Z_s^k)$, obtained by processing the data of the sensors $s = 1, \dots, S$ individually:

$$\{p(\mathbf{x}_l|Z_s^l)\}_{s,l=1}^{S,k} \xrightarrow[\text{fusion}]{\text{track-to-track}} p(\mathbf{x}_k|\{Z_s^k\}_{s=1}^S). \quad (3.7)$$

In Sect. 6 selected aspects of track-to-track fusion are discussed and exact update formulae for certain special cases are derived.

3.1.4 A First Look at Initiation

At time t_0 , the probability density $p(X_0|Z^0)$ describes the initial knowledge of the object state. As an example let us consider state vectors $\mathbf{x}_k = (\mathbf{r}_k^\top, \dot{\mathbf{r}}_k^\top)^\top$, consisting of the object position and velocity, and a first position measurement \mathbf{z}_0 with a measurement error covariance matrices \mathbf{R}_0 . Based on \mathbf{z}_0 and the context information on the maximum object speed v_{\max} to be expected, a reasonable initiation is given by $p(\mathbf{x}_0|\mathbf{z}_0) = \mathcal{N}(\mathbf{x}_0; \mathbf{x}_{0|0}, \mathbf{P}_{0|0})$ with:

$$\mathbf{x}_{0|0} = (\mathbf{z}_0^\top, \mathbf{0}^\top)^\top, \quad \mathbf{P}_{0|0} = \text{diag}[\mathbf{R}_0, v_{\max}^2 \mathbf{1}]. \quad (3.8)$$

In the case of an IMM evolution model, we consider the probability density $p(\mathbf{x}_0, i_0|Z^0) = p_{0|0}^{i_0} \mathcal{N}(\mathbf{x}_0; \mathbf{x}_{0|0}^{i_0}, \mathbf{P}_{0|0}^{i_0})$ with $p_{0|0}^{i_0} = \frac{1}{r}$. For a numerically robust and quick initiation scheme even from incomplete measurements see [21, 22] and the literature cited therein.

3.2 Object State Prediction

The probability density function $p(X_k|Z^{k-1})$ describes the predicted knowledge of the object state X_k referring to the instant of time t_k based on all the measurements received in the past up to and including the time t_{k-1} . According to the Chapman-Kolmogorov Equation, the prediction density can be calculated by combining the available knowledge on the object state at the past time t_{k-1} , given by $p(X_{k-1}|Z^{k-1})$ with the available knowledge on the object evolution, given by the evolution model $p(X_k|X_{k-1})$. Marginalization and the Markov assumption directly yield:

$$p(X_k|Z^{k-1}) = \int dX_{k-1} p(X_k, X_{k-1}|Z^{k-1}) \quad (3.9)$$

$$= \int dX_{k-1} p(X_k|X_{k-1}) p(X_{k-1}|Z^{k-1}). \quad (3.10)$$

3.2.1 Kalman Prediction

Let us consider a Gauß-Markov evolution model, such as provided by van Keuk's model (Eq. 2.8), where its deterministic part is characterized by the evolution matrix $\mathbf{F}_{k|k-1}$ and the stochastic part by the evolution covariance matrix $\mathbf{D}_{k|k-1}$, and a Gaußian previous filtering density, given by $p(\mathbf{x}_{k-1}|Z^{k-1}) = \mathcal{N}(\mathbf{x}_{k-1}; \mathbf{x}_{k-1|k-1}, \mathbf{P}_{k-1|k-1})$. Then the prediction density is also provided by a Gaußian:

$$p(\mathbf{x}_k|Z^{k-1}) = \int d\mathbf{x}_{k-1} \mathcal{N}(\mathbf{x}_k; \mathbf{F}_{k|k-1}\mathbf{x}_{k-1}, \mathbf{D}_{k|k-1}) \times \mathcal{N}(\mathbf{x}_{k-1}; \mathbf{x}_{k-1|k-1}, \mathbf{P}_{k-1|k-1}) \quad (3.11)$$

$$= \mathcal{N}(\mathbf{x}_k; \mathbf{x}_{k|k-1}, \mathbf{P}_{k|k-1}) \quad (3.12)$$

with an expectation vector $\mathbf{x}_{k|k-1}$ and a covariance matrix $\mathbf{P}_{k|k-1}$ given by the Kalman prediction update equations:

$$\mathbf{x}_{k|k-1} = \mathbf{F}_{k|k-1}\mathbf{x}_{k-1|k-1} \quad (3.13)$$

$$\mathbf{P}_{k|k-1} = \mathbf{F}_{k|k-1}\mathbf{P}_{k-1|k-1}\mathbf{F}_{k|k-1}^\top + \mathbf{D}_{k|k-1}. \quad (3.14)$$

This directly results from a product formula for Gaußians stated and proven in Appendix A.5, Eq. A.28. Note that after applying this formula, the integration variable \mathbf{x}_{k-1} in Eq. 3.11 is no longer contained in the first Gaußian of the product and can be drawn in front of the integral. The integration thus becomes trivial since probability densities are normalized by definition.

3.2.2 Expectation Gates

As a by-product of the prediction process, the statistical properties of object measurements Z_k that are expected at time t_k can be calculated on the basis of previously obtained measurements Z^{k-1} :

$$p(Z_k|Z^{k-1}) = \int dX_k p(Z_k, X_k|Z^{k-1}) \quad (3.15)$$

$$= \int dX_k p(Z_k|X_k) p(X_k|Z^{k-1}). \quad (3.16)$$

In the special case of Kalman prediction and with a Gaussian likelihood function, we obtain:

$$p(\mathbf{z}_k | Z^{k-1}) = \int d\mathbf{x}_k \mathcal{N}(\mathbf{z}_k; \mathbf{H}_k \mathbf{x}_k, \mathbf{R}_k) \mathcal{N}(\mathbf{x}_k; \mathbf{x}_{k|k-1}, \mathbf{P}_{k|k-1}) \quad (3.17)$$

$$= \mathcal{N}(\mathbf{z}_k; \mathbf{H}_k \mathbf{x}_{k|k-1}, \mathbf{S}_{k|k-1}). \quad (3.18)$$

Via the product formula (Eq. A.28), the matrix $\mathbf{S}_{k|k-1}$ results from the previous filtering covariance matrix $\mathbf{P}_{k-1|k-1}$ exploiting both the evolution and the sensor model:

$$\mathbf{S}_{k|k-1} = \mathbf{H}_k \mathbf{P}_{k|k-1} \mathbf{H}_k^\top + \mathbf{R}_k. \quad (3.19)$$

This means in particular that the *innovation vector* $\mathbf{v}_{k|k-1} = \mathbf{z}_k - \mathbf{H}_k \mathbf{x}_{k|k-1}$ is a normally distributed zero mean random variable characterized by the covariance matrix $\mathbf{S}_{k|k-1}$, which is thus called *innovation covariance matrix*. For this reason, the quadratic form

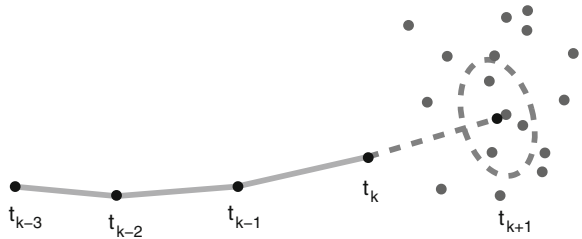
$$|\mathbf{v}_{k|k-1}|_{\mathbf{S}_{k|k-1}}^2 = (\mathbf{z}_k - \mathbf{H}_k \mathbf{x}_{k|k-1})^\top \mathbf{S}_{k|k-1}^{-1} (\mathbf{z}_k - \mathbf{H}_k \mathbf{x}_{k|k-1}), \quad (3.20)$$

called *innovation square* or *Mahalanobis distance* between predicted and actually produced measurements, is a χ_n^2 -distributed random variable with n degrees of freedom where n is the dimension of the measurement vector \mathbf{z}_k . The ellipsoid defined by:

$$|\mathbf{v}_{k|k-1}|_{\mathbf{S}_{k|k-1}}^2 \leq \chi_n^2(1 - P_c) \quad (3.21)$$

thus contains the expected measurement with a *correlation probability* P_c . The concrete value of $\chi_n^2(1 - P_c)$ can be looked up in a χ^2 -table. Such expectation gates are useful to exclude measurements from the fusion process that are very unlikely to belong to a given object. Figure 3.2 schematically illustrates the use of expectation gates in an object tracking example.

Fig. 3.2 Schematic illustration of expectation gates as a means of excluding measurements belonging to an object with a low probability $1 - P_c$



3.2.3 IMM Prediction

According to the discussion in the Sects. 2.1 and 2.2.2, let the filtering density $p(X_{k-1}|Z^{k-1})$ at time t_{k-1} be given by

$$p(X_{k-1}|Z^{k-1}) = p(\mathbf{x}_{k-1}, i_{k-1}|Z^{k-1}) \quad (3.22)$$

$$= p(\mathbf{x}_{k-1}|i_{k-1}, Z^{k-1}) p(i_{k-1}|Z^{k-1}) \quad (3.23)$$

$$= p_{k-1|i_{k-1}}^{i_{k-1}} \mathcal{N}(\mathbf{x}_{k-1}; \mathbf{x}_{k-1|i_{k-1}}^{i_{k-1}}, \mathbf{P}_{k-1|i_{k-1}}^{i_{k-1}}), \quad (3.24)$$

i.e. by a weighted Gaußian. In this case, the prediction update according to Eq. 3.10 and the product formula for Gaußians (Eq. A.28) yield:

$$p(\mathbf{x}_k, i_k|Z^{k-1}) = \sum_{i_{k-1}} \int d\mathbf{x}_{k-1} p(\mathbf{x}_k, i_k, \mathbf{x}_{k-1}, i_{k-1}|Z^{k-1}) \quad (3.25)$$

$$= \sum_{i_{k-1}} \int d\mathbf{x}_{k-1} p(\mathbf{x}_k, i_k|\mathbf{x}_{k-1}, i_{k-1}) p(\mathbf{x}_{k-1}, i_{k-1}|Z^{k-1}) \quad (3.26)$$

$$= \sum_{i_{k-1}} p_{k|k-1}^{i_k i_{k-1}} \mathcal{N}(\mathbf{x}_k; \mathbf{x}_{k|k-1}^{i_k i_{k-1}}, \mathbf{P}_{k|k-1}^{i_k i_{k-1}}), \quad (3.27)$$

where the parameters $p_{k|k-1}^{i_k i_{k-1}}$, $\mathbf{x}_{k|k-1}^{i_k i_{k-1}}$, $\mathbf{P}_{k|k-1}^{i_k i_{k-1}}$ of the density are given by:

$$p_{k|k-1}^{i_k i_{k-1}} = p_{i_k i_{k-1}} p_{k-1|i_{k-1}}^{i_{k-1}} \quad (3.28)$$

$$\mathbf{x}_{k|k-1}^{i_k i_{k-1}} = \mathbf{F}_{k|k-1}^{i_k} \mathbf{x}_{k-1|i_{k-1}}^{i_{k-1}} \quad (3.29)$$

$$\mathbf{P}_{k|k-1}^{i_k i_{k-1}} = \mathbf{F}_{k|k-1}^{i_k} \mathbf{P}_{k-1|i_{k-1}}^{i_{k-1}} \mathbf{F}_{k|k-1}^{i_k \top} + \mathbf{D}_{k|k-1}^{i_k}. \quad (3.30)$$

In standard IMM applications, $p(\mathbf{x}_k, i_k|Z^{k-1})$ is approximated via moment matching (see [23, p. 56 ff] and the discussion in Appendix A.6) yielding

$$p(\mathbf{x}_k, i_k|Z^{k-1}) \approx p_{k|k-1}^{i_k} \mathcal{N}(\mathbf{x}_k; \mathbf{x}_{k|k-1}^{i_k}, \mathbf{P}_{k|k-1}^{i_k}) \quad (3.31)$$

with parameters $p_{k|k-1}^{i_k}$, $\mathbf{x}_{k|k-1}^{i_k}$ and $\mathbf{P}_{k|k-1}^{i_k}$ given by:

$$p_{k|k-1}^{i_k} = \sum_{i_{k-1}=1}^r p_{k|k-1}^{i_k i_{k-1}} \quad (3.32)$$

$$\mathbf{x}_{k|k-1}^{i_k} = \frac{1}{p_{k|k-1}^{i_k}} \sum_{i_{k-1}=1}^r p_{k|k-1}^{i_k i_{k-1}} \mathbf{x}_{k|k-1}^{i_k i_{k-1}} \quad (3.33)$$

$$\mathbf{P}_{k|k-1}^{i_k} = \frac{1}{P_{k|k-1}^{i_k}} \sum_{i_{k-1}=1}^r P_{k|k-1}^{i_k i_{k-1}} (\mathbf{P}_{k|k-1}^{i_k i_{k-1}} \quad (3.34)$$

$$+ (\mathbf{x}_{k|k-1}^{i_k i_{k-1}} - \mathbf{x}_{k|k-1}^{i_k})(\mathbf{x}_{k|k-1}^{i_k i_{k-1}} - \mathbf{x}_{k|k-1}^{i_k})^\top). \quad (3.35)$$

If the predictions of the kinematic state variables \mathbf{x}_k are the only objects of interest, $p(\mathbf{x}_k|Z^{k-1})$ is a direct result from marginalization and is given by a Gaußian sum with r mixture components:

$$p(\mathbf{x}_k|Z^{k-1}) = \sum_{i_k=1}^r P_{k|k-1}^{i_k} \mathcal{N}(\mathbf{x}_k; \mathbf{x}_{k|k-1}^{i_k}, \mathbf{P}_{k|k-1}^{i_k}). \quad (3.36)$$

3.3 Data Update: Filtering

The filtering update equation for the conditional probability density function $p(X_k|Z^k)$ that represents our knowledge of the present object state given all available information can be represented according to Bayes' Theorem by:

$$p(X_k|Z^k) = p(X_k|Z_k, m_k, Z^{k-1}) \quad (3.37)$$

$$= \frac{p(Z_k, m_k|X_k) p(X_k|Z^{k-1})}{\int dX_k p(Z_k, m_k|X_k) p(X_k|Z^{k-1})}. \quad (3.38)$$

This equation states how $p(X_k|Z^k)$ is obtained by combining the prediction density $p(X_k|Z^{k-1})$ with the sensor model $p(Z_k, m_k|X_k)$. As the sensor model appears both in the denominator and the numerator, the conditional densities $p(Z_k, m_k|X_k)$ need to be known up to a factor independent of the object state X_k only. Each function $\ell(X_k; Z_k, m_k) \propto p(Z_k, m_k|X_k)$ provides the same result. This observation is the reason for introducing the term “likelihood function” for denoting functions that are proportional to the conditional probability density $p(Z_k, m_k|X_k)$.

3.3.1 Kalman Filtering

Let us consider kinematic object states only, $X_k = \mathbf{x}_k$, and sensors that produce measurements related to them. Under conditions where the data-to-object associations are unambiguous, e.g. for well-separated objects without false sensor data ($\rho_F = 0$), and in the case of a Gauß-Markov evolution model, such as given by Eq. 2.8, and a Gaußian sensor model (Eq. 2.19), the Bayesian approach leads to the well-known Kalman filter update equations. Kalman filtering can thus be considered as a simple straight-forward realization of the more general Bayesian filtering paradigm.

Equation 3.38 yields according to the product formula for Gaussians (Eq. A.28):

$$p(\mathbf{x}_k | Z^k) = \frac{\mathcal{N}(\mathbf{z}_k; \mathbf{H}_k \mathbf{x}_k, \mathbf{R}_k) \mathcal{N}(\mathbf{x}_k; \mathbf{x}_{k|k-1}, \mathbf{P}_{k|k-1})}{\int d\mathbf{x}_k \mathcal{N}(\mathbf{z}_k; \mathbf{H}_k \mathbf{x}_k, \mathbf{R}_k) \mathcal{N}(\mathbf{x}_k; \mathbf{x}_{k|k-1}, \mathbf{P}_{k|k-1})} \quad (3.39)$$

$$= \frac{\mathcal{N}(\mathbf{z}_k; \mathbf{H}_k \mathbf{x}_{k|k-1}, \mathbf{S}_{k|k-1}) \mathcal{N}(\mathbf{x}_k; \mathbf{x}_{k|k}, \mathbf{P}_{k|k})}{\int d\mathbf{x}_k \mathcal{N}(\mathbf{z}_k; \mathbf{H}_k \mathbf{x}_{k|k-1}, \mathbf{S}_{k|k-1}) \mathcal{N}(\mathbf{x}_k; \mathbf{x}_{k|k}, \mathbf{P}_{k|k})} \quad (3.40)$$

$$= \mathcal{N}(\mathbf{x}_k; \mathbf{x}_{k|k}, \mathbf{P}_{k|k}), \quad (3.41)$$

where the parameters $\mathbf{x}_{k|k}$, $\mathbf{P}_{k|k}$ of the resulting Gaussian are alternatively given by:

$$\mathbf{x}_{k|k} = \begin{cases} \mathbf{x}_{k|k-1} + \mathbf{W}_{k|k-1}(\mathbf{z}_k - \mathbf{H}_k \mathbf{x}_{k|k-1}) \\ \mathbf{P}_{k|k}(\mathbf{P}_{k|k-1}^{-1} \mathbf{x}_{k|k-1} + \mathbf{H}_k^\top \mathbf{R}_k^{-1} \mathbf{z}_k) \end{cases} \quad (3.42)$$

$$\mathbf{P}_{k|k} = \begin{cases} \mathbf{P}_{k|k-1} - \mathbf{W}_{k|k-1} \mathbf{S}_{k|k-1} \mathbf{W}_{k|k-1}^\top \\ (\mathbf{P}_{k|k-1}^{-1} + \mathbf{H}_k^\top \mathbf{R}_k^{-1} \mathbf{H}_k)^{-1} \end{cases} . \quad (3.43)$$

Note that there are equivalent formulations of the Kalman update formulae according to various versions of the product formula (Eq. A.28). The innovation covariance matrix $\mathbf{S}_{k|k-1}$ has already appeared earlier in our considerations (see Eq. 3.19), while the *Kalman Gain* matrix is given by:

$$\mathbf{W}_{k|k-1} = \mathbf{P}_{k|k-1} \mathbf{H}_{k|k-1}^\top \mathbf{S}_{k|k-1}^{-1}. \quad (3.44)$$

In Eq. 3.41, the factor $\mathcal{N}(\mathbf{z}_k; \mathbf{H}_k \mathbf{x}_{k|k-1}, \mathbf{S}_k)$ does not depend on the integration variable \mathbf{x}_k and can be drawn in front of the integral, thus canceling the corresponding quantity in the numerator. Note that the matrix $\mathbf{S}_{k|k-1}$ to be inverted when calculating the Kalman gain matrix has the same dimension as the measurement vector \mathbf{z}_k , i.e. $\mathbf{S}_{k|k-1}$ is a low-dimensional matrix in general.

3.3.2 IMM Filtering

This update philosophy can easily be generalized to apply to situations where IMM evolution models are used, i.e. if the object state is given by $X_k = (\mathbf{x}_k, i_k)$. We immediately obtain:

$$p(\mathbf{x}_k, i_k | Z^k) = \frac{p_{k|k-1}^{i_k} \mathcal{N}(\mathbf{z}_k; \mathbf{H}_k \mathbf{x}_k, \mathbf{R}_k) \mathcal{N}(\mathbf{x}_k; \mathbf{x}_{k|k-1}^{i_k}, \mathbf{P}_{k|k-1}^{i_k})}{\sum_{i_k} p_{k|k-1}^{i_k} \int d\mathbf{x}_k \mathcal{N}(\mathbf{z}_k; \mathbf{H}_k \mathbf{x}_k, \mathbf{R}_k) \mathcal{N}(\mathbf{x}_k; \mathbf{x}_{k|k-1}^{i_k}, \mathbf{P}_{k|k-1}^{i_k})} \quad (3.45)$$

$$= \frac{p_{k|k-1}^{i_k} \mathcal{N}(\mathbf{z}_k; \mathbf{H}_k \mathbf{x}_{k|k-1}^{i_k}, \mathbf{S}_{k|k-1}^{i_k}) \mathcal{N}(\mathbf{x}_k; \mathbf{x}_{k|k}^{i_k}, \mathbf{P}_{k|k}^{i_k})}{\sum_{i_k} p_{k|k-1}^{i_k} \mathcal{N}(\mathbf{z}_k; \mathbf{H}_k \mathbf{x}_{k|k-1}^{i_k}, \mathbf{S}_{k|k-1}^{i_k}) \int d\mathbf{x}_k \mathcal{N}(\mathbf{x}_k; \mathbf{x}_{k|k}^{i_k}, \mathbf{P}_{k|k}^{i_k})} \quad (3.46)$$

$$= p_{k|k}^{i_k} \mathcal{N}(\mathbf{x}_k; \mathbf{x}_{k|k}^{i_k}, \mathbf{P}_{k|k}^{i_k}), \quad (3.47)$$

where the parameters $\mathbf{x}_{k|k}^{i_k}$, $\mathbf{P}_{k|k}^{i_k}$ are given by a Kalman filtering update based on $\mathbf{x}_{k|k-1}^{i_k}$, $\mathbf{P}_{k|k-1}^{i_k}$ and $\mathbf{S}_{k|k-1}^{i_k} = \mathbf{H}_k \mathbf{P}_{k|k-1}^{i_k} \mathbf{H}_k^\top + \mathbf{R}_k$, while the weighting factors $p_{k|k}^{i_k}$ depend on the sensor data \mathbf{z}_k and are given by:

$$p_{k|k}^{i_k} = \frac{p_{k|k-1}^{i_k} \mathcal{N}(\mathbf{z}_k; \mathbf{H}_k \mathbf{x}_{k|k-1}^{i_k}, \mathbf{S}_{k|k-1}^{i_k})}{\sum_{i_k} p_{k|k-1}^{i_k} \mathcal{N}(\mathbf{z}_k; \mathbf{H}_k \mathbf{x}_{k|k-1}^{i_k}, \mathbf{S}_{k|k-1}^{i_k})}. \quad (3.48)$$

If only the kinematic state variables \mathbf{x}_k are of interest, $p(\mathbf{x}_k | Z^k)$ is given by a Gaussian sum with r mixture components via marginalization:

$$p(\mathbf{x}_k | Z^k) = \sum_{i_k} p_{k|k}^{i_k} \mathcal{N}(\mathbf{x}_k; \mathbf{x}_{k|k}^{i_k}, \mathbf{P}_{k|k}^{i_k}). \quad (3.49)$$

An Alternative

So-called ‘Generalized Pseudo-Bayesian’ realizations of the IMM filtering problem (GPB, [24, 25]) fit well into this framework. The difference between GPB and standard IMM filtering is simply characterized by the instant of time when the moment-matching step is performed. While in standard IMM this is done after the prediction step and before the new sensor data are processed, GPB filtering approximates the probability density

$$\begin{aligned} p(\mathbf{x}_k, i_k | Z^k) &\propto \mathcal{N}(\mathbf{z}_k; \mathbf{H}_k \mathbf{x}_k, \mathbf{R}_k) \sum_{i_{k-1}} p_{k|k-1}^{i_k i_{k-1}} \mathcal{N}(\mathbf{x}_k; \mathbf{x}_{k|k-1}^{i_k i_{k-1}}, \mathbf{P}_{k|k-1}^{i_k i_{k-1}}) \\ &= \sum_{i_{k-1}} p_{k|k-1}^{i_k i_{k-1}} \mathcal{N}(\mathbf{z}_k; \mathbf{H}_k \mathbf{x}_{k|k-1}^{i_k i_{k-1}}, \mathbf{S}_{k|k-1}^{i_k i_{k-1}}) \mathcal{N}(\mathbf{x}_k; \mathbf{x}_{k|k}^{i_k i_{k-1}}, \mathbf{P}_{k|k}^{i_k i_{k-1}}) \\ &\approx p_{k|k}^{i_k} \mathcal{N}(\mathbf{x}_k; \mathbf{x}_{k|k}^{i_k}, \mathbf{P}_{k|k}^{i_k}) \end{aligned}$$

with appropriately defined mixture parameters that are directly given by the product formula A.28. Since the moment matching is done with the updated weighting factors, GPB methods show a better reaction to abrupt maneuvers. For a more rigorous discussion of these topics see [26].

3.3.3 MHT Filtering

In the case of ambiguous sensor data, likelihood functions such as in Eq. 2.40 are essentially characterized by taking different data interpretation hypotheses into

account. They are the basis for *Multiple Hypothesis Tracking* techniques (MHT, [27, 28]). In such situations, the origin of a time series $Z^k = \{Z_k, m_k, Z^{k-1}\}$ of sensor data accumulated up to the time t_k can be interpreted by interpretation histories $\mathbf{j}_k = (j_k, \dots, j_1)$, $0 \leq j_k \leq m_k$ that assume a certain data interpretation j_l to be true at each data collection time t_l , $1 \leq l \leq k$.

Via marginalization, for kinematic object states $X_{k-1} = \mathbf{x}_{k-1}$, the previous filtering density $p(\mathbf{x}_{k-1}|Z^{k-1})$ can be written as a mixture over the interpretation histories \mathbf{j}_{k-1} . Let us furthermore assume that its components are given by Gaussians:

$$p(\mathbf{x}_{k-1}|Z^{k-1}) = \sum_{\mathbf{j}_{k-1}} p(\mathbf{x}_{k-1}|\mathbf{j}_{k-1}, Z^{k-1}) p(\mathbf{j}_{k-1}|Z^{k-1}) \quad (3.50)$$

$$= \sum_{\mathbf{j}_{k-1}} p_{\mathbf{j}_{k-1}} \mathcal{N}(\mathbf{x}_{k-1}; \mathbf{x}_{k-1|k-1}^{\mathbf{j}_{k-1}}, \mathbf{P}_{k-1|k-1}^{\mathbf{j}_{k-1}}). \quad (3.51)$$

With a Gauß-Markov evolution model such as in Eq. 2.8, the prediction densities obey a similar representation:

$$p(\mathbf{x}_k|Z^{k-1}) = \sum_{\mathbf{j}_{k-1}} p_{\mathbf{j}_{k-1}} \mathcal{N}(\mathbf{x}_k; \mathbf{x}_{k|k-1}^{\mathbf{j}_{k-1}}, \mathbf{P}_{k|k-1}^{\mathbf{j}_{k-1}}), \quad (3.52)$$

where $\mathbf{x}_{k|k-1}^{\mathbf{j}_{k-1}}$, $\mathbf{P}_{k|k-1}^{\mathbf{j}_{k-1}}$ result from the Eqs. 3.13 and 3.14. By making use of the likelihood function for uncertain data discussed earlier (Eq. 2.40) and according to Bayes' Theorem, we obtain:

$$p(\mathbf{x}_k|Z^k) = \frac{\sum_{\mathbf{j}_k, \mathbf{j}_{k-1}} \ell_{j_k}(\mathbf{x}_k) p_{\mathbf{j}_{k-1}} \mathcal{N}(\mathbf{x}_k; \mathbf{x}_{k|k-1}^{\mathbf{j}_{k-1}}, \mathbf{P}_{k|k-1}^{\mathbf{j}_{k-1}})}{\sum_{\mathbf{j}_k, \mathbf{j}_{k-1}} \int d\mathbf{x}_k \ell_{j_k}(\mathbf{x}_k) p_{\mathbf{j}_{k-1}} \mathcal{N}(\mathbf{x}_k; \mathbf{x}_{k|k-1}^{\mathbf{j}_{k-1}}, \mathbf{P}_{k|k-1}^{\mathbf{j}_{k-1}})} \quad (3.53)$$

$$= \sum_{\mathbf{j}_k} p_{\mathbf{j}_k} \mathcal{N}(\mathbf{x}_k; \mathbf{x}_{k|k}^{\mathbf{j}_k}, \mathbf{P}_{k|k}^{\mathbf{j}_k}) \quad (3.54)$$

by using the product formula for Gaussians. The weighting factors $p_{\mathbf{j}_k}$ are given by:

$$p_{\mathbf{j}_k} = \frac{p_{\mathbf{j}_k}^*}{\sum_{\mathbf{j}_k} p_{\mathbf{j}_k}^*} \quad (3.55)$$

with the unnormalized weighting update:

$$p_{\mathbf{j}_k}^* = p_{\mathbf{j}_{k-1}} \begin{cases} (1 - P_D) \rho_F & \text{for } j_k = 0 \\ P_D \mathcal{N}(\mathbf{z}_k^{j_k}; \mathbf{H}_k \mathbf{x}_{k|k-1}^{\mathbf{j}_{k-1}}, \mathbf{S}_{k|k-1}^{\mathbf{j}_{k-1}}) & \text{for } j_k \neq 0 \end{cases}, \quad (3.56)$$

while $\mathbf{x}_{k|k}^{\mathbf{j}_k}$ and $\mathbf{P}_{k|k}^{\mathbf{j}_k}$ result from:

$$\mathbf{x}_{k|k}^j = \begin{cases} \mathbf{x}_{k|k-1}^j & \text{for } j_k = 0 \\ \mathbf{x}_{k|k-1}^j + \mathbf{W}_{k|k-1}^j (\mathbf{z}_k^j - \mathbf{H}_k \mathbf{x}_{k|k-1}^j) & \text{for } j_k \neq 0 \end{cases} \quad (3.57)$$

$$\mathbf{P}_{k|k}^j = \begin{cases} \mathbf{P}_{k|k-1}^j & \text{for } j_k = 0 \\ \mathbf{P}_{k|k-1}^j - \mathbf{W}_{k|k-1}^j \mathbf{S}_{k|k-1}^j \mathbf{W}_{k|k-1}^{j\top} & \text{for } j_k \neq 0 \end{cases} \quad (3.58)$$

with the corresponding innovation covariance and Kalman gain matrices

$$\mathbf{S}_{k|k-1}^j = \mathbf{H}_k \mathbf{P}_{k|k-1}^j \mathbf{H}_k^\top + \mathbf{R}_k^j \quad (3.59)$$

$$\mathbf{W}_{k|k-1}^j = \mathbf{P}_{k|k-1}^j \mathbf{H}_{k|k-1}^\top (\mathbf{S}_{k|k-1}^j)^{-1}, \quad (3.60)$$

which are defined in analogy to the expressions in Eqs. 3.19 and 3.44. This filtering update philosophy can directly be generalized to IMM-MHT-type techniques [29].

According to the previous discussion, each mixture component

$$p_{k|k}^j p(\mathbf{x}_k | \mathbf{j}_k, Z^k)$$

of the resulting densities $p(\mathbf{x}_k | Z^k)$ represents a *track hypothesis*. The structure of a Gaussian mixture for $p(\mathbf{x}_k | Z^k)$ also occurs if an IMM prediction $p(\mathbf{x}_k | Z^{k-1})$ (see previous subsection) is updated by using a Gaussian likelihood according to Eq. 3.49, where $p(i_k | Z^k) p(\mathbf{x}_k | i_k, Z^k)$ can be considered as a *model hypothesis*. IMM filtering may thus be considered as a multiple hypothesis tracking method as well. See [30, 31] for an alternative treatment of the multiple hypothesis tracking problem by exploiting expectation maximization techniques.

Figure 3.3 provides a schematic illustration of MHT filtering. A mixture component p^i of the filtering density at time t_k is predicted to time t_{k+1} . Due to uncertainty in the object evolution, the predicted component is broadened (dashed line). Let us assume that three measurements are in the expectation gate, which can be interpreted by four data interpretation hypotheses. The likelihood function is thus a sum of three Gaussians and a constant. The subsequent filtering thus spawns the predicted component into four filtering components with different weights depending on the innovation square of the sensor measurement belonging to each component.

Approximations

In case of a more severe clutter background or in a multiple object tracking task with expectation gates overlapping for a longer time, Bayesian tracking filters inevitably lead to mixture densities $p(\mathbf{x}_k | Z^k)$ with an exponentially growing number of mixture components involved. In contrast to the rigorous Bayesian reasoning, the choice of a prudent approximation scheme is in some sense an “art” depending on the particular application considered.

Practical experience in many real-world applications (see [32–34], for example) shows, however, that the densities are usually characterized by several distinct modes. By using

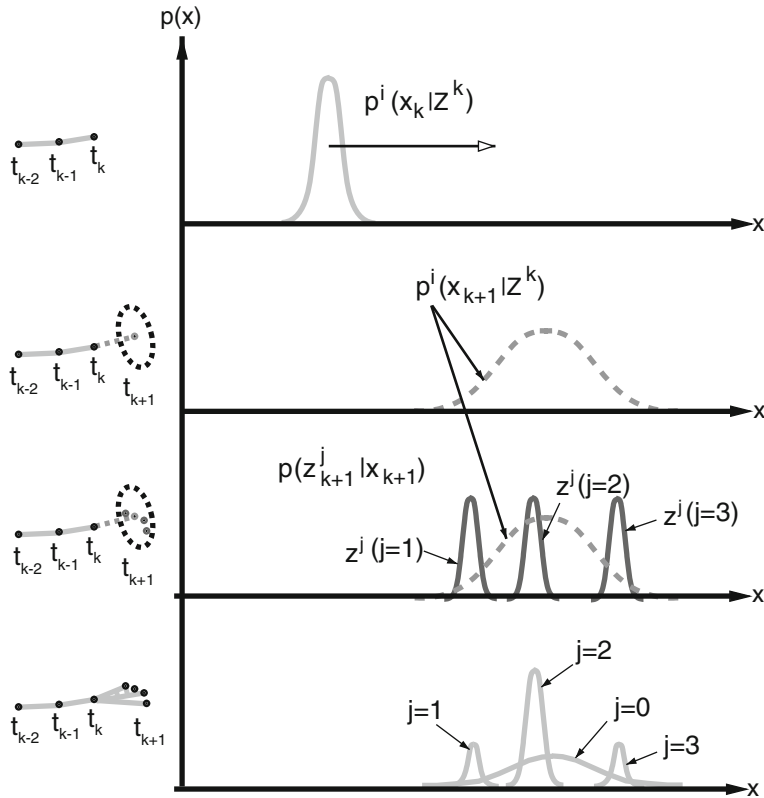


Fig. 3.3 Simplified schematic illustration of the MHT filtering process with 4 measurements to be processed at time t_{k+1}

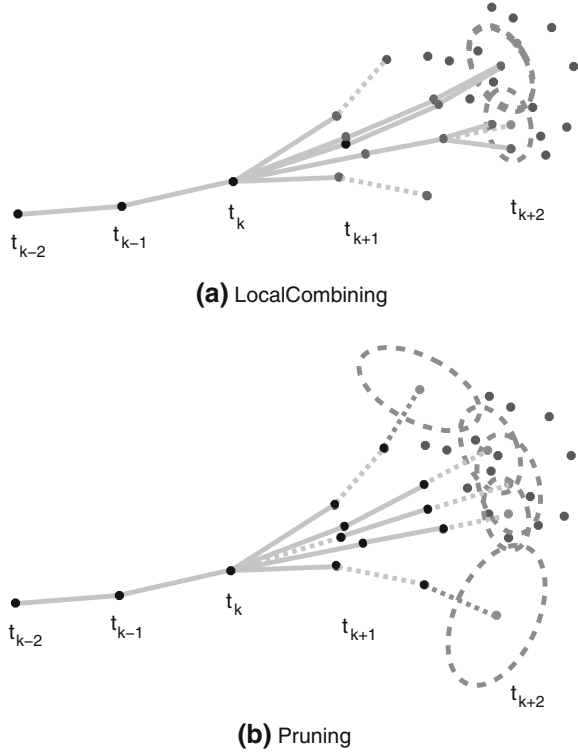
- *individual gating* for each track hypothesis,
- *local combining* of similar components via moment matching, and
- *pruning* of irrelevant mixture components,

memory explosions can be avoided without destroying the multi-modal structure of the densities $p(\mathbf{x}_k | Z^k)$. Provided this is carefully done with data-driven adaptivity, all statistically relevant information can be preserved, while keeping the number of mixture components under control, i.e. the number of mixture components involved may be fluctuating and even large in critical situations, but does not grow explosively [35–38]. This strategy was first applied by van Keuk et al. [39] and is illustrated in Fig. 3.4.

PDA-type filtering according to Bar Shalom, where *all* mixture components are combined via moment matching, is a limiting case of such techniques [23]. As the phenomenon of distinct modes is inherent in the uncertain origin of the received data, however, relevant statistical information would get lost if global combining

Fig. 3.4 Schematic illustration: local combining of similar components via moment matching and pruning of irrelevant mixture components.

a Local combining, **b** Pruning



were applied to such cases. The use of PDA-type filtering is thus confined to a relatively restricted area in parameter space (defined by ρ_F , P_D , for instance).

3.4 Object State Retrodiction

For making statements about past object states X_l at time instants t_l with $l < k$, given that sensor information Z^k is available up to the present time t_k , the probability density functions $p(X_l|Z^k)$, i.e. the retrodiction densities, must be calculated. As before in filtering, Bayes Theorem is the key to an iterative calculation scheme, which starts with the knowledge on the object $p(X_k|Z^k)$ available at the present time t_k and is directed towards the past. In deriving a retrodiction update formula, which relates $p(X_l|Z^k)$ to the previously obtained retrodiction density $p(X_{l+1}|Z^k)$ calculated for time t_{l+1} , the object state X_{l+1} at this very time is brought into play via marginalization,

$$p(X_l|Z^k) = \int dX_{l+1} p(X_l, X_{l+1}|Z^k) \quad (3.61)$$

$$= \int dX_{l+1} p(X_l|X_{l+1}, Z^k) p(X_{l+1}|Z^k). \quad (3.62)$$

Since in this equation $p(X_{l+1}|Z^k)$ is assumed to be available, it remains to understand the meaning of the density $p(X_l|X_{l+1}, Z^k)$ in the integrand of the previous equation. It seems to be intuitively clear that the knowledge on the object state X_l at time t_l does not depend on the sensor data produced at t_{l+1}, \dots, t_k , i.e. $p(X_l|X_{l+1}, Z^k) = p(X_l|X_{l+1})$. In Appendix A.7, a more formal argumentation is given. A subsequent use of Bayes' Theorem yields:

$$p(X_l|X_{l+1}, Z^k) = p(X_l|X_{l+1}, Z^l) \quad (3.63)$$

$$= \frac{p(X_{l+1}|X_l) p(X_l|Z^l)}{\int dX_l p(X_{l+1}|X_l) p(X_l|Z^l)}. \quad (3.64)$$

The retrodiction update equation for $p(X_l|Z^k)$ is thus given by:

$$p(X_l|Z^k) = \int dX_{l+1} \frac{p(X_{l+1}|X_l) p(X_l|Z^l)}{p(X_{l+1}|Z^l)} p(X_{l+1}|Z^k) \quad (3.65)$$

and combines the previously obtained retrodiction, filtering, and prediction densities as well as the object evolution model.

We assemble several characteristic features of retrodiction techniques:

1. In the given formulation, retrodiction applies to single as well as multiple objects, to well-separated objects, object formations, and objects characterized by a more general state.
2. The retrodicted density for time l is completely determined by the filtering density at time l and the following instants of time up to the present ($l \leq k$). Retrodiction is thus decoupled from filtering and prediction and may be switched off without affecting the tracking filter performance (e.g. in overload situations).
3. Accurate filtering and prediction is prerequisite to accurate retrodiction. Provided these processing steps were performed approximately optimally, the retrodiction loop provides an approximately optimal description of the past object states.
4. Besides making use of the underlying evolution model of the objects, retrodiction refers to no other modeling assumption. In particular, the sensor data are not reprocessed by retrodiction.
5. Retrodiction can provide highly precise reconstructions on object trajectory, including their velocity and acceleration histories that may contribute to object classification (see Sect. 1.3.5).
6. The classification of an air target as a helicopter, for example, could be based on precisely retrodicted velocity estimates equal to Zero. Since such retrodiction-based classifications have impact on the evolution model chosen for the future,

the example illustrates in which way retrodiction results may improve available knowledge even on present and future object states.

3.4.1 Fixed Interval Smoothing

Let us consider kinematic object states only, $X_l = \mathbf{x}_l$, and conditions where Kalman filtering is applicable. Under these conditions and using the product formula for Gaussians, Eq. 3.64 can be written as:

$$p(X_l|X_{l+1}, Z^l) = \frac{\mathcal{N}(\mathbf{x}_{l+1}; \mathbf{F}_{l+1|l}\mathbf{x}_l, \mathbf{D}_{l+1|l}) \mathcal{N}(\mathbf{x}_l; \mathbf{x}_{l|l}, \mathbf{P}_{l|l})}{\mathcal{N}(\mathbf{x}_{l+1}; \mathbf{x}_{l+1|l}, \mathbf{P}_{l+1|l})} \quad (3.66)$$

$$= \mathcal{N}(\mathbf{x}_l; \mathbf{h}_{l|l+1}(\mathbf{x}_{l+1}), \mathbf{R}_{l|l+1}) \quad (3.67)$$

with the abbreviations:

$$\mathbf{h}_{l|l+1}(\mathbf{x}_{l+1}) = \mathbf{x}_{l|l} + \mathbf{W}_{l|l+1}(\mathbf{x}_{l+1} - \mathbf{x}_{l+1|l}) \quad (3.68)$$

$$\mathbf{R}_{l|l+1} = \mathbf{P}_{l|l} - \mathbf{W}_{l|l+1}\mathbf{P}_{l+1|l}\mathbf{W}_{l|l+1}^\top \quad (3.69)$$

and a “retrodiction gain” matrix

$$\mathbf{W}_{l|l+1} = \mathbf{P}_{l|l}\mathbf{F}_{l+1|l}^\top\mathbf{P}_{l+1|l}^{-1}. \quad (3.70)$$

Note that $\mathcal{N}(\mathbf{x}_l; \mathbf{h}_{l|l+1}(\mathbf{x}_{l+1}), \mathbf{R}_{l|l+1})$ can be interpreted in analogy to a Gaussian likelihood function with a linear measurement function $\mathbf{h}_{l|l+1}(\mathbf{x}_{l+1})$. For this reason, a second use of the product finally yields:

$$p(\mathbf{x}_l|Z^k) = \int d\mathbf{x}_{l+1} p(\mathbf{x}_l|\mathbf{x}_{l+1}, Z^k) \mathcal{N}(\mathbf{x}_{l+1}; \mathbf{x}_{l+1|k}, \mathbf{P}_{l+1|k}) \quad (3.71)$$

$$= \mathcal{N}(\mathbf{x}_l; \mathbf{x}_{l|k}, \mathbf{P}_{l|k}), \quad (3.72)$$

where the parameters of the retrodicted density $p(\mathbf{x}_l|Z^k)$ are given the *Rauch-Tung-Striebel* [4] retrodiction update equations:

$$\mathbf{x}_{l|k} = \mathbf{x}_{l|l} + \mathbf{W}_{l|l+1}(\mathbf{x}_{l+1|k} - \mathbf{x}_{l+1|l}) \quad (3.73)$$

$$\mathbf{P}_{l|k} = \mathbf{P}_{l|l} + \mathbf{W}_{l|l+1}(\mathbf{P}_{l+1|k} - \mathbf{P}_{l+1|l})\mathbf{W}_{l|l+1}^\top. \quad (3.74)$$

The retrodicted state estimates $\mathbf{x}_{l|k}$ do not depend on the corresponding error covariance matrices $\mathbf{P}_{l|k}$. Their computation may thus be omitted in case of limited resources.

3.4.2 Continuous Time Retrodiction

In certain applications, there is a need to produce suitable interpolations between two retrodicted densities $p(X_l|Z^k)$ and $p(X_{l+1}|Z^k)$ at two subsequent data collection times t_l and t_{l+1} by taking full advantage of the available knowledge of the objects' evolution model [40]. For this reason, let us consider probability densities $p(X_{l+\theta}|Z^k)$ with $0 < \theta < 1$, which represent the available knowledge about the object state at an intermediate instant of time $t_l < t_{l+\theta} < t_{l+1}$. In analogy to the previous reasoning, we obtain:

$$p(X_{l+\theta}|Z^k) = \int dX_{l+1} p(X_{l+\theta}|X_{l+1}, Z^k) p(X_{l+1}|Z^k) \quad (3.75)$$

with a modified version of the density in Eq. 3.64:

$$p(X_{l+\theta}|X_{l+1}, Z^k) = \frac{p(X_{l+1}|X_{l+\theta}) p(X_{l+\theta}|Z^l)}{p(X_{l+1}|Z^l)}. \quad (3.76)$$

Note that the prediction densities $p(X_{l+\theta}|Z^l)$, $p(X_{l+1}|Z^l)$ are available according to Eq. 3.10.

Under conditions, where Kalman filtering is applicable, the Markov transition density $p(X_{l+1}|X_{l+\theta})$ is given by the Gaußian:

$$p(\mathbf{x}_{l+1}|\mathbf{x}_{l+\theta}) = \mathcal{N}(\mathbf{x}_{l+1}; \mathbf{F}_{l+1|l+\theta}\mathbf{x}_{l+\theta}, \mathbf{D}_{l+1|l+\theta}), \quad (3.77)$$

yielding as a special case of Eq. 3.67:

$$p(\mathbf{x}_{l+\theta}|\mathbf{x}_{l+1}, Z^k) = \mathcal{N}(\mathbf{x}_{l+\theta}; \mathbf{h}_{l+\theta|l+1}(\mathbf{x}_{l+1}), \mathbf{R}_{l+\theta|l+1}), \quad (3.78)$$

with the abbreviations:

$$\mathbf{h}_{l+\theta|l+1}(\mathbf{x}_{l+1}) = \mathbf{x}_{l+\theta|l} + \mathbf{W}_{l+\theta|l+1}(\mathbf{x}_{l+1} - \mathbf{x}_{l+1|l}) \quad (3.79)$$

$$\mathbf{R}_{l+\theta|l+1} = \mathbf{P}_{l+\theta|l} - \mathbf{W}_{l+\theta|l+1}\mathbf{P}_{l+1|l}\mathbf{W}_{l+\theta|l+1}^\top \quad (3.80)$$

$$\mathbf{W}_{l+\theta|l+1} = \mathbf{P}_{l+\theta|l}\mathbf{F}_{l+1|l+\theta}^\top\mathbf{P}_{l+1|l+\theta}^{-1} \quad (3.81)$$

$p(\mathbf{x}_{l+\theta}|\mathbf{x}_{l+1}, Z^k)$ directly provides an expression for the continuous time retrodiction density $p(\mathbf{x}_{l-\theta}|Z^k)$ according to the product formula:

$$p(\mathbf{x}_{l-\theta}|Z^k) = \frac{p(\mathbf{x}_{l+1}|\mathbf{x}_{l+\theta}) p(\mathbf{x}_{l+\theta}|Z^l)}{p(\mathbf{x}_{l+1}|Z^l)} \quad (3.82)$$

$$= \mathcal{N}(\mathbf{x}_{l-\theta}; \mathbf{x}_{l-\theta|k}, \mathbf{P}_{l-\theta|k}) \quad (3.83)$$

with parameters given by modified Rauch-Tung-Striebel update formulae:

$$\mathbf{x}_{l-\theta|k} = \mathbf{x}_{l-\theta|l-1} + \mathbf{W}_{l|l-\theta}(\mathbf{x}_{l|k} - \mathbf{x}_{l|l-1}) \quad (3.84)$$

$$\mathbf{P}_{l-\theta|k} = \mathbf{P}_{l-\theta|l-1} + \mathbf{W}_{l|l-\theta}(\mathbf{P}_{l|k} - \mathbf{P}_{l|l-1})\mathbf{W}_{l|l-\theta}^\top \quad (3.85)$$

$$\mathbf{W}_{l|l-\theta} = \mathbf{P}_{l-\theta|l-1}\mathbf{F}_{l|l-\theta}^\top\mathbf{P}_{l|l-1}^{-1}. \quad (3.86)$$

3.4.3 IMM Retrodiction

With an underlying IMM evolution model, we obtain the following expression for the retrodiction density:

$$p(\mathbf{x}_l, i_l|Z^k) = \sum_{i_{l+1}} \int d\mathbf{x}_{l+1} p(\mathbf{x}_l, i_l|\mathbf{x}_{l+1}, i_{l+1}, Z^k) p(\mathbf{x}_{l+1}, i_{l+1}|Z^k), \quad (3.87)$$

where we assume that the previous retrodiction density is in analogy to IMM filtering given by a weighted Gaussian:

$$p(\mathbf{x}_{l+1}, i_{l+1}|Z^k) = p_{l+1|k}^{i_{l+1}} \mathcal{N}(\mathbf{x}_{l+1}; \mathbf{x}_{l+1|k}^{i_{l+1}}, \mathbf{P}_{l+1|k}^{i_{l+1}}), \quad (3.88)$$

while the remaining factor in the integral results from:

$$p(\mathbf{x}_l, i_l|\mathbf{x}_{l+1}, i_{l+1}, Z^k) = \frac{p(\mathbf{x}_{l+1}, i_{l+1}|\mathbf{x}_l, i_l) p(\mathbf{x}_l, i_l|Z^l)}{\sum_{i_l} \int d\mathbf{x}_l p(\mathbf{x}_{l+1}, i_{l+1}|\mathbf{x}_l, i_l) p(\mathbf{x}_l, i_l|Z^l)}. \quad (3.89)$$

With $p(\mathbf{x}_l, i_l|Z^l)$ approximately given by Eq. 3.48 and the IMM evolution model in Eq. 2.11, the product formula yields in analogy to Eq. 3.67:

$$p(\mathbf{x}_l, i_l|\mathbf{x}_{l+1}, i_{l+1}, Z^k) = c_{l|l+1}^{i_l}(\mathbf{x}_{l+1}) \mathcal{N}(\mathbf{x}_l; \mathbf{h}_{l|l+1}^{i_{l+1}, i_l}(\mathbf{x}_{l+1}), \mathbf{R}_{l|l+1}^{i_{l+1}, i_l}) \quad (3.90)$$

with abbreviations $\mathbf{h}_{l|l+1}^{i_{l+1}, i_l}(\mathbf{x}_{l+1})$ and $\mathbf{R}_{l|l+1}^{i_{l+1}, i_l}$ given by:

$$\mathbf{h}_{l|l+1}^{i_{l+1}, i_l}(\mathbf{x}_{l+1}) = \mathbf{x}_{l|l}^{i_l} + \mathbf{W}_{l|l+1}^{i_{l+1}, i_l}(\mathbf{x}_{l+1} - \mathbf{F}_{l+1|l}^{i_{l+1}}\mathbf{x}_{l|l}^{i_l}) \quad (3.91)$$

$$\mathbf{R}_{l|l+1}^{i_{l+1}, i_l} = \mathbf{P}_{l|l}^{i_l} - \mathbf{W}_{l|l+1}^{i_{l+1}, i_l} \mathbf{S}_{l+1|l}^{i_{l+1}, i_l} \mathbf{W}_{l|l+1}^{i_{l+1}, i_l \top}, \quad (3.92)$$

where we used:

$$\mathbf{S}_{l+1|l}^{i_{l+1}, i_l} = \mathbf{F}_{l+1|l}^{i_{l+1}} \mathbf{P}_{l|l}^{i_l} \mathbf{F}_{l+1|l}^{i_{l+1} \top} + \mathbf{D}_{l+1|l}^{i_{l+1}} \quad (3.93)$$

$$\mathbf{W}_{l|l+1}^{i_{l+1}, i_l} = \mathbf{P}_{l|l}^{i_l} \mathbf{F}_{l+1|l}^{i_{l+1} \top} (\mathbf{S}_{l+1|l}^{i_{l+1}, i_l})^{-1} \quad (3.94)$$

and factors $c_{l|l}^{i_l}(\mathbf{x}_{l+1})$, which can be interpreted as normalized weighting factors depending on the object state \mathbf{x}_{l+1} :

$$c_{l|l+1}^{i_l}(\mathbf{x}_{l+1}) = \frac{p_{l+1|i_l} p_{l+1|l}^{i_l} \mathcal{N}(\mathbf{x}_{l+1}; \mathbf{F}_{l+1|l}^{i_{l+1}} \mathbf{x}_{l+1|l}^{i_l}, \mathbf{S}_{l+1|l}^{i_{l+1}i_l})}{\sum_{i_l} p_{l+1|i_l} p_{l+1|l}^{i_l} \mathcal{N}(\mathbf{x}_{l+1}; \mathbf{F}_{l+1|l}^{i_{l+1}} \mathbf{x}_{l+1|l}^{i_l}, \mathbf{S}_{l+1|l}^{i_{l+1}i_l})}. \quad (3.95)$$

According to these considerations, $p(\mathbf{x}_l, i_l | \mathbf{x}_{l+1}, i_{l+1}, Z^k)$ can no longer be interpreted in analogy to a Gaussian likelihood and be evaluated by exploiting the product formula. The problems are caused by the weighting factors $c_{l|l+1}^{i_l}(\mathbf{x}_{l+1|k})$, which explicitly depend on the kinematic object state at time t_{l+1} in a rather complicated way. The product formula would be directly applicable only if they were constant. The best knowledge on \mathbf{x}_{l+1} available at time t_k , however, is given by the expectation $\mathbf{x}_{l+1|k}$ calculated in the previous retrodiction step. We thus consider the approximation:

$$c_{l|l+1}^{i_l}(\mathbf{x}_{l+1}) \approx c_{l|l+1}^{i_l}(\mathbf{x}_{l+1|k}), \quad (3.96)$$

which leads to an approximate expression for the retrodicted density:

$$p(\mathbf{x}_l, i_l | Z^k) \approx \sum_{i_{l+1}} \int d\mathbf{x}_{l+1} c_{l|l+1}^{i_l} p_{l+1|k}^{i_{l+1}} \mathcal{N}(\mathbf{x}_l; \mathbf{h}_{l|l+1}^{i_{l+1}, i_l}(\mathbf{x}_{l+1}), \mathbf{R}_{l|l+1}^{i_{l+1}, i_l}) \times \mathcal{N}(\mathbf{x}_{l+1}; \mathbf{x}_{l+1|k}^{i_{l+1}}, \mathbf{P}_{l+1|k}^{i_{l+1}}) \quad (3.97)$$

$$= \sum_{i_{l+1}} p_{l|k}^{i_{l+1}i_l} \mathcal{N}(\mathbf{x}_l; \mathbf{x}_{l|k}^{i_{l+1}i_l}, \mathbf{P}_{l|k}^{i_{l+1}i_l}) \quad (3.98)$$

with $p_{l|k}^{i_{l+1}i_l} = c_{l|l+1}^{i_l} p_{l+1|k}^{i_{l+1}}$, while the parameters $\mathbf{x}_{l|k}^{i_{l+1}i_l}$ and $\mathbf{P}_{l|k}^{i_{l+1}i_l}$ are obtained by the Rauch-Tung-Striebel formulae 3.73, 3.74. As in standard IMM prediction, $p(\mathbf{x}_k, i_k | Z^{k-1})$ is approximated via moment matching ([23, p. 56 ff], Appendix A.6) yielding

$$p(\mathbf{x}_l, i_l | Z^k) \approx p_{l|k}^{i_l} \mathcal{N}(\mathbf{x}_l; \mathbf{x}_{l|k}^{i_l}, \mathbf{P}_{l|k}^{i_l}) \quad (3.99)$$

with parameters $p_{l|k}^{i_l}$, $\mathbf{x}_{l|k}^{i_l}$, and $\mathbf{P}_{l|k}^{i_l}$ given by:

$$\begin{aligned} p_{l|k}^{i_l} &= \sum_{i_{l+1}=1}^r p_{l|k}^{i_{l+1}i_l} \\ \mathbf{x}_{l|k}^{i_l} &= \frac{1}{p_{l|k}^{i_l}} \sum_{i_{l+1}=1}^r p_{l|k}^{i_{l+1}i_l} \mathbf{x}_{l|k}^{i_{l+1}i_l} \\ \mathbf{P}_{l|k}^{i_l} &= \frac{1}{p_{l|k}^{i_l}} \sum_{i_{l+1}=1}^r p_{l|k}^{i_{l+1}i_l} (\mathbf{P}_{k|k-1}^{i_k i_{k-1}} + (\mathbf{x}_{l|k}^{i_{l+1}i_l} - \mathbf{x}_{l|k}^{i_l})(\mathbf{x}_{l|k}^{i_{l+1}i_l} - \mathbf{x}_{l|k}^{i_l})^\top). \end{aligned} \quad (3.100)$$

If only the retrodictions of the kinematic state variables \mathbf{x}_l are of interest, $p(\mathbf{x}_l|Z^k)$ is given by a Gaussian sum with r mixture components:

$$p(\mathbf{x}_l|Z^k) = \sum_{i_l=1}^r p(\mathbf{x}_l, i_l|Z^k) \quad (3.101)$$

$$\approx \sum_{i_l=1}^r p_{l|k}^{i_l} \mathcal{N}(\mathbf{x}_l; \mathbf{x}_{l|k}^{i_l}, \mathbf{P}_{l|k}^{i_l}). \quad (3.102)$$

3.4.4 MHT Retrodiction

As discussed before in the case of MHT filtering, data interpretation histories \mathbf{j}_k provide possible explanations of the origin of a time series Z^k consisting of ambiguous sensor data. The notion of retrodiction can also be applied to those situations. Due to the total probability theorem and under the conditions discussed in Sect. 2.3.3, the retrodiction $p(\mathbf{x}_l|Z^k)$ may be represented by a mixture:

$$p(\mathbf{x}_l|Z^k) = \sum_{\mathbf{j}_k} p(\mathbf{x}_l, \mathbf{j}_k|Z^k) \quad (3.103)$$

$$= \sum_{\mathbf{j}_k} p_{\mathbf{j}_k} \mathcal{N}(\mathbf{x}_l; \mathbf{x}_{l|k}^{\mathbf{j}_k}, \mathbf{P}_{l|k}^{\mathbf{j}_k}). \quad (3.104)$$

Since for any given data interpretation history \mathbf{j}_k the conditional probability densities $p(\mathbf{x}_l|\mathbf{j}_k, Z^k)$ are unambiguous, the parameters $\mathbf{x}_{l|k}^{\mathbf{j}_k}$, $\mathbf{P}_{l|k}^{\mathbf{j}_k}$ of the retrodiction density $p(\mathbf{x}_l|Z^k)$ directly result from the Rauch-Tung-Striebel formulae, while the weighting factors $p_{\mathbf{j}_k}$ are those obtained in the filtering step. In other words, the retrodiction process proceeds along the branches of the data interpretation hypotheses tree.

In the following, we assemble several aspects of MHT retrodiction.

1. For well-separated objects and a single evolution model under ideal operational conditions, i.e. without false measurements and assuming perfect detection, the approach comes down to the Rauch-Tung-Striebel fixed-interval smoothing as a limiting case. Hence, the Rauch-Tung-Striebel formulae play a role in MHT retrodiction that is completely analogous to the Kalman update formulae in MHT filtering.
2. MHT retrodiction can be combined with IMM evolution models. Under ideal conditions with well-separated objects, we obtain a hierarchy of approximations to the original retrodiction problem. Adopting the standard terminology [4], the Fraser-Potter-type algorithms in [41, 42] are approximations to optimal retrodiction in the two-filter form insofar as the results of backward and forward filters are combined. In our view, however, the Rauch-Tung-Striebel-type formulation of approximate IMM-smoothing offers advantages over Fraser-Potter-type

algorithms insofar as computational effort is concerned (e.g. matrix inversions involved). In addition, Rauch-Tung-Striebel-type algorithms are initialized by the filtering results (no diffuse prior density).

3. In order to avoid memory explosions such as mentioned in Sect. 3.3.3, those mixture components in the filtering process are neglected ($p_{\mathbf{j}_k} \rightarrow 0$) that are either statistically irrelevant or can be combined with other mixture components. This has useful consequences: If all hypotheses with the same prehistory \mathbf{j}_{k-1} are canceled, \mathbf{j}_{k-1} is irrelevant itself ($p_{\mathbf{j}_{k-1}} \rightarrow 0$). This scheme may be applied repeatedly to all subsequent prehistories $\mathbf{j}_l, l < k - 1$, finally leading to a unique track. This process is called *reconstruction of histories* [28, 29, 32]. The work reported in [43] also points in that direction. As observed in [28, 32], we assemble the following facts.

- (a) The history is correctly reconstructed with high probability.
- (b) The number of relevant hypotheses to be stored can be drastically reduced.
- (c) The number of missed detections in a reconstructed history provides on-line estimations of the detection probability that are otherwise not easily obtainable.

4. Oliver Drummond's *Retrodiction of Probabilities* [2, 3] is an approximation of the retrodiction density $p(\mathbf{x}_k|Z^k)$ that omits the Rauch-Tung-Striebel update of the retrodicted expectation vector and the corresponding covariance matrix. In other words, we assume:

$$\mathcal{N}(\mathbf{x}_l; \mathbf{x}_{l|k}^{\mathbf{j}_k}, \mathbf{P}_{l|k}^{\mathbf{j}_k}) \approx \mathcal{N}(\mathbf{x}_l; \mathbf{x}_{l|l}^{\mathbf{j}_l}, \mathbf{P}_{l|l}^{\mathbf{j}_l}). \quad (3.105)$$

As a direct consequence, we yield approximations to the density functions

$$p(\mathbf{x}_l|Z^k) \approx \sum_{\mathbf{j}_l} p_{\mathbf{j}_l}^* \mathcal{N}(\mathbf{x}_l; \mathbf{x}_{l|l}^{\mathbf{j}_l}, \mathbf{P}_{l|l}^{\mathbf{j}_l}) \quad (3.106)$$

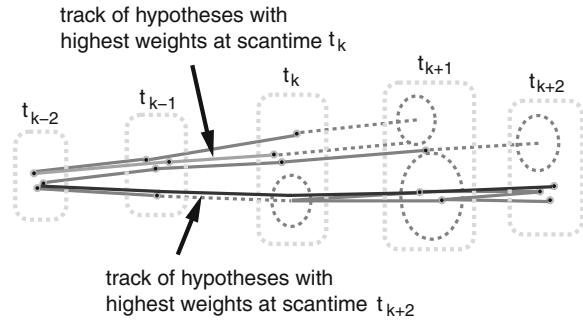
with mixture coefficients $p_{\mathbf{j}_l}^*$ that are recursively defined by

$$p_{\mathbf{j}_l}^* = \begin{cases} p_{\mathbf{j}_k} & \text{for } l = k \\ \sum_{\mathbf{j}_{l+1} \in J_{l+1}|\mathbf{j}_l} p_{\mathbf{j}_{l+1}}^* & \text{for } l < k, \end{cases} \quad (3.107)$$

where the sum is taken over all histories \mathbf{j}_{l+1} with the same prehistory \mathbf{j}_l . True hypotheses that incidentally have had a small weight in at the time, when they were originally created, may well increase in weight incrementally during this procedure as time goes by. Retrodiction of discrete probabilities is computationally cheap since only weighting factors are to be re-processed, leaving the state estimates and their error covariance matrices unchanged.

5. In principle, retrodiction methods do not affect the description of the current object states provided the filtering was done correctly. As previously discussed (Sect. 3.3.3), however, in any practical realization approximations must be applied

Fig. 3.5 Schematic overview of retrodiction within a multiple hypothesis framework



to avoid memory explosions. In this context, retrodiction-based pruning offers the potential of improved approximations to optimal filtering. The scheme generalizes the strategy in [1, 3] in that, as each set of sensor data becomes available, the modification of earlier track hypotheses has impact on subsequent tracks (Multiple Frame Data Association).

- (a) In *retrodiction-based cut-off*, we first permit hypotheses with even very small weights at present. By retrodiction of probabilities, retrospectively some past hypotheses increase in weight, while others decrease. Then, starting at a certain time in the past, hypotheses with insignificant weights are neglected. This has impact up to the present scan since all descending track hypotheses vanish themselves, while the remaining weighting factors are renormalized. This scheme may be applied repeatedly over several data collection times.
- (b) In close analogy to retrodiction-based cut-off, we might also delay the decision if two hypotheses are to be combined, thus leading to *retrodiction-based local combining*.

Retrodiction-based pruning seems to be particularly useful in track initiation/extraction [44], an issue addressed below (Sect. 4).

Figure 3.5 provides a schematic overview of retrodiction within a multiple hypothesis framework.

3.4.5 Discussion of an Example

The following aspects are illustrated by an example with real radar data:

1. Data association conflicts arise even for well-separated objects if a high false return background is to be taken into account, which cannot completely be suppressed by clutter filtering at the signal processing level.
2. Even in the absence of unwanted sensor reports, ambiguous correlations between newly received sensor data and existing tracks are an inherent problem for objects

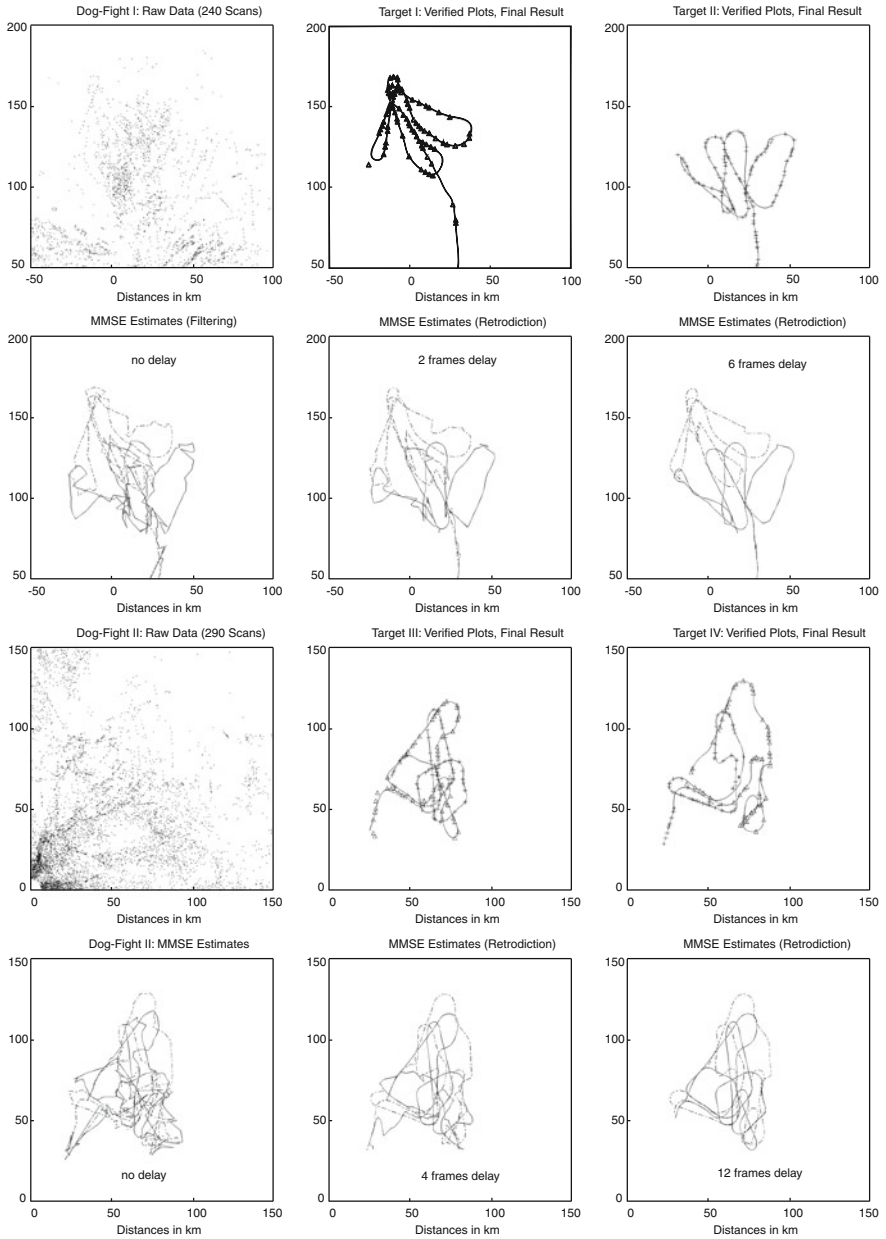


Fig. 3.6 An example taken from wide-area ground-based air surveillance: two pairs of highly maneuvering aircraft in a training situation (high residual clutter background)

moving closely-spaced for some time. Furthermore, resolution phenomena make the data association task even harder.

3. Additional problems arise from poor quality sensor data, due to large measurement errors, low signal-to-noise ratios, or fading phenomena (i.e. successively missing plots). Besides that, the scan rates may be low (especially in long-range surveillance applications).

Figure 3.6 shows a radar data set accumulated over about 240 and 290 scans, respectively. As well as many false alarms, the data of two pairs of highly maneuvering aircraft in a training situation were recorded. The detection probability is between 40 and 60%. The data were collected from a rotating S-band long-range radar measuring target range and azimuth (scan period: 10 s, range accuracy: 350 ft, bearing accuracy: 0.22° , range resolution: 1,600 ft, bearing resolution: 2.4°). Information on the real object position is crucial for evaluating tracking filters. Here a secondary radar was used. The verified primary plots are indicated by \triangle and $+$ in the figures right to the raw data along with the final tracking result (i.e. tracking output according to multiple data association hypotheses and subsequent retrodiction until no further improvement is obtained).

The 2nd and 4th row in 3.6 show for both scenarios the MMSE-estimates of the objects' positions are displayed for a retrodiction delay of zero, 2, 4, 6, and 12 scans. The estimates with no delay are simply obtained by MHT-type filtering. The resulting trajectories seem to be of small value for assessing the air situation. The related variances (very large) are not indicated. The high inaccuracy observed reflects the complex hypothesis tree resulting from ambiguous data interpretations. Multiple dynamics model filtering (IMM) does outperform single model filtering in some particular situations that are characterized by fewer data association conflicts and at least one non-maneuvering target. Aside from those situations, however, the overall impression of the pure filtering result is similar for both cases.

By using MHT-retrodiction, even a delay of two frames significantly improves the filtering output. We displayed the MMSE estimates derived from $p(\mathbf{x}_l|Z^k)$ for $l = 2, 4, 6, 12$. A delay of 6 frames (i.e. 1 min) provides easily interpretable trajectories, while the maximum gain by retrodiction is obtained after 12 frames delay. Evidently the final retrodiction results fit the verified primary plots very well. If IMM-retrodiction is used, we essentially obtain the same final trajectory. However, in certain flight phases (not too many false returns, no maneuvers) it is obtained by a shorter delay (about 1–3 frames less). i.e. Under certain circumstances, accurate speed and heading information is available earlier than in case of a single dynamics model.

References

1. O.E. Drummond, Target tracking with retrodicted discrete probabilities, in *Proceedings of SPIE 3163, Signal and Data Processing of Small Targets*, 1997, p. 249

2. O.E. Drummond, Multiple sensor tracking with multiple frame, probabilistic data association, in *SPIE 2561, Signal and Data Processing of Small Targets*, 1995, p. 322
3. O.E. Drummond, Multiple target tracking with multiple frame, probabilistic data association, in *Proceedings of SPIE 1954, Signal and Data Processing of Small Targets*, 1993, p. 394
4. A. Gelb (ed.), *Applied Optimal Estimation* (M.I.T Press, Cambridge, 1974)
5. M.E. Liggins, D.L. Hall, J. Llinas (eds.), *Handbook of Multisensor Data Fusion - Theory and Practice*, 2nd edn. (CRC Press, Boca Raton, 2008)
6. D.M. Titterton, A.F.M. Smith, U.E. Makov, *Statistical Analysis of Finite Mixture Distributions* (Wiley, New York, 1985)
7. D.L. Alspach, H.W. Sorenson, Nonlinear Bayesian estimation using gaussian sum approximation. *IEEE Trans. Autom. Control* **20**, 439–447 (1972)
8. M. Ulmke, O. Erdinc, and P. Willett, Ground moving target tracking with cardinalized Gaussian mixture PHD filtering, in *Proceedings of the 10th International Conference on Information Fusion FUSION 2007*, Quebec, Canada, July 2007
9. N. Gordon, A hybrid bootstrap filter for target tracking in clutter, *IEEE Trans. Aerosp. Electron. Syst.* **33**, 353–358 (1997)
10. B. Ristic, S. Arulampalam, N. Gordon, *Beyond the Kalman Filter: Particle Filters for Tracking Applications* (Artech House Radar Library, London, 2004)
11. D. Fox, W. Burgard, F. Dellaert, S. Thrun, Monte Carlo localization: Efficient position estimation for mobile robots, in *Proceedings of AAAI-99*.
12. A. Doucet, N. de Freitas, N. Gordon (eds.), *Sequential Monte Carlo Methods in Practice* (Springer, Berlin, 2001)
13. M. Ulmke, W. Koch, Road-map assisted ground moving target tracking. *IEEE Trans. Aerosp. Electron. Syst. AES-42* **4**, 1264–1274 (2006)
14. V. Algeier, B. Demissie, W. Koch, R. Thomä, State space initiation for blind mobile terminal position tracking. *EURASIP J. Adv. Sig. Process* **2008**(394219), 14. doi:[10.1155/2008/394219](https://doi.org/10.1155/2008/394219)
15. W. Koch, Perspectives for a Backbone technology: tracking and fusion in real-world applications, in *11th International Conference on Information Fusion, Cologne, Germany (2008)*. Under review: *IEEE AESS Magazine*
16. V. Klumpp, F. Sawo, U.D. Hanebeck, D. Franken, The sliced Gaussian mixture filter for efficient nonlinear estimation, in *11th International Conference on Information Fusion, Cologne, Germany, 2008*
17. K.-C. Chang, T. Zhi, R.K. Saha, Performance evaluation of track fusion with information matrix filter. *IEEE Trans. Aerosp. Electron. Syst.* **38**(2), 455 (2002)
18. H. Chen, T. Kirubarajan, Y. Bar-Schalom, Performance limits of track-to-track fusion versus centralized fusion: Theory and applications. *IEEE Trans. Aerosp. Electron. Syst.* **39**(2), 386 (2003)
19. C.-Y. Chong, S. Mori, H. Barker, K.-C. Chang, Architectures and algorithms for track association and fusion, in *IEEE Aerospace and Electronic Systems Society Magazine*, Jan, 2000
20. S. Mori, W.H. Barker, C.-Y. Chong, K.-C. Chang, Track association and track fusion with nondeterministic target dynamics. *IEEE Trans. Aerosp. Electron. Syst.* **38**(2), 659 (2002)
21. C.R. Berger, M. Daun, W. Koch, Low complexity track initialization from a small set of non-invertible measurements. *EURASIP J. Adv. Signal Process.*, special issue on track-before-detect techniques **2008**(756414), 15 (2008)
22. Ch. Berger, M. Daun, W. Koch, Track initialization from incomplete measurements, in *Proceedings of 10th ISIF International Conference on Information Fusion, Quebec, Canada, 2007*
23. Y. Bar-Shalom, X.-R. Li, T. Kirubarajan, *Estimation with Applications to Tracking and Navigation* (Wiley, New York, 2001)
24. Rong X. Li, V.P. Jilkov, Survey of maneuvering target tracking. Part V. Multiple model methods. *IEEE Trans. Aerosp. Electron. Syst.* **41**(4), 1255–1321 (2005)
25. X.R. Li, Hybrid Estimation Techniques, in *Control and Dynamic Systems*, ed. by C.T. Leondes, vol. 76 (Academic Press, San Diego, 1996)
26. H.A.P. Blom, J. Jygeros (Eds.), *Stochastic Hybrid Systems: Theory and Safety Critical Applications*, (Springer, Berlin, 2006)

27. S.S. Blackman, Multiple Hypothesis Methods. in *IEEE AES Magazine* **19**(1), 41–52 (2004)
28. W. Koch, On Bayesian MHT for well-separated targets in a densely cluttered environment, in *Proceedings of the IEEE International Radar Conference, RADAR'95*, Washington, May 1995, p. 323
29. W. Koch, Fixed-interval retrodiction approach to Bayesian IMM-MHT for maneuvering multiple targets, *IEEE Trans. Aerosp. Electron. Syst.* AES-36 **1**, (2000)
30. R. Streit, T. E. Luginbuhl, *Probabilistic Multi-Hypothesis Tracking*. Naval Undersea Warfare Center Dahlgren Division, *Research Report NUWC-NPT/10/428* (1995)
31. M. Wieneke, W. Koch, The PMHT: Solutions to some of its problems *In Proceedings of SPIE Signal and Data Processing of Small Targets*, San Diego, USA, Aug 2007
32. W. Koch, M. Blanchette, Tracking in densely cluttered environment - concepts and experimental results, in *Proceedings of ISATA Robotics, Motion, and Machine Vision*, Aachen, Germany, 1994, p. 215 ff
33. W. Koch, Experimental results on Bayesian MHT for maneuvering closely-spaced objects in a densely cluttered environment, in *IEE International Radar Conference RADAR'97*, Edinburgh, UK, 1999, p. 729
34. W. Koch, Generalized smoothing for multiple model/multiple hypothesis filtering: Experimental results, in *Proceedings of European Control Conference ECC'99*, Karlsruhe, Germany, CD ROM, 1999
35. D. Salmond, Mixture reduction algorithms for target tracking in clutter. *SPIE signal Data Process. Small Targets* **1305**, 434–445 (1990)
36. L.Y. Pao, Multisensor Multitarget Mixture Reduction Algorithms for Tracking. *J. Guidance Control Dyn.* **17**, 1205 (1994)
37. R. Danchick, G.E. Newnam, A fast method for finding the exact N -best hypotheses for multi-target tracking, *IEEE Trans. Aerosp. Electron. Syst.* AES-29 **2**, (1993)
38. I.J. Cox, M.L. Miller, On finding ranked assignments with application to multitarget tracking and motion correspondence. *IEEE Trans. Aerosp. Electron. Syst.* AES-31, **1**, (1995)
39. W. Fleskes, G. van Keuk, On single target tracking in dense clutter environment - Quantitative results, in *Proceedings of IEE International Radar Conference RADAR 1987*, 1987, pp. 130–134
40. W. Koch, J. Koller, M. Ulmke, Ground target tracking and road-map extraction. *ISPRS J. Photogram. Remote Sens.* **61**, 197–208 (2006)
41. H.A.P. Blom, Y. Bar-Shalom, Time-reversion of a hybrid state stochastic difference system with a jump-linear smoothing application, *IEEE Trans. Inf. Theory* **36**(4), 1990
42. R.E. Helmick, W.D. Blair, S.A. Hoffman, Fixed-interval smoothing for Markovian switching systems. *IEEE Trans. Info. Technol.* **41**(6) (1995)
43. I. Cox, J.J. Leonard, Modeling a dynamic environment using a Bayesian multiple hypothesis approach. *Artif. Intell.* **66**, 311 (1994)
44. G. van Keuk, Sequential track extraction. *IEEE Trans. Aerosp. Electron. Syst.* **34**, 1135 (1998)

Chapter 4

Sequential Track Extraction

Iterative tracking algorithms must be initiated appropriately. Under simple conditions, this is not a difficult task, as has been shown above (Eq. 3.8). For low observable objects, i.e. objects embedded in a high clutter background [1–5] or in case of incomplete measurements [6, 7], more than a single set of observations at particular data collection times are usually necessary for detecting all objects of interest moving in the sensors' fields of view. Only then, the probability density iteration can be initiated based on 'extracted' object tracks, i.e. by tentative tracks, whose existence is 'detected' by a detection process working on a higher level of abstraction. This process makes use of a time series of accumulated sensor data $Z^k = \{Z_i\}_{i=1}^k$.

4.1 Well-Separated Objects

Assuming at first that the objects are well-separated, for the sake of simplicity, we thus have to decide between two alternatives before a tracking process can be initiated:

- h_1 : Besides false data, Z^k also contains real object measurements.
- h_0 : There is no object in the FoV; all sensor data in Z^k are false.

As a special case of the more general theory of statistical decision processes, the performance of a track extraction algorithm is characterized by two probabilities related to the decision errors of first and second kind:

1. $P_1 = P(\text{accept } h_1|h_1)$, i.e. the conditional probability that h_1 is accepted given h_1 is actually true (corresponding to the detection probability P_D of a sensor discussed in Sect. 2.3.4).
2. $P_0 = P(\text{accept } h_1|h_0)$: the conditional probability that h_1 is accepted given it is actually false (corresponding to the false alarm probability P_F of a sensor).

4.1.1 Sequential Likelihood Ratio Test

In typical tracking applications, the decisions between the alternatives must be made as quickly as possible on average for given decision probabilities P_0, P_1 . The decision algorithm discussed below fulfills this requirement and is of enormous practical importance. It is called *Sequential Likelihood Ratio Test* and was first proposed by Abraham Wald [2–4, 8, 9].

The starting point for sequential decision-making in the context of track extraction is the ratio of the conditional probabilities $p(h_1|Z^k)$ of h_1 being true given all data have been processed appropriately and $p(h_0|Z^k)$ of h_0 being true given the sensor data. If $p(h_1|Z^k)$ is close to One and $p(h_0|Z^k)$ close to Zero, the ratio is large, while it is small if $p(h_1|Z^k)$ is close to Zero and $p(h_0|Z^k)$ close to One. If both hypotheses are more or less equally probable, the ratio is of an intermediate size. According to Bayes' Theorem, we obtain:

$$\frac{p(h_1|Z^k)}{p(h_0|Z^k)} = \frac{p(Z^k|h_1)}{p(Z^k|h_0)} \frac{p(h_1)}{p(h_0)}. \quad (4.1)$$

Since the a priori probabilities $p(h_1)$ and $p(h_0)$ are in most applications assumed to be equal, this defines a test function, which is called *likelihood ratio*:

$$\text{LR}(k) = \frac{p(Z^k|h_1)}{p(Z^k|h_0)} \quad (4.2)$$

and can be calculated iteratively by exploiting the underlying object evolution and sensor models $p(X_k|X_{k-1})$ and $p(Z_k|X_k)$.

An intuitively plausible sequential test procedure starts with a time window of length $k = 1$ and iteratively calculates the test function $\text{LR}(k)$ until a decision can be made. At each step of this iteration the likelihood ratio is compared with two thresholds A and B :

$\text{LR}(k) < A$, accept the hypothesis h_0 (i.e. no object existent)
 for $\text{LR}(k) > B$, accept the hypothesis h_1 (i.e. an object exists)
 $A < \text{LR}(k) < B$, expect new data Z_{k+1} , repeat the test with $\text{LR}(k + 1)$.

4.1.2 Properties Relevant to Tracking

Note that the iterative calculation of likelihood ratios has a meaning, which is completely different from the iterative calculation of probability density functions, although similar formulae and calculations are implied, as will become clear below. By iteratively calculated likelihood ratios we wish to decide, whether an iterative tracking process should be initiated or not.

1. The most important theoretical result on sequential likelihood ratio tests is the fact that the test has a *minimum decision length on average* given predefined statistical

decision errors of first and second kind, which have to be specified according to the requirements in a given application.

2. Furthermore, the thresholds A , B can be expressed as functions of the decision probabilities P_0 , P_1 , i.e. they can be expressed as functions of the statistical decision errors of first and second kind and are thus not independent test parameters to be chosen appropriately. A useful approximation in many applications is given by:

$$A \approx \frac{1 - P_1}{1 - P_0}, \quad B \approx \frac{P_1}{P_0}. \quad (4.3)$$

4.1.3 Relation to MHT Tracking

Likelihood ratios $\text{LR}(k)$ can be calculated iteratively as a by-product of the standard Bayesian tracking methodology previously discussed, provided we look upon it from a different perspective. This can be seen directly:

$$\text{LR}(k) = \frac{p(Z^k|h_1)}{p(Z^k|h_0)} \quad (4.4)$$

$$= \frac{\int d\mathbf{x}_k p(Z_k, m_k, \mathbf{x}_k, Z^{k-1}|h_1)}{p(Z_k, m_k, Z^{k-1}, h_0)} \quad (4.5)$$

$$= \frac{\int d\mathbf{x}_k \underbrace{p(Z_k, m_k|\mathbf{x}_k, h_1)}_{\text{likelihood}} \underbrace{p(\mathbf{x}_k|Z^{k-1}, h_1)}_{\text{prediction}}}{\underbrace{|\text{FoV}|^{-m_k} p_F(m_k)}_{\text{clutter model}}} \text{LR}(k-1). \quad (4.6)$$

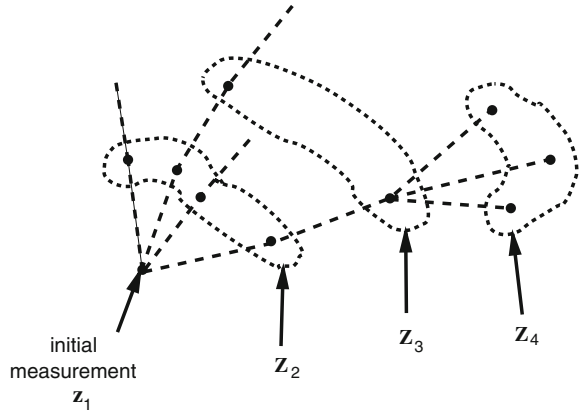
According to these considerations, the likelihood ratio is in general a sum of a temporally increasing number of individual likelihood ratios,

$$\text{LR}(k) = \sum_i \lambda_k^i. \quad (4.7)$$

In order to avoid memory explosion in calculating the likelihood ratio, the same type of mixture approximation techniques as discussed in Sect. 3.3.3 can be applied (merging of similar, pruning of summands λ_k^i that are too small). Figure 4.1 provides a schematic illustration of the hypothesis tree structure, which is created by sequentially calculating the likelihood ratio test function. As soon as a decision in favor of object existence is made, e.g. at time t_k , the normalized individual likelihood ratios can be used for initializing the tracking process:

$$p(\mathbf{x}_k|Z^k) = \sum_i \frac{\lambda_k^i}{\sum_j \lambda_k^j} \mathcal{N}(\mathbf{x}_k; \mathbf{x}_{k|k}^i, \mathbf{P}_{k|k}^i), \quad (4.8)$$

Fig. 4.1 Schematic illustration of the hypothesis tree structure created by sequentially calculating the likelihood ratio test function



where $\mathbf{x}_{k|k}^i$ and $\mathbf{P}_{k|k}^i$ are by-products of the calculation of λ_k^i . As soon as the track has been initiated, the calculation of the likelihood ratio can be restarted as it is a by-product of track maintenance. The output of these subsequent sequential ratio tests can serve to re-confirm track existence or track deletion, depending on the test output. See [1, 2] for details. So far, the problem of multiple well-separated object track extraction, track maintenance, and track deletion, i.e. the full life cycle of a track, is solved in principle. See [5] for an alternative calculation of $LR(k)$ by using PMHT techniques and [10] for a proof that for well-separated objects, this scheme is identical with Gaußian Mixture Cardinalized PHD filtering (GM-CPHD). Careful quantitative performance evaluations can be found in [11].

4.2 Object Clusters

Sequential likelihood testing can be extended to the problem of extracting object clusters with an unknown number of objects involved. To this end let us assume that the number n of objects involved is limited by N (not too large). The discussed method is confined to N being less than around 10. This means that it can be applied to aircraft formations and convoys of ground moving objects, which are practically relevant examples of object clusters. It is not applicable to larger object clouds or swarms.

4.2.1 Generalized Likelihood Ratio

The ratio of the probability $p(h_1 \vee h_2 \vee \dots \vee h_N | Z^k)$ that a cluster consisting of at least one and at most N objects exists versus the probability of having false returns only can be written as:

$$\frac{p(h_1 \vee \dots \vee h_N | Z^k)}{p(h_0 | Z^k)} = \frac{\sum_{n=1}^N p(h_n | Z^k)}{p(h_0 | Z^k)} \quad (4.9)$$

$$= \sum_{n=1}^N \frac{p(Z^k | h_n)}{p(Z^k | h_0)} \frac{p(h_n)}{p(h_0)}. \quad (4.10)$$

We thus very naturally obtain a generalized test function

$$\text{LR}(k) = \frac{1}{N} \sum_{n=1}^N \text{LR}_n(k) \quad \text{with} \quad \text{LR}_n(k) = \frac{p(Z^k | h_n)}{p(Z^k | h_0)} \quad (4.11)$$

to be calculated in analogy to the case $n = 1$. In practical applications the finite resolution capabilities of the sensors involved have to be taken into account (see section IV.A). For the sake of simplicity this has been omitted here.

4.2.2 On Cluster Cardinality

It seems to be reasonable to interpret the normalized individual likelihood ratios as a ‘cardinality’, i.e. as a measure of the probability of having n objects in the cluster.

$$c_k(n) = \frac{\text{LR}_n(k)}{\sum_{n=1}^N \text{LR}_n(k)}. \quad (4.12)$$

An estimator for the number of objects within the cluster is thus given by

$$\bar{n} = \sum_{i=1}^N n c_k(n). \quad (4.13)$$

See [2, 3] for a more detailed description of the iterative calculation of the likelihood ratios, practical implementation issues and quantitative results.

References

1. W. Koch, J. Koller, M. Ulmke, Ground target tracking and road-map extraction. *ISPRS J. Photogram. Remote Sens.* **61**, 197–208 (2006)
2. G. van Keuk, Sequential track extraction. *IEEE Trans. Aerosp. Electron. Syst.* **34**, 1135 (1998)
3. G. van Keuk, MHT extraction and track maintenance of a target formation. *IEEE Trans. Aerosp. Electron. Syst.* **38**, 288 (2002)
4. Y. Boers, Hans Driessen, in *IEE Proceedings on Radar, Sonar, Navigation*. A particle filter multi target track before detect application, vol. 151, no. 6 (2004)

5. M. Wieneke, W. Koch, On Sequential Track Extraction within the PMHT Framework. EURASIP J. Adv. Signal Process. **2008**, Article ID 276914, 13 (2008). doi:[10.1155/2008/276914](https://doi.org/10.1155/2008/276914)
6. C.R. Berger, M. Daun, W. Koch, Low complexity track initialization from a small set of non-invertible measurements. EURASIP J. Adv. Signal Process. special issue on track-before-detect techniques **2008**, Article ID 756414, 15 (2008). doi:[10.1155/2008/756414](https://doi.org/10.1155/2008/756414)
7. Ch. Berger, M. Daun, W. Koch, Track initialization from incomplete measurements, in *Proceedings of 10th ISIF International Conference on Information Fusion*, Quebec, Canada (2007)
8. A. Wald, *Sequential Analysis*, (John Wiley and Sons, New York, 1947)
9. A. Wald, *Statistical Decision Functions*, (John Wiley and Sons, New York, 1950)
10. M. Ulmke, O. Erdinc, and P. Willett, Ground moving target tracking with cardinalized gaussian mixture PHD filtering, in *Proceedings of the 10th International Conference on Information Fusion FUSION 2007*, Quebec, Canada, July (2007)
11. J. Koller, H. Bos, M. Ulmke, Track extraction and multiple hypothesis tracking for GMTI sensor data. FKIE, Report 90 (2005)